

**PARTICULATE ORGANIC MATTER (POM) COMPOSITION IN
STREAM RUNOFF FOLLOWING LARGE STORM EVENTS:
ROLE OF POM SOURCES, PARTICLE SIZE,
AND EVENT CHARACTERISTICS**

by

Erin R. Johnson

A thesis submitted to the Faculty of the University of Delaware in partial fulfillment of the requirements for the degree of Master of Science in Water Science and Policy

Summer 2017

© 2017 Erin Ruth Johnson
All Rights Reserved

**PARTICULATE ORGANIC MATTER (POM) COMPOSITION IN
STREAM RUNOFF FOLLOWING LARGE STORM EVENTS:
ROLE OF POM SOURCES, PARTICLE SIZE,
AND EVENT CHARACTERISTICS**

by

Erin R. Johnson

Approved: _____
Shreeram P. Inamdar, Ph.D.
Professor in charge of thesis on behalf of the Advisory Committee

Approved: _____
Shreeram P. Inamdar, Ph.D.
Director of the Program of Water Science and Policy

Approved: _____
Mark W. Rieger, Ph.D.
Dean of the College of Agriculture and Natural Resources

Approved: _____
Ann L. Ardis, Ph.D.
Senior Vice Provost for Graduate and Professional Education

ACKNOWLEDGMENTS

I would like to thank Dr. Shreeram Inamdar for the support, guidance, and advice he has provided as I have pursued my Masters degree. Thanks to my committee member Dr. Rodrigo Vargas for his technical expertise and support for the analyses done in this project. Special thanks to my committee member Dr. Jinjun Kan for his continuous support, encouragement, and valuable expertise.

A heartfelt thank you to my fellow graduate students who have taken this journey with me, Chelsea Krieg, Doug Rowland, Catherine Winters, and Dan Warner, your endless help, support, and friendship have meant so much. Thank you to the summer interns who assisted with this project, Jack Protokowicz, Shawn Del Percio, John Dougherty, Caraline Canning and Margaret Orr.

Thanks to the staff of the Fair Hill Natural Resource Management Area for providing us with assistance and access to the study site, the Delaware Environmental Observing System (DEOS) for providing climatological data for this study and the researchers and staff of the Duke Environmental Isotope Lab (DEVIL) and UD Soil Testing Laboratory for their assistance with sample analysis. This work would not have been possible with generous funding from USDA grant number 2015-67020-23585.

Finally, a special thanks to my parents and to my family, for always being supportive and encouraging for both the ups and downs of this journey, and to Michael, for believing in me every step of the way and always encouraging me to follow my dreams!

TABLE OF CONTENTS

LIST OF TABLES	vi
LIST OF FIGURES	vii
ABSTRACT	xiii

Chapter

1	INTRODUCTION	1
2	LITERATURE REVIEW	5
2.1	Environmental Significance of POM	5
2.2	Characterization of POM composition and quality	10
2.3	POM variations with watershed source	12
2.4	POM variations with particle class size	13
2.5	POM variation with storm event	15
2.6	POM variation with drainage location	16
3	SITE DESCRIPTION AND METHODS	18
3.1	Site Description	18
3.2	Analyses	24
4	RESULTS	29
4.1	Composition of POM in watershed sources	29
4.2	Differences in fluvial POM for storm events and particle size class	49
4.3	Comparison of watershed sources against fluvial POM in chemical and isotopic mixing space	69
5	DISCUSSION	85
5.1	POM composition for Watershed Sources	85
5.2	Fluvial POM composition with particle size class and storm events	89
5.3	POM compositional changes with Particle Size Class	92
5.4	Broader environmental implications of POM composition	94
6	CONCLUSION	99

REFERENCES	102
------------------	-----

Appendix

A SUPPLEMENTAL DATA	109
A.1 Inorganic Nitrogen species	109
A.2 Average values for extracted and solid POM metrics	115
A.3 Correlation Matrix	117

LIST OF TABLES

Table 3.1: The sediment samples were sieved into three discrete particle class sizes for analysis based on previous studies performed in the watershed and a review of the literature.....	23
Table 4.1: Storm event metrics for the five events examined in this study. API is the antecedent precipitation index, calculated as the total rainfall, in mm, for 7 or 14 days prior to the event.....	41
Table 4.2: Amount of material collected (g), separated by size class for each event. All five CSS locations were summed for these calculations.....	43
Table 4.3: Percent distribution of sediment within each particle size class for the storm events. All five CSS sites were summed and averaged to get a whole event composite. Percentages were calculated from this average.....	44
Table A1: Average values and standard deviations of solid POM metrics.....	115
Table A2: Average and standard deviations of extracted event POM metric.....	116
Table A3: Correlation matrix for all POM samples.....	117
Table A4: p-values of correlation matrix presented in Table A3.....	118

LIST OF FIGURES

Figure 3.1:	Nested catchments in the Fair Hill NRMA. A 12 ha catchment was nested inside of a larger 79 ha catchment. The two main 1 st order stream branches (ST10 and ST11) converge to form a 2 nd order stream (ST12). The catchment drains to the Big Elk Creek. Map includes sampling locations for composite suspended sediment samplers (CSS). Five CSS sampler locations are showed in red.....	19
Figure 3.2:	Photo of Composite Suspended Sampler (CSS) apparatus at baseflow conditions. Note orange flag for scale.....	22
Figure 3.3:	Schematic of composite sediment samplers (CSS). Panel (a) shows the front view of the sampler where the holes in the PVC pipe face upstream. At baseflow there is no water or POM being collected. Panel (b) shows a rear view of the sampler. Note that there are no holes on the back, and that the sampler is anchored with a stake into the stream bed and attached to the stake with metal gear clamps (grey horizontal lines). Panel (c) shows a side view of the passive sampler in action during a high flow event. POM and sediments can enter the holes and are retained within the PVC tube. POM and sediments settle to the bottom PVC cup due to a reduction in velocity. Samples are collected after storm flow has receded.	23
Figure 3.4:	Sediment was sieved into three discrete size fractions using brass sieves. The percent weight for each size class was determined after sieving.	24
Figure 4.1:	The percent carbon (C) values are presented for each of the seven watershed sources. Different letters indicate significant differences. Note that the axis has been placed on a log scale.....	30
Figure 4.2:	Percent nitrogen (N) values are presented for each of the seven watershed sources. Significant differences are indicated by different letters.	30
Figure 4.3:	C:N ratio (atomic) values are presented for each of the seven watershed sources. Significant differences are indicated by the letters.	31

Figure 4.4: Isotopic separation of sources, based on $\delta^{15}\text{N}$ and $\delta^{13}\text{C}$. Sources are represented as an average value and error bars represent one standard deviation.	32
Figure 4.5: Dissolved organic carbon (DOC) values for each of the seven watershed sources. Note that the axis is on a log scale.	33
Figure 4.6: DOC values within each source, separated by size class. Note that the axis is on a log scale.	34
Figure 4.7: Total Nitrogen (TN) leached by all seven watershed sources. Note that the axis is on a log scale.	35
Figure 4.8: The percent protein-like fluorescence values presented for each of the seven watershed sources. Significant differences are indicated with letters.	36
Figure 4.9: Percent humic-like fluorescence values for each of the seven watershed sources. Significant differences are noted by letters.	37
Figure 4.10: Percent fulvic-like fluorescence for all seven watershed sources. Significant differences are indicated with letters.	38
Figure 4.11: SUVA values for all seven watershed sources. Significant differences are indicated with letters.	39
Figure 4.12: The DOC:TN ratio (atomic) is presented for all seven watershed sources. Significant differences are indicated with letters.	40
Figure 4.13: Storm event metrics showing total precipitation, maximum intensity, and duration of events	42
Figure 4.14: Sediment mass (g) collected from composite sediment samplers (CSS) for all events. Reported masses are a sum of all five sampling locations. The proportion of each size class collected is represented in the stacked bars.	43
Figure 4.15a-e: Percentage of sediment in the three particle size classes for individual storm events. Samples from all CSS sites were summed to generate an event average.	45
Figure 4.16: Particulate organic carbon (POC) generated by each of the events, separated by size class. This trend was driven by the amount of material generated (Figure 4.3).	46

Figure 4.17a-e: Particulate organic carbon (POC) percent contributed by size class. All CSS sampling locations were summed and percent contributions of each size class were calculated from the total.....	47
Figure 4.18: Particulate Nitrogen (PN) by size class for each event. All CSS sampling locations were summed and percent contributions of each size class were calculated from the total. This trend was partially a function of the amount of material generated (Figure 4.14).	48
Figure 4.19: Percent PN contributed by each size class. All CSS sampling locations were summed and percent contributions of each size class were calculated from the total.	49
Figure 4.20: Percent C and %N values by event are presented. Significant differences are indicated by letters.	50
Figure 4.21: Percent C and %N presented by size class. Significant differences are indicated by letters.....	51
Figure 4.22: C:N ratio separated by event and size class. Significant differences are indicated by letters.....	52
Figure 4.23: C:N ratio presented for each of the three size classes. Significant differences are indicated by letters.	52
Figure 4.24: $\delta^{15}\text{N}$ and $\delta^{13}\text{C}$ mixing space shows separation between the sizes classes on the $\delta^{15}\text{N}$ axis.	53
Figure 4.25: Isotopic values for $\delta^{15}\text{N}$ are presented by size class. Significant differences are indicated by letters.	54
Figure 4.26: Average DOC concentration leached from each size class by event. Significant differences are indicated by letters.	55
Figure 4.27: DOC amounts leached from different size classes of POM. Significant differences are noted by letters.....	55
Figure 4.28a-e: DOC was leached from 0.5g of each size class. The DOC concentration obtained was multiplied by the total sample mass (Table 4.2) and the percent contribution was calculated to better understand the DOC contribution from each size class, for each event.	57
Figure 4.29: Average TN concentration leached from each size class, for each event. Significant differences are indicated by letters.....	58

Figure 4.30: TN concentrations by size class are shown, and significant differences are indicated by letters.	59
Figure 4.31a-e: TN was leached from 0.5g of each size class. The TN concentration obtained was multiplied by the total sample mass (Table 4.2) and the percent contribution was calculated to better understand the TN contribution from each size class, for each event	60
Figure 4.32: Protein-like fluorescence values are presented by event and size class. Significant differences are indicated by letters.	61
Figure 4.33: Percent protein-like fluorescence is presented by size class. Significant differences are indicated by letters.	62
Figure 4.34: Percent humic-like fluorescence is presented by event and size class. Significant differences are indicated by letters.	63
Figure 4.35: Percent humic-like fluorescence is shown by size class. Significant differences are indicated by letters.	63
Figure 4.36: Percent fulvic-like fluorescence presented by event and size class. Significant differences are indicated by letters.	64
Figure 4.37: Percent fulvic-like fluorescence presented by size class. No significant differences were found.	65
Figure 4.38: SUVA values presented by event. Significant differences indicated by letters.	66
Figure 4.39: SUVA presented by size class. Significant differences indicated by letters.	66
Figure 4.40: DOC:TN ratio presented by size class. Significant differences are indicated by letters. Similar results are presented in Figure 4.23.....	67
Figure 4.41: DOC:TN ratio presented by event. Significant differences are indicated by letters.....	68
Figure 4.42: Isotope mixing space of $\delta^{15}\text{N}$ and $\delta^{13}\text{C}$ with sources plotted as letters and event POM plotted as dots. Dots are sized by size class and colored by event.	70
Figure 4.43: Coarse material only is presented for all five events, along with the sources.	71

Figure 4.44: Medium material only is presented for each of the five events, along with the sources.	72
Figure 4.45: The Fine material only is presented by event, along with the sources. ...	73
Figure 4.46: Loading plot of PCA components shows that PC1 was best explained by the carbon and nitrogen components, while PC2 was best explained by the “quality” components.	74
Figure 4.47: Comparing the sources in component space with the PC component loadings (Figure 4.46) provides information about the quality of the sources.	76
Figure 4.48: Average values for POM, by size class, for each event. Plotted with sources in PCA mixing space.	77
Figure 4.49: The average value of Coarse material for each event is presented. Sources are also plotted in this PCA mixing space.	78
Figure 4.50: The average value of Medium material for each event is presented. Sources are also plotted in this PCA mixing space.	79
Figure 4.51: The average value of Fine material for each event is presented. Sources are also plotted in this PCA mixing space.	80
Figure 4.52: POM averaged by location for all events shows is presented, along with the sources in PCA mixing space.	81
Figure 4.53: The average value of Coarse material for each location is presented. Sources are also plotted in this PCA mixing space.	82
Figure 4.54: The average value of Medium material for each location is presented. Sources are also plotted in this PCA mixing space.	83
Figure 4.55: The average value of Fine material for each location is presented. Sources are also plotted in this PCA mixing space.	84
Figure A1: Nitrate, measured as NO ₃ -N, showed no significant differences by event. The horizontal line represents the average streamwater concentration, from which the event values did not significantly deviate.	110
Figure A2: Nitrate, measured as NO ₃ -N, showed no significant differences by size class. The horizontal line represents the average streamwater blank sample from which the size classes did not deviate significantly.	111

Figure A3: Ammonium, measured as $\text{NH}_4\text{-N}$, only showed a significant difference between the 2/16/16 and 8/21/16 events, and was significantly higher than streamwater blank which read below the detection limit of the instrument.	112
Figure A4: Ammonium, measured as $\text{NH}_4\text{-N}$, showed no significant difference between size classes.	113
Figure A5: DON (ppm), calculated as $\text{TN} - \text{NO}_3\text{-N} - \text{NH}_4\text{-N}$. The Coarse size class was significantly different from Medium and Fine. No significant differences were found between events. This trend mirrors the TN trend by size class indicating that this relationship was an artifact of the TN values and was not influenced by the $\text{NO}_3\text{-N}$ or $\text{NH}_4\text{-N}$ values.	114

ABSTRACT

Large storm events have tremendous erosive energy which is capable of mobilizing large amounts of material from watershed sources into fluvial systems. This complex mixture of sediments and particulate organic matter (POM) are important nutrient sources that have the potential to impact downstream water quality. This study investigates how the composition and quality of storm events mobilized POM varies as a function of the source, particle size, event characteristics, and drainage location. Storm event POM and source sediments were collected from a forested headwater (second order stream) catchment in the Piedmont region of Maryland. Streamwater extractions were performed for three particle class sizes and bulk source materials, and the resulting fluorescent organic matter was analyzed. Carbon (C) and Nitrogen (N) amount, C:N ratio and isotopic analysis of ^{13}C and ^{15}N were performed on solid state materials from events and sources. Key findings from this study are: (1) Composition and quality varied greatly between sources. Carbon/nitrogen rich and isotopically depleted sources have the ability to contribute large amounts of labile material to the stream, while the carbon/nitrogen poor and isotopically enriched sources likely contribute more recalcitrant material. (2) Event characteristics such as storm magnitude, intensity, and antecedent conditions regulated the sources that were mobilized. Summer storms mobilized more carbon and nitrogen rich labile sources, while winter events mobilized more carbon and nitrogen poor refractory material from near stream sources. (3) POM quality was distinct in different size classes, with the Coarse size showing more C/N rich and labile properties while

the Fine size showing more degraded and refractory properties. (4) POM quality varied by drainage location and was most strongly regulated by the sources available at each location within the stream network. Future climate variability will likely increase the frequency and intensity of large storm events, thus mobilizing more POM into aquatic systems. POM has the potential to impact water quality, aquatic nutrient cycling, and greenhouse gas fluxes and therefore should be accounted for in future management decisions.

Chapter 1

INTRODUCTION

The transport and processing of terrestrial organic matter through fluvial networks provides a critical link between terrestrial and aquatic systems (Vannote et al. 1980). In natural headwater streams, allochthonous material serves as a key energy source for aquatic food webs, maintains organic matter budgets, and contributes to ecosystem metabolism (Tank et al. 2010). Disturbances related to land use or climate change can increase organic matter inputs to aquatic systems, undermining the water quality and valuable ecosystem services provided by these ecosystems (Tank et al. 2010; Stanley et al. 2012; Kaushal et al. 2014). Organic forms of carbon and nitrogen can contribute to eutrophication of estuarine and coastal ecosystems with detrimental consequences for fisheries and recreational opportunities (Seitzinger et al. 2002). Elevated inputs of organic carbon in particulate and dissolved forms can pose challenges for drinking water utilities due to increased costs associated with filtration and the formation of carcinogenic disinfection byproducts (DBPs; Karanfil et al. 2008; Hrudey 2009) following water treatment. Organic matter inputs can increase greenhouse gas fluxes from inland waters through mineralization, thereby increasing CO₂ fluxes as well as other more potent greenhouse gases such as CH₄ and N₂O (Kaushal et al. 2014; Worrall et al. 2016). Therefore, developing a comprehensive understanding of organic matter inputs to fluvial ecosystems as a result of large storm events is critical to understanding nutrient cycling and water quality.

While much of the focus on organic matter contributions from large storm events has been dedicated to the dissolved organic matter (DOM), the mobilization and transport of particulate organic matter (POM) has recently received increased attention. Several

studies have found that particulate forms of carbon (C) and nitrogen (N) transported during high intensity, large storm events can greatly exceed the amount contributed by dissolved forms (Dhillon and Inamdar 2013; Inamdar et al. 2015; Jeong et al. 2012; Jung et al. 2012). For example, in a mountainous watershed in South Korea, Jeong et al. (2012) found that POC export during storm events accounted for 84% of the annual export and one extreme event represented 62% of the total annual export. Similarly, in a forested mid-Atlantic watershed Inamdar et al. (2015) found that 65% of the annual PN export occurred during storm events. These findings are particularly critical as the frequency and intensity of the largest (top 1%) storm events are predicted to increase as a result of global climate change (Barker 2007; Melillo et al. 2014). With an increase in large storm events, mobilization of terrestrial C to fluvial systems could lead to changes in biogeochemical cycling in aquatic systems (Battin et al. 2009b). Similar to carbon, nitrogen was also found to be preferentially transported with the particulate fraction during storm events and identified as “highly relevant” to achieving water quality goals (Hirsch 2012; Inamdar et al. 2015). Large inputs of POM could produce important “hot moments” and “hot spots” for carbon and nitrogen fluxes and cycling in fluvial ecosystems (McClain et al. 2003; Goulsbra et al. 2016).

While the increase in POM mobilization and transport with storm intensity and magnitude is well recognized, a largely unexplored topic is how these large events alter the composition and quality of POM exported to aquatic ecosystems. Event characteristics can have a direct control on the composition and quality of POM depending on the sources that are mobilized. For example, in a small forested watershed, Dhillon and Inamdar (2014) found that smaller storms tended to transport near stream sources while larger, more intense storms tended to transport more distal upland sources. POM quality directly regulates the quality of leached DOM (Yoshimura et al. 2008), the thus has a strong influence on the biodegradability of the organic matter (Fellman et al. 2009). Bianchi and Bauer (2011) classify the degradation of POC in estuarine systems

into three phases: leaching, decomposition, and refractory; all of which have the potential to influence biogeochemical cycles in both the water and sediments. POM quality can influence the initial leaching phase of organic matter, as both amount and rate of organic matter release can be influenced by the organic matter quality (Yoshimura et al. 2008; Yoshimura et al. 2010). Differences in the quality of POM can have a direct impact on the degradation of POM, as labile components can be preferentially utilized by microbes over refractory components (Hur et al. 2009). Understandably, the material left after initial degradation was traditionally thought to be degraded and refractory and therefore not easily utilized (Battin et al. 2009a). However, more recent studies suggest that the remobilization of this refractory material in concert with a labile carbon source, such as autochthonous production, can cause a “priming effect” and subsequently allow for the material to be further processed and degraded (Guenet et al. 2014).

The impact of POM on fluvial systems is not well understood, and therefore the influence of POM from large storm events warrants further investigation. Specifically, the key missing knowledge gaps are: (1) how POM composition and quality changes with storm magnitude and intensity, (2) how the sources change in their contribution to storm event POM with differing runoff events, (3) what the compositional and quality differences are between the different particle size classes of POM, (4) what are the differences in quality of the leached POM, and (5) how these differences may subsequently affect biogeochemical responses on both short and long term scales.

In order to develop a better understanding of how climate-driven large storm inputs/pulses of POM entering fluvial systems could contribute to downstream nutrient fluxes and/or alter aquatic metabolism and nutrient cycling, this study characterizes the storm-event POM by assessing its composition and quality through multiple analytical techniques including traditional isotopic source tracking and elemental analysis coupled with fluorescence analysis of extracted organic matter. Based on a review of current literature, no study has combined these analyses to comprehensively examine POM

fluxes and the subsequent influence on the surrounding environment. The study was conducted in a 79ha headwater forested watershed in which five storm events over a one year period were sampled. Specific questions that were addressed in this study included:

- (1) What are the sources of POM in watersheds and how do they vary in composition and quality?
- (2) How is the composition of fluvial POM affected by – sources, storm event magnitude and intensity, particle size class, and drainage location?

Key hypotheses associated with the questions above are:

- (1) Fluvial POM composition will vary with the contributions from watershed sources.
- (2) Fluvial POM composition will vary with the magnitude/intensity of the storms and its seasonal occurrence.
- (3) Fluvial POM was also expected to differ by size class with Coarse POM being fresher and more carbon and nitrogen rich and Fine POM being more degraded and carbon and nitrogen poor.

Chapter 2

LITERATURE REVIEW

This review addresses the environmental significance of particulate organic matter (POM) and its impact on fluvial systems when mobilized by large storm events. Specifically addressed is the quality of POM in both solid and leached/solution forms and how that quality differs as a function of POM source, particle size class, and drainage location. Also examined are the potential impacts and influence of POM on water quality, aquatic nutrient cycling, and greenhouse gas fluxes (GHG).

2.1 Environmental Significance of POM

Much of the research on organic matter impacts from large storm events has focused on the dissolved phase of organic matter (DOM). However, multiple recent studies show that large intense storm events can mobilize significant amounts of POM relative to annual POM budgets (Jung et al. 2012; Dhillon and Inamdar 2013; Jung et al. 2014b). While transport of POM and DOM both significantly increase during storm flow (Alvarez-Cobelas et al. 2012), Jeong et al. (2012) found that stormflow export of POC accounted for 84% of the annual export in a mountainous headwater stream in South Korea and one extreme event represented 62% of the total annual export. Similarly, working in a small forested watershed in the mid-Atlantic, USA, Dhillon and Inamdar (2013) found that the vast majority of POC export (88%) occurred during elevated flows ($>0.5\text{mm/hr}$) which occurred at a frequency of less than 1% during the study period. In a similar study and in the same watershed, Inamdar et al. (2015) found that 65% of the annual PN export occurred during storm events. These large POM fluxes indicate that storm events are key drivers in organic matter transport and that POM inputs can

contribute a significant portion of an annual carbon or nitrogen budget over a very short period of time. Understanding organic matter inputs therefore requires a better understanding of present and future storm event patterns.

Stronger and more intense storm events have been shown to induce larger (Trimmer et al. 2012) and more variable responses from natural systems (Kaushal et al. 2014). Examining storm event POM, and its influence on fluvial systems, can help develop a better understanding of the potential impacts of increased storm frequency and intensity resulting from climate change (Melillo et al. 2014). Similar to previous research on DOM, large storm events appear to trigger a “pulse” response from POM where a large amount of material is transported through the fluvial network and delivered to downstream waters, resulting in water quality concerns due to high loadings of contaminants or nutrients (Kaushal et al. 2014). A similar “pulse-shunt” concept is defined by Raymond et al. (2016) which suggests that large infrequent storm events can be the driving factor controlling amount of DOM transported through the network and the level of processing that it has undergone. While both of these theories focus on the dissolved phase of organic matter, they are likely more relevant to the transport and processing of POM due to the particle size, inertial effects, and greater dependency of POM on storm flows. With increases in climate extremes, these POM “pulses” may become more environmentally significant as they deliver large loads of nutrients to downstream systems, influencing water and drinking water quality, aquatic food webs, and greenhouse gas fluxes.

The effects of POM on water quality are not currently well understood, and notably absent from water quality improvement plans. However, as a result of leaching, degradation, and microbial processing of POM, it is hypothesized that POM additions could result in excess nutrient loading (Bianchi and Bauer 2011), eutrophication and oxygen depletion (Anderson et al. 2002), and increased greenhouse gas fluxes (Worrall et al. 2016). The lateral transfer of organic matter from terrestrial to aquatic systems as a

result of storm events can result in large inputs of carbon, nitrogen, and other nutrients to aquatic systems making them available for degradation and processing (Kaushal et al. 2014). Large inputs of POM, even of refractory composition, may be broken down when stimulated by an aquatic “priming” effect (Guenet et al. 2014). For example, in a study of soil carbon mineralization, Guenet et al. (2014) found that addition of labile organic matter stimulated the degradation of soil organic matter by 63% in an aquatic system. This shows that aquatic priming has the potential to induce breakdown of material previously considered to be recalcitrant, generating an even larger nutrient supply than originally estimated. These large inputs of organic matter and subsequent breakdown processes could lead to significant downstream impacts on water quality (Kaushal et al. 2014), and these water quality impacts likewise extend to human health implications. Water bodies used as sources of drinking water may face increased challenges due to increases in sediment and POM loads to drinking water facilities (Park et al. 2010), as these POM inputs could increase water filtration and coagulation costs for the water utilities. Increased leaching of DOM from POM could react with the chlorine used for disinfection and form disinfectant byproducts (DBP) such as trihalomethanes, which are known carcinogens (Kraus et al. 2008). In a study of DBP formation from POM mobilized by a large storm event, Jung et al. (2014b) found that the dissolution of reactive DOM from the POM and subsequent treatment had the potential to form DBPs, indicated that storm events could be a public health concern for drinking water quality. It is therefore critical to develop a better understanding of the fundamental importance of POM, and evaluate how excess loading of POM can have impacts on water quality.

While large contributions of POM may pulse excess nutrients into aquatic systems, allochthonous POM also serves as a key source of energy to microbial communities, especially in headwater streams (Vannote et al., 1980). This allochthonous material fuels food web dynamics through leaching of soluble compounds, physical fractionation, microbial conditioning, and macroinvertebrate processing (Tank et al.

2010). This extensive processing has led to the notion that POM in fluvial systems is comprised primarily of refractory material (Battin et al., 2009); however, multiple studies suggest that although the material moving through streams has already been biologically processed, the inefficiencies in the previous processes allow POM to act as an energy source for biological activity in downstream reaches (Vannote et al., 1980, Webster et al., 1999, Tank et al., 2010). The POM naturally sequestered in streams, either as a result of reduced stream velocity, debris dams, snags, or other obstacles, provides a large pool of nutrients to microbial communities for processing (Tank et al. 2010). While this natural process is key for food web dynamics, large pulses of POM may overwhelm the system, leading to higher inefficiency in processing and more “leaking” of nutrients. This leaky system could be facilitated by nutrient enrichment which has been found to increase the rate of respiration, especially on the coarser POM, indicating an enhancement of this carbon loss pathway and stimulation of the aquatic food web (Tant et al. 2013).

Disruption of the aquatic food web has water quality implications as well as ecosystem implications as natural cycles are disrupted. Anthropogenic sources of nutrients in particulate and dissolved forms have been shown to contribute to eutrophication in aquatic systems. In a study by Seitzinger et al. (2002), N loading to aquatic systems was recognized as a contributing factor to eutrophication. The study evaluated multiple watershed sources, including urban/suburban and forested/pasture systems, along with the bioavailability of the dissolved N from these sources. They found that ~80% of the dissolved N from urban/suburban runoff was bioavailable while less, 20-60%, from forested and pasture systems was bioavailable (Seitzinger et al. 2002). This indicates that nutrient inputs from highly bioavailable sources will have a greater impact on the aquatic system and could simulate whole-system changes, such as eutrophication (Anderson et al. 2002). These changes in nutrient inputs can occur as a result of human influence, but can also happen in natural system as a result of changes in climate, and more extreme weather events. For example, Sadro and Melack (2012) found

that the dissolved organic carbon (DOC) and particulate organic carbon (POC) inputs to a high elevation oligotrophic lake from one extreme event caused the lake to flip from a slightly autotrophic system to a strongly heterotrophic system. These findings indicate that large storm events can have critical consequences for aquatic nutrient cycling in both naturally and anthropogenically influenced systems.

The carbon cycle can be greatly influenced by excessive POM inputs, as inland waters serve as a large transport and processing site for organic matter with nearly twice as much terrestrial carbon entering fluvial systems as is exported to the ocean (Cole et al. 2007). Often neglected in these assessments is an understanding of the CO₂ fluxes from inland waters, though they can be dominant pathways of carbon loss at both baseflow and stormflow (Bass et al. 2014). In a study of POC fluxes from peatland watersheds in the UK, Worrall et al. (2014) determined that loss of carbon in the form of CO₂ resulted in the soil becoming a net source of carbon as opposed to a net sink. Similarly, in a lab experiment, Goulsbra et al. (2016) also found that POC additions to streamwater resulted in large initial fluxes of CO₂ over the first 24 hours. This indicates that the storm inputs of POM could result in large fluxes of CO₂ to the atmosphere. While CO₂ dominates the gas flux from POM additions to fluvial systems, smaller amounts of even more potent greenhouse gases such as CH₄ and N₂O, have also been observed (Worrall et al. 2016). This pathway of carbon cycling and loss is a key component to understanding the impacts of storm even POM pulses on the global carbon cycle.

While the potential environmental significance of POM is clear, the magnitude of its effect is further regulated by the amount of POM mobilized, as well as its composition (i.e. elemental content) and quality (i.e. bioavailability). Other studies have provided a comprehensive assessment of POM fluxes (Alvarez-Cobelas et al. 2012; Jeong et al. 2012; Dhillon and Inamdar 2013; Worrall et al. 2014; Jung et al. 2014b; Inamdar et al. 2015), and therefore this study focuses specifically on the composition and quality of

POM as a function of the watershed source, particle size class, fluvial drainage location and storm event characteristics.

2.2 Characterization of POM composition and quality

Evaluating the composition of POM entering fluvial systems can provide insights into the degradability and bioavailability of this energy source and its potential influence on aquatic biogeochemical cycles. A variety of analytical techniques can be employed to evaluate the composition of POM. Bianchi and Bauer (2011) provided a detailed overview of basic bulk analyses used in estuarine systems, such as elemental composition, stable isotopes, and NMR (nuclear magnetic resonance) for the determination of functional groups in POC. The authors noted, however, that these bulk analyses are limited in their ability to provide information on the character and cycling of POC. Additionally, they noted that compound specific analyses such as chemical biomarkers could be used to better characterize POC (Bianchi and Bauer 2011). An alternative approach was taken by Yoshimura et al. (2008) in which the chemical differences in POM composition were examined as coarse POM (CPOM) was converted to fine POM (FPOM) by shredding macroinvertebrates. The authors examined the degradability and bioavailability of these two POM fractions using metrics such as C:N content, C:P content, lignin and cellulose composition, and microbial metabolism. From these analytical metrics, they were able to conclude that FPOM exhibited less microbial respiration (lower O₂ consumption), slower decomposition, and more refractory behavior compared to the original CPOM (Yoshimura et al. 2008). While bulk analyses provide valuable information about general POM composition, additional levels of analysis can be used to more accurately characterize the intricate differences influencing the cycling and processing of POM.

One analytical technique that can provide additional information on POM is fluorescence spectroscopy. This technique has been widely used to characterize the

composition of DOM which has been extracted from POM (Osburn et al. 2012; Jung et al. 2014a; Larsen et al. 2015). While this is not a direct measure of POM composition, the leaching of POM can provide insights into the compounds that would become available to fluvial systems with inputs of POM - a key focus of this study. Fluorescence spectroscopy is an analytical technique that provides detailed information about chromophoric dissolved organic matter (CDOM) present in water samples which serves as a tracer for DOM (Stedmon et al. 2003; Cory and McKnight 2005). The CDOM fraction of the larger DOM pool is analyzed colorimetrically based on both how the CDOM absorbs and how a smaller subset of fluorescent dissolved organic matter (FDOM) emits certain wavelengths of light. This occurs through the excitation of atoms by the absorption of energy and the movement of an electron to an “excited” energy state, and the subsequent fluorescence when the electron returns to its ground state (Fellman et al. 2010). The excitation and emission wavelengths are distinct to specific compounds/fluorophores, which can be related to their functional groups (Fellman et al. 2010). In aquatic systems fluorescent signatures are classified into two main categories: humic-like, and protein-like fluorescence (Fellman et al. 2010). These metrics, along with the use of a parallel factor analysis (PARAFAC) can allow for detailed interpretation of naturally occurring DOM (Stedmon et al. 2003). This technique is rapid, relatively inexpensive, and has the ability to provide valuable detailed information about the bioavailability and degradation state of DOM (Fellman et al., 2010).

Several studies have explored the POM and DOM interface by leaching POM to create DOM (Osburn et al. 2012; Gabor et al. 2014; Jung et al. 2014b; Gabor et al. 2015; Larsen et al. 2015). They used fluorescence coupled with a variety of additional metrics, to characterize organic matter in a wide array of ecosystems. Osburn et al. (2012) evaluated POM and DOM composition in a river dominated estuary using fluorescence spectroscopy. They examined DOM as well as the base extractable organic matter (BEOM) portion of the POM and were able to elucidate similarities and differences

between the two major sources of organic matter inputs to the system (Osburn et al. 2012). Larsen et al. (2015) found that fluorescence spectroscopy was a valuable fingerprinting technique to track sources of FPOM and to better understand the dynamics of FPOM transport. A broader analysis was performed by Jung et al. (2014a) where a combination of BDOC incubations, fluorescence spectroscopy, isotopes, solution-state ^1H NMR, and lipid biomarkers were used to assess the alterations in POC composition and quality with transport downstream.

The coupling of intricate analyses such as fluorescence with bulk analyses of isotopes and elemental analysis have been used in tandem to more holistically characterize organic matter. Elemental analysis of C and N as well as ^{13}C and ^{15}N stable isotopes can provide a detailed characterization of the POM, and subsequently help to determine the source of storm event mobilized POM (Kendall et al. 2001). It can also provide information about the degradation status of POM as fractionation occurs during decomposition, leading to more isotopic enrichment with increased degradation (Engle and Macko 1993). Traditionally, isotopic analyses use isotopic signatures of specific end members to create a mixing model, in which samples can be plotted to determine relative contributions from multiple sources (Finlay & Kendall, 2007; Kendall et al. 2001; Larsen et al. 2015). Coupling traditional source tracking measurements with fluorescence metrics provides a more comprehensive picture of POM composition and quality across spatial and temporal scales for large storm events.

2.3 POM variations with watershed source

Different sources of POM can have a significant impact on the quality of POM transported to fluvial systems. In a study characterizing DOM sources during storm events, Inamdar et al. (2011) observed changes in DOM fluorescence when comparing stormflow and baseflow. This indicates that the sources of organic matter activated during storm events directly influence the quality of DOM in streamwater (Inamdar et al.

2011). For POM, event flow paths are likely more variable, and are dependent on the rainfall amount, intensity, and duration. For example, in a study of a small forested catchment, Dhillon and Inamdar (2014) found that the sources of POC were more similar to near stream sources for small events and had higher contributions of upland sources in larger and more intense storms. In a study of sources of fine sediment in a subtropical Australian catchment Garzon-Garcia et al. (2016) found that the subsoil sources of sediment were both the dominant sediment source as well as the main source of N transfer in dry years. However, litter sources were the main export of organic C, and the dominant source of N in wet years (Garzon-Garcia et al. 2016). Differences in source contributions were also found between restored and unrestored urban streams using fluorescence as a source tracking technique (Larsen et al. 2015). Larsen et al. (2015) found that during storm events, restored streams transported more material from banks and soil, while the unrestored streams transported more bed material. Using fluorescence as a source tracking technique can provide information on both the source and quality of organic matter. These findings indicate that sources with differing quality can cause different ecological impacts, and highlight the importance of developing a comprehensive understanding of the POM sources.

2.4 POM variations with particle class size

The size classes in this study were chosen based on a review of the literature as well as previous studies performed in the same catchment (Rowland et al. 2017). Within the literature, defining size classes was dependent on the context of the study, with much overlap between different studies. In a review of allochthonous material influences on stream systems, Tank et al. (2010) broadly defined size classes in the stream ecology context as CPOM >1mm and FPOM as 0.45µm to 1mm. In a study centered on POM quality generated by shredding amphipods Yoshimura et al. (2008) defined FPOM as 100-500µm. Akamatsu et al. (2011) defined three size classes including FPOM from 1.2-

100 μm , MPOM from 100-250 μm , and CPOM from 250-1000 μm in a study examining seasonal and longitudinal changes in POM. Tant et al. (2013) defined CPOM ($>1\text{mm}$) and FPOM ($<1\text{mm}$) in terms of the detritivore groups that used these size classes in a study on nutrient enrichments. The size classes in this study remain consistent with many other studies that define CPOM as $>1\text{mm}$, and has a more liberal definition of MPOM (1mm-250 μm) and FPOM ($<250\mu\text{m}$) in order to capture enough material for analysis, and to remain consistent with previous studies in the catchment.

Separating the POM into different size classes is critical, as POM can exhibit distinct composition and quality differences as an artifact of source and degradation state (Kendall et al. 2001; Yoshimura et al. 2010). Since FPOM can be a direct product of CPOM breakdown (Sakamaki and Richardson 2011) it follows that CPOM would tend to be fresher and less degraded compared to FPOM. This has implications for the different impacts each size class may have on water quality, nutrient cycling and aquatic metabolism. CPOM has been found to exhibit higher carbon and nitrogen content while FPOM was found to have lower and more degraded carbon and nitrogen content, based on compositional and isotopic analyses (Yoshimura et al. 2008; Akamatsu et al. 2011; Sakamaki and Richardson 2011). CPOM was also found to release more DOC compared to FPOM in an investigation of POM leaching from different sources (Yoshimura et al. 2010). This indicates that the amount of DOM contributed to fluvial systems during storm events is likely regulated in part by the size classes of POM mobilized. In addition to the amount of DOM released by the different size fractions, the quality of POM by size has also been found to differ greatly. CPOM, composed of fresher plant material, was found to support higher levels of respiration compared to FPOM which was composed of more processed and refractory compounds (Yoshimura et al., 2008). In a study on nutrient enrichment, this size class relationship was maintained. Tant et al. (2013) found that when microbial communities were stimulated by labile energy sources, there was a subsequent increase of the respiration rates on both FPOM and CPOM, though CPOM

was respired at a vastly greater rate. Tant et al. (2013) attributed the difference in respiration partially to the difference in POM quality of the substrate, though the microbial communities colonizing the size classes may also differ. For example, Stelzer et al. (2003) found that the fungal biomass was stimulated more by increased nutrients, and that fungal communities dominated on large sized particles, therefore explaining why higher rates of respiration are found on larger particles. This indicates that examining POM by size class and not simply as a bulk measurement can provide important insights into the composition and quality of POM generated by storm events.

2.5 POM variation with storm event

As previously discussed, storm events can supply large fluxes of POM to fluvial systems; however the POM sources that are activated during each storm event can be highly dependent on the event characteristics, antecedent conditions, seasonality, and present and historic land use within the watershed. Dhillon and Inamdar (2014) found that variability in storm intensity resulted in differences in the POM sources mobilized in a small forested watershed. During small events, near stream sources (generally of lower quality) were mobilized while more intense events activated more distal and upland sources (generally of higher quality). These storm event POM responses can also be strongly influenced by antecedent conditions within the watershed. Gellis and Noe (2013) found that fine grained sediment was primarily sourced from stream banks, and that this contribution was highest during winter months as a result of the erosive capability of freeze-thaw processes, coupled with high flow events. Other studies have also found that rain events occurring after prolonged dry periods could result in large pulses of DOC and POC due to build up and degradation within the catchment over the dry period, potentially releasing more nutrients (Bass et al. 2014). On the contrary, back to back events have the potential to exhaust POM supplies and therefore result in lower POM mobilization in the second event (Dhillon and Inamdar 2014; Inamdar et al. 2015).

Land use is another large regulating factor in POM transport in watersheds. Lu et al. (2014) examined four different land use types, forest, pasture, cropland, and urban, and found that the quality of POM at baseflow differed between all of these land uses. The overall finding in this study was that human land use in the watershed significantly altered the nutritional value of the POM, with more urban influence resulting in higher nutritional value, likely due to excess nutrients (Lu et al. 2014). Similarly, Hoover and MacKenzie (2009) found significant changes in fluxes due to land use during storm events. When comparing conservation, urban, and agricultural land uses they found the highest POC and PON fluxes coming from the conservation land use, and attribute this to the loss of organic matter from cultivated soils (Hoover and MacKenzie 2009). Finally, Goñi et al. (2013) examined contrasting catchments in two small mountainous rivers in the Pacific Northwest, and found that while the yields of sediment and POM were best explained by geological differences, the composition and quality of POM was regulated more strongly by ecological factors such as vegetation coverage and soil carbon. These studies demonstrate that land use can be a strong controlling factor regulating the POM sources and subsequently the POM exports at baseflow and during storm events.

2.6 POM variation with drainage location

POM can change in composition and quality with movement downstream either as a function of increased processing and degradation, contribution from different allochthonous sources or due to increased contribution from autochthonous sources (Atkinson et al. 2009; Akamatsu et al. 2011; Jung et al. 2014a; Rowland et al. 2017; Vannote et al. 1980). In a detailed study of POM composition in a forested headwater catchment, Rowland et al. (2017) found that CPOM was comprised mainly of the litter layer, especially at the upstream locations. Stream bed and bank sources became more important contributors to FPOM with movement downstream and also showed lower carbon and nitrogen content and lower C:N ratios with movement downstream (Rowland

et al. 2017). Similarly, Akamatsu et al. (2011) found lowering C:N ratios in all size classes with movement downstream, and attributed this to an increase in periphyton. Jung et al. (2014a) suggests that while microbially degraded POC would be expected to become depleted in OM with movement downstream, new stimulation from labile sources could continue to fuel its degradation. This indicates that while POM may change in composition and quality with movement downstream, the material does not necessarily become less ecologically important.

Chapter 3

SITE DESCRIPTION AND METHODS

3.1 Site Description

The study site was located at the Fair Hill Natural Resource Management Area (NRMA) in Cecil County Maryland (Inamdar et al. 2011; Inamdar et al. 2012; Dhillon and Inamdar 2013). The catchment had a nested 12 ha watershed within a larger 79 ha watershed draining to the Big Elk Creek (Figure 3.1), which is part of the Chesapeake Bay watershed. The study site was within the Piedmont region and was underlain by the Mt. Cuba Wissahickon formation and underlying bedrock composed of pelitic gneiss, pelitic schist (Blackmer 2005). The climate is a humid, continental climate with well-defined seasons. The mean annual temperature is 13°C, the mean annual rainfall is 1205 mm, and the mean annual snowfall is 447 mm (Maryland State Climatologist Office Data Page, <http://metosrv2.umd.edu/~climate/weather/marylandnormals.htm>, accessed March 4, 2016). The soils were of the Glenelg series and were deep and well drained with nearly level to moderately steep topography and an elevation of 252 to 430m above mean sea level. The vegetation is comprised primarily (61%) of deciduous forest with pasture on the perimeter of the drainage area. Dominant tree species included *Fagus grandifolia* (American Beech), *Liriodendron tulipifera* (Yellow Poplar), and *Acer rubrum* (Red Maple) (Levia et al. 2010).

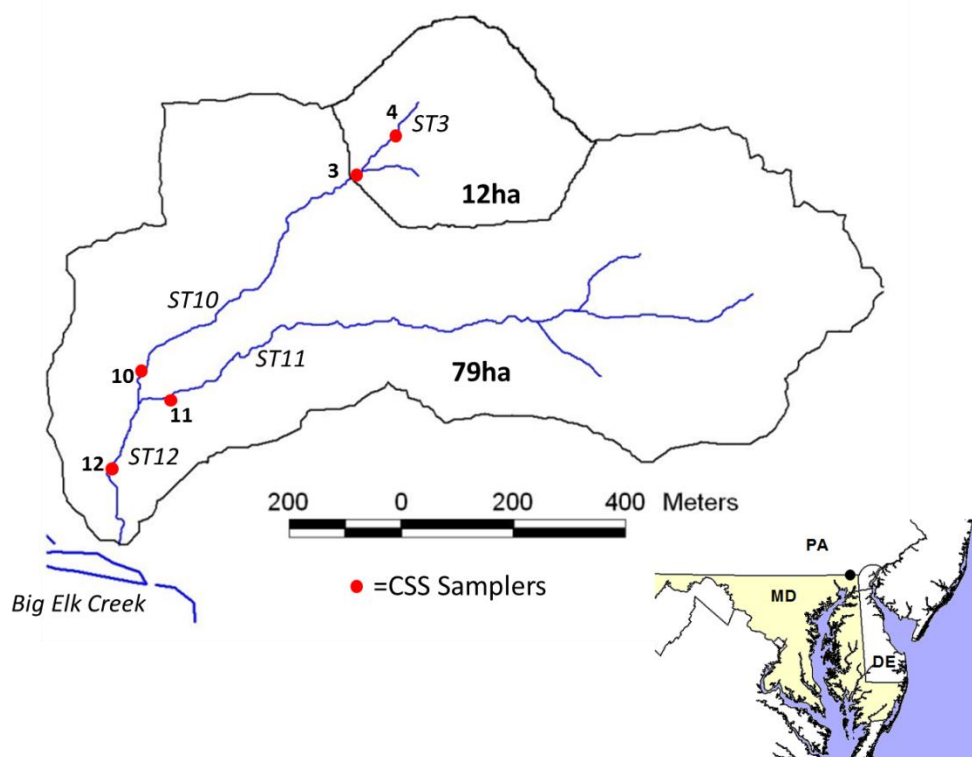


Figure 3.1: Nested catchments in the Fair Hill NRMA. A 12 ha catchment was nested inside of a larger 79 ha catchment. The two main 1st order stream branches (ST10 and ST11) converge to form a 2nd order stream (ST12). The catchment drains to the Big Elk Creek. Map includes sampling locations for composite suspended sediment samplers (CSS). Five CSS sampler locations are showed in red.

Source Sampling for POM

Watershed source sampling for POM was performed using the methodology of Rowland et al. (2017). Seven potential watershed sources, Forest Floor Litter, Forest Floor Humus, Upland A Horizon, Wetland A Horizon, Stream Bank A Horizon, Stream Bank B Horizon, and Stream Bed, were sampled at four locations within the watershed to account for spatial heterogeneity. Samples were collected with a clean, ethanol rinsed and dried trowel or auger and placed into sterile Whirl-pack sampling bags. Forest Floor Litter and Forest Floor Humus samples were collected at equidistant points along 20m transects at low gradient locations in areas with mixed tree stands. Upland A Horizon

(Upland A) samples were collected at equidistant points along 20 m transects spanning forested hillslopes. Wetland A Horizon (Wetland A) sampling locations occurred at three randomly selected points within the boundaries of the valley bottom wetland areas. Stream Bank A and B Horizon (Stream Bank A, Stream Bank B) sources were collected separately from areas with exposed banks; three locations were selected approximately three meters apart from each other and were composited for each location. In areas where Stream Bank A and Stream Bank B were collected from the same location, care was taken to collect the Stream Bank B horizon first in order to avoid contamination. The Stream Bed source was collected at each location from nine composited samples that formed a grid pattern on the stream, care was taken to collect downstream samples prior to disturbing the upstream sediments. Samples were transported on ice to the lab and were placed into ethanol wiped glass dishes to air dry. Once dry, samples, excluding the Forest Floor Litter, were pre-sieved at 2mm, and a bulk sample was retained for analysis. The remainder of the sample was sieved into three discrete size classes (Table 3.1). The samples were then frozen until further analysis.

Storm event sampling

Over the course of one year (2015-2016) five storm events were studied. These storm events were selected based on their magnitude and intensity. Each event produced greater than one inch of rainfall, and had an hourly rainfall intensity in the top 2% of events at the study location since 2008 (Table 4.1). Weather and precipitation data for these events such as duration, intensity, and total rainfall were obtained from GEONOR gauge maintained by the Delaware Environmental Observing System (DEOS) which is located at approximately 450m from the 79ha catchment outlet.

Composite Suspended Sediments (CSS) Sample Collection

Composite suspended sediments (CSS) were retrieved after each storm event from five passive samplers (Figure 3.1) located within the flowing channel of the stream (Figure 3.2). These samplers collected suspended sediment over the duration of the storm (composite sample) and allowed for comparison between different drainage locations.

CSS samplers (Figure 3.2) were made from a perforated PVC tube. The sampler was approximately two feet tall with 1/2 inch holes drilled into the pipe, in the pattern seen in Figure 3.2. There were PVC caps on both ends of the pipe. The bottom cap collected the POM and sediments transported during storm events, and the top cap prevented any other material from contaminating the sample. The samplers were anchored into the stream bed using rebar stakes, and the PVC was secured to the stake using metal gear hose clamps. During elevated flows, POM in the streamwater was captured in the sampler and settled to the bottom cap as illustrated in Figure 3.3.

CSS Sample Processing

CSS samples were recovered from the samplers within 24 hours of an event. The samples were frozen, then thawed and dried in an oven at 60°C. The samples were sieved into three discrete particle class sizes (Table 3.1) for further analysis. Once the samples were dried and sieved, they were stored frozen until further analysis.



Figure 3.2: Photo of Composite Suspended Sampler (CSS) apparatus at baseflow conditions. Note orange flag for scale.

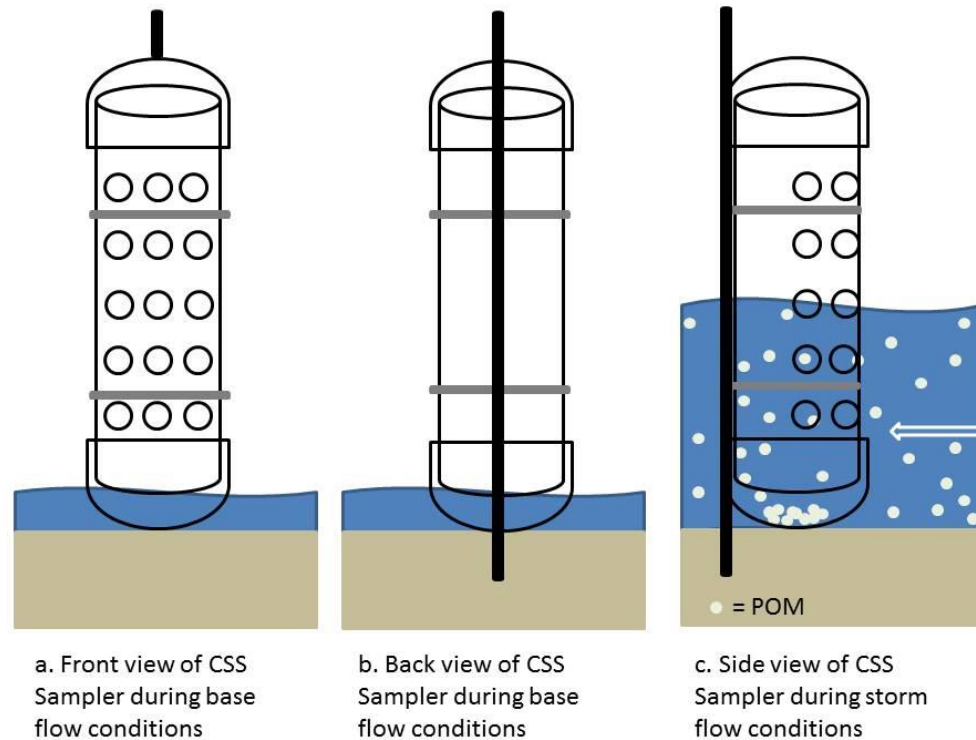


Figure 3.3: Schematic of composite sediment samplers (CSS). Panel (a) shows the front view of the sampler where the holes in the PVC pipe face upstream. At baseflow there is no water or POM being collected. Panel (b) shows a rear view of the sampler. Note that there are no holes on the back, and that the sampler is anchored with a stake into the stream bed and attached to the stake with metal gear clamps (grey horizontal lines). Panel (c) shows a side view of the passive sampler in action during a high flow event. POM and sediments can enter the holes and are retained within the PVC tube. POM and sediments settle to the bottom PVC cup due to a reduction in velocity. Samples are collected after storm flow has receded.

Table 3.1: The sediment samples were sieved into three discrete particle class sizes for analysis.

Sediment Size Fractions	
Coarse	>1 mm
Medium	1mm-250 μ m
Fine	<250 μ m



Figure 3.4: Sediment was sieved into three discrete size fractions using brass sieves. The percent weight for each size class was determined after sieving.

No widely accepted definition of “Coarse”, “Medium” or “Fine” POM existed in the literature and previous research has taken a liberal approach to defining size class. This study divides POM into three size classes to more accurately capture the heterogeneity between them. This remains consistent with many studies that define CPOM as $>1\text{mm}$, and has a more liberal definition of MPOM ($1\text{mm}-250\mu\text{m}$) and FPOM ($<250\mu\text{m}$). These divisions provide enough material in each size class in order to perform the majority of analyses on the material (Figure 3.4). These size classes also remain consistent with previous size class analyses performed in this watershed (Rowland et al. 2017).

3.2 Analyses

POM Extractions

In order to evaluate POM quality and composition using fluorescence, TOC/TN, $\text{NO}_3\text{-N}$, and $\text{NH}_4\text{-N}$ analyses, the POM was extracted into aqueous solution and the resulting extracted dissolved fraction was analyzed. Extractions were performed on the different particle size classes achieved through the sieving of the CSS and Sources.

Within the Sources, no significant differences were found in all extracted parameters between the size classes, using a standard least-squares regression, and therefore only bulk measurements were considered. $\text{NO}_3\text{-N}$ and $\text{NH}_4\text{-N}$ analysis was also not performed on the sources. The sieved sediments were ground with a mortar and pestle and 0.5 g of the ground sediment was placed into an amber glass vial with 40 ml of 0.2 μm -filtered streamwater. The sediment and streamwater mixture was placed on a reciprocating shaker for one hour at 150 rpm at room temperature and was then incubated at 4°C for 24 hours. The solution was filtered through a 0.7 μm Sterlitech GF/F filter into an amber glass vial and stored in the dark at 4°C until further analysis. This liberally follows the methodologies of Perdrial and Perdrial (2016) with a few notable differences, including the drying, sieving, and grinding of the material. Following Yoshimura et al. (2010), extraction with streamwater was used in order to realistically represent the interactions of POM and streamwater during storm events. After extraction three separate analyses were performed on the aqueous solution; (1) Fluorescence Spectroscopy, (2) TOC/TN analysis, and (3) analysis for $\text{NO}_3\text{-N}$ and $\text{NH}_4\text{-N}$.

Fluorescence Spectroscopy on POM leachates

The extracted solutions were analyzed using fluorescence spectroscopy which measured the fluorescent dissolved organic matter (FDOM) within the aqueous samples. A Horiba Aqualog ® fluorometer (Horiba, Kyoto, Japan) was used to produce fluorescence Excitation-Emission Matrices (EEMs). Samples were analyzed with an excitation wavelength range from 700-240 nm at 4 nm increments. The emission wavelengths were measured from 700-240 nm with an estimated interval of 4.66 nm. Several daily checks were performed to ensure consistent performance by the instrument including a manufacturer's excitation check, emission check, cuvette check, and Raman water scan. Additionally, post-processing steps were applied the Aqualog ® which

corrected for inner filter effects and applied 1st and 2nd order Rayleigh Masking with the sum of slit width set to 10. Post-processing was done in Matlab (Version R2015b V 8.6.0) where the absorbance and fluorescence data was used to create excitation emission matrices (EEMs). The EEMs were run through a PARAFAC model as described in Singh et al. (2013) and that information was used to calculate multiple quality metrics including %protein-like, %humic-like, and %fulvic-like fluorescence, as well as SUVA, which was calculated as the absorbance at UV wavelength 254 divided by the DOC(ppm).

TOC/TN analyses on POM leachates

The aqueous extracted samples were analyzed for total organic carbon (TOC) and total nitrogen (TN) on a Shimadzu TOC-L, TNM-L analyzer (Shimadzu, Colombia, MD) using catalytic thermal decomposition/chemiluminescence methods. The instrument measured TN as well as TOC using a TC-IC method. Before each run, initial cleaning steps and maintenance were performed to ensure the instrument baselines were correct. Standard curves were created for TC, IC, and TN for each run to ensure proper instrument area readings. Data were processed through standard QA/QC procedures to ensure their fit within the standard curve relationship.

Nitrate-N and ammonium-N on POM leachates

An AQ2 Discrete Analyzer (Seal Analytical, Mequon, Wisconsin) was used to analyze nitrate-N and ammonium-N in the extracted samples through a colorimetric method. The extracted POM samples were analyzed for nitrate and ammonium using the methods of EPA-127-A Rev 8 for nitrate-N and EPA-148-A Rev 2 for ammonium-N. Source samples were not analyzed. No significant trends were found between the events or size classes; therefore data are presented in Appendix A.

Percent Carbon, Nitrogen, and Isotopic Analysis (^{13}C and ^{15}N) for POM

The dried and sieved sediment (Table 3.1) was lyophilized for 24 hours, and then ground with a mortar and pestle. Based on estimated C and N content, an appropriate sample weight was calculated to ensure that the samples would fall within the detection range of the instrument. The sample was then placed into 5x9mm tin capsule (Costech, Valencia, CA). The capsules were sealed tightly and placed into a 96 well plate and stored in a desiccator until shipment for analysis. Samples were sent to the Duke Environmental Stable Isotope Laboratory (DEVIL) (Durham, NC) for isotopic analysis of ^{13}C and ^{15}N as well as %C and %N. These values were determined by coupled elemental analysis and isotope ratio mass spectrometry (EA-IRMS). The atomic C:N ratio was calculated from the %C and %N data.

Statistical analyses

Standard least squares regressions and ANOVAs were performed on the Source and POM data to compare differences in each of the variables by event and size class. Significant differences were tested using a Tukey HSD test. In addition, multiple linear regressions were performed on the some variables to control for differences in size class and drainage location. When significant, these were tested with a Tukey HSD test, and the significantly different variables were reported. Correlations were also performed to compare the relationship between the different compositional metrics. A correlation matrix (Figure A3) was created for all POM samples and is presented in Appendix A along with the p-values for the correlations (Figure A4).

Principal Component Analysis (PCA)

A principal component analysis was performed on for the Source and fluvial POM data using the variables of %C, %N, C:N, $\delta^{13}\text{C}$, $\delta^{15}\text{N}$, DOC, TN, %protein-like fluorescence, %humic-like fluorescence, and %fulvic-like fluorescence. A PCA was chosen due to the multicollinearity of the variables. The PCA has the ability to show the interrelationships between variables as each principal component is a linear combination of the original variables. For this analysis PC1 and PC2 are graphed, as the first two components explain the largest amount of variance in the samples. ANOVAs were performed on the first two principal components and, when significant, post hoc Tukey HSD tests were performed.

Chapter 4

RESULTS

4.1 Composition of POM in watershed sources

Characteristics of solid phase POM

Percent C and N were both lowest in the near stream sources such as the Stream Bed and Stream Banks, and increased gradually in the sources, with the highest amount found in the Forest Floor Humus and Litter (Figure 4.1, 4.2). This progressive increase in %C and %N was reflected in the C:N ratio, though not as distinctly (Figure 4.3). Forest Floor Litter vastly exceeded all of the other sources in terms of its carbon and nitrogen content. For all box and whisker plots presented, box edges represent the first and third quartiles with the horizontal line inside the box representing the median value. Whiskers represent points that fall outside the quartiles but are within 1.5 times the interquartile range.

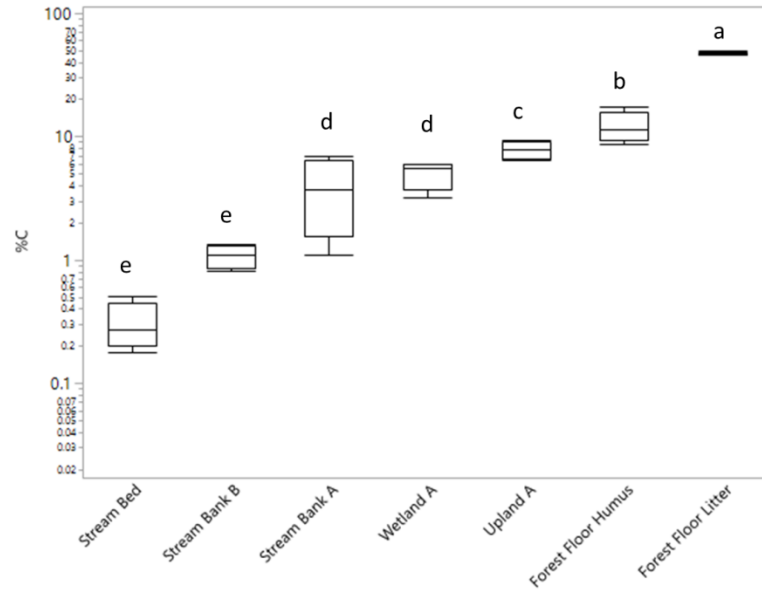


Figure 4.1: The percent carbon (C) values are presented for each of the seven watershed sources. Different letters indicate significant differences. Note that the axis has been placed on a log scale.

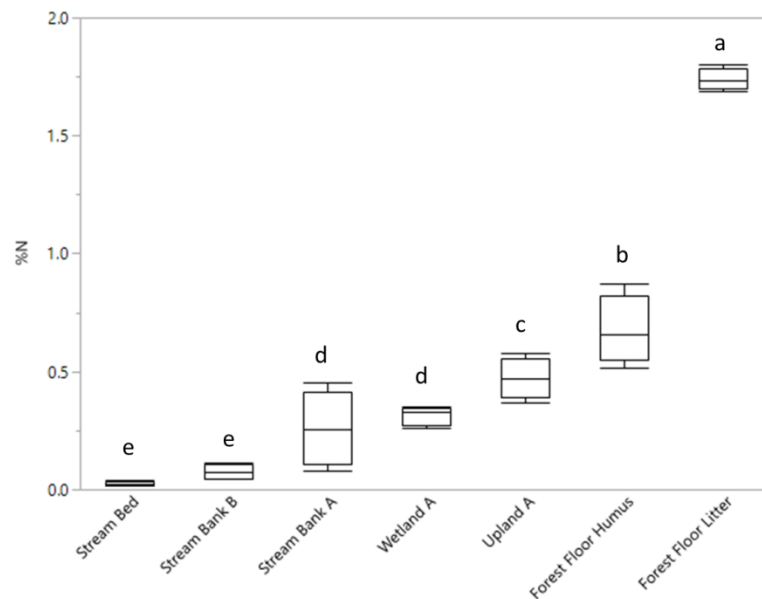


Figure 4.2: Percent nitrogen (N) values are presented for each of the seven watershed sources. Significant differences are indicated by different letters.

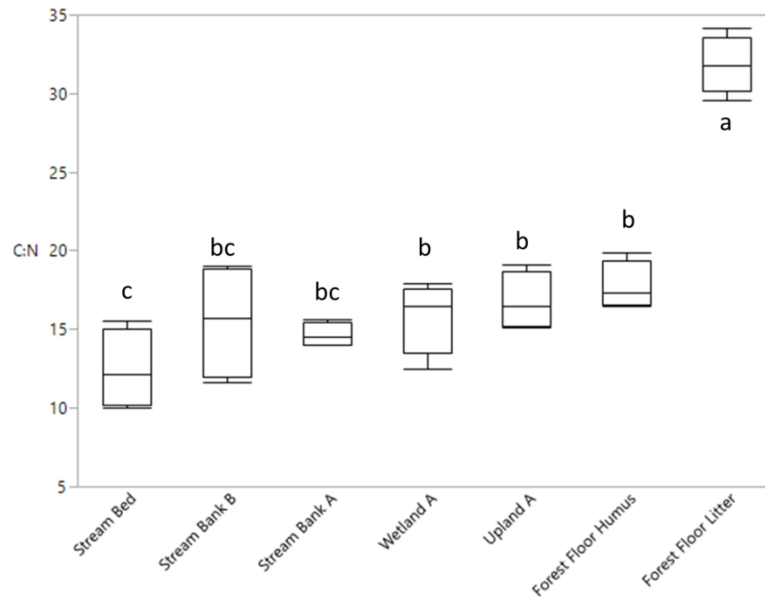


Figure 4.3: C:N ratio (atomic) values are presented for each of the seven watershed sources. Significant differences are indicated by the letters.

Most of the separation between isotopes occurred on the $\delta^{15}\text{N}$ axis (Figure 4.4). There was also separation of the sources on the $\delta^{13}\text{C}$ axis, but with smaller per mil changes. Forest Floor Litter contained the most depleted (most negative) $\delta^{15}\text{N}$ and $\delta^{13}\text{C}$ values, while the Stream Banks contained the most enriched (more positive) $\delta^{15}\text{N}$ and $\delta^{13}\text{C}$ values. The other sources were intermediate to these two extremes.

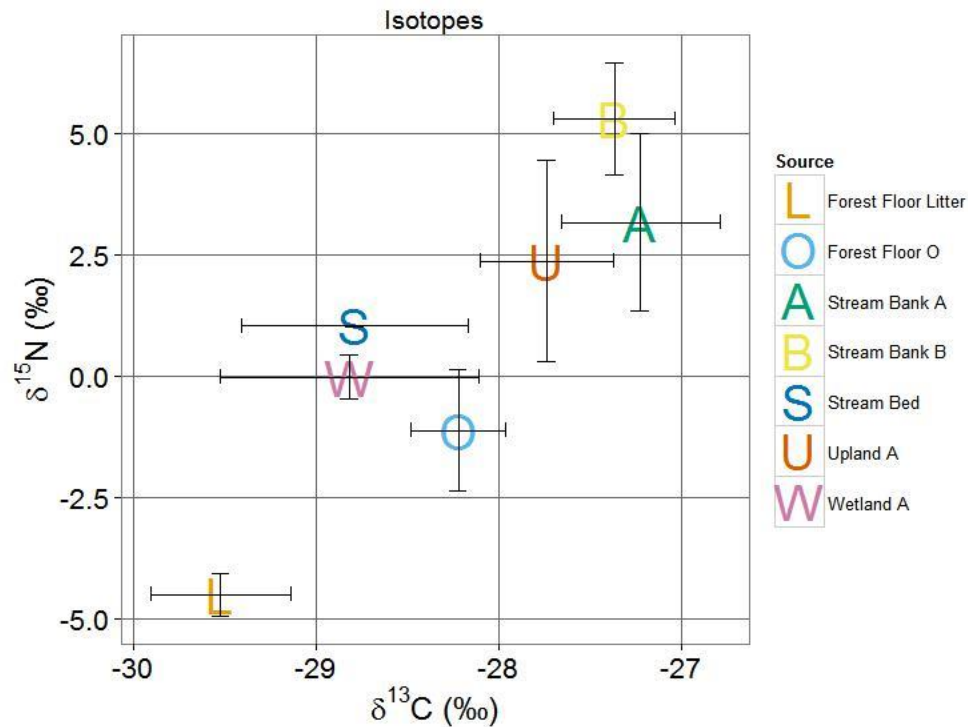


Figure 4.4: Isotopic separation of sources, based on $\delta^{15}\text{N}$ and $\delta^{13}\text{C}$. Sources are represented as an average value and error bars represent one standard deviation.

Characteristics of leached/extracted POM

DOC leached from the sources varied greatly by source, and was similar to the %C pattern, with some differences. In both solid and dissolved phases the Forest Floor Litter source overwhelmingly contained the highest amount of carbon, while the lowest was found in the Stream Bed. The other sources were intermediate and did not necessarily maintain the same order in the amount of DOC leached (Figure 4.5) as they did in the %C amounts (Figure 4.1).

The sources were also extracted by particle size class, however little distinction was found for leachate DOC concentrations between the size classes within each source. The results for DOC by size class showed no significant difference between size classes

within each source (Figure 4.6). This pattern was consistent for the other extracted concentrations such as TN and the fluorescence metrics and therefore the DOC pattern shown in Figure 4.6 serves as an accurate representation of this lack of separation in all other extracted metrics.

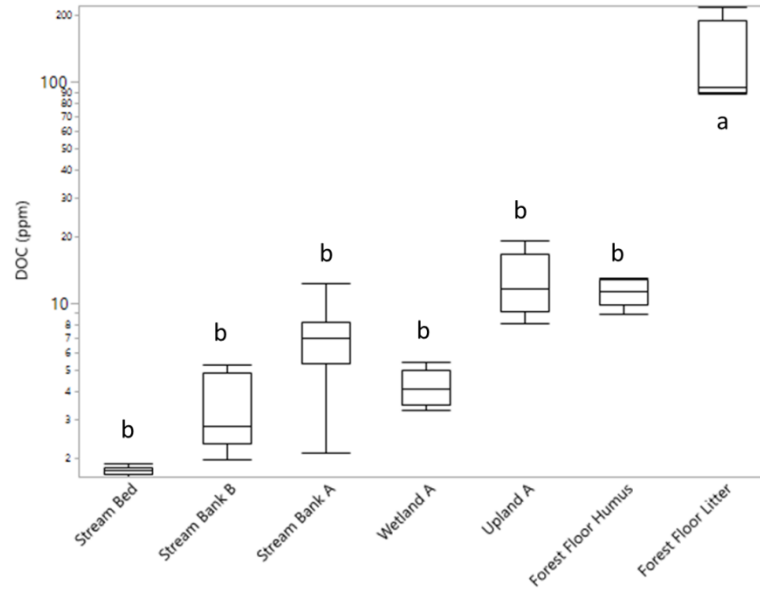


Figure 4.5: Dissolved organic carbon (DOC) values for each of the seven watershed sources. Note that the axis is on a log scale.

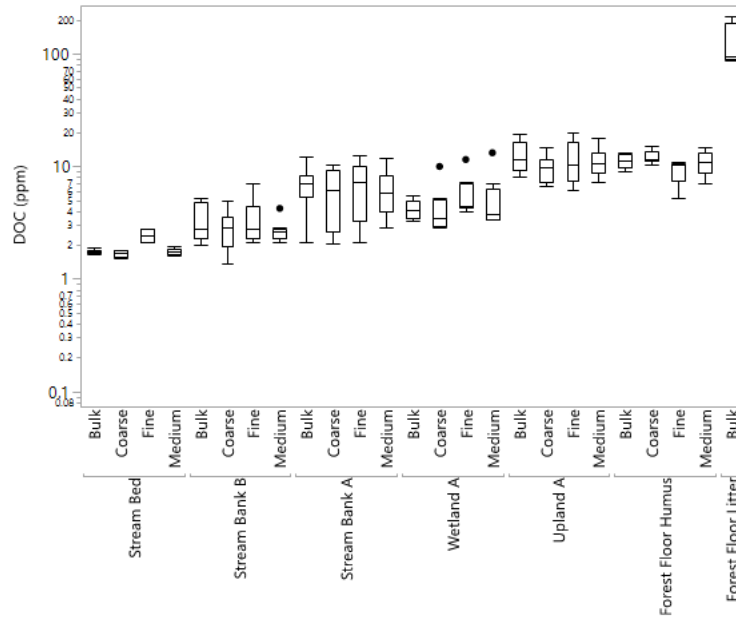


Figure 4.6: DOC values within each source, separated by size class. Note that the axis is on a log scale.

Similar to DOC (Figure 4.5), the Forest Floor Litter had significantly higher TN concentrations in the leached extracts compared to all other sources (Figure 4.7). The remaining sources did not follow the same pattern in both DOC and TN. For example, Stream Bed showed the lowest DOC but exceeded the TN in Stream Bank B, though not significantly.

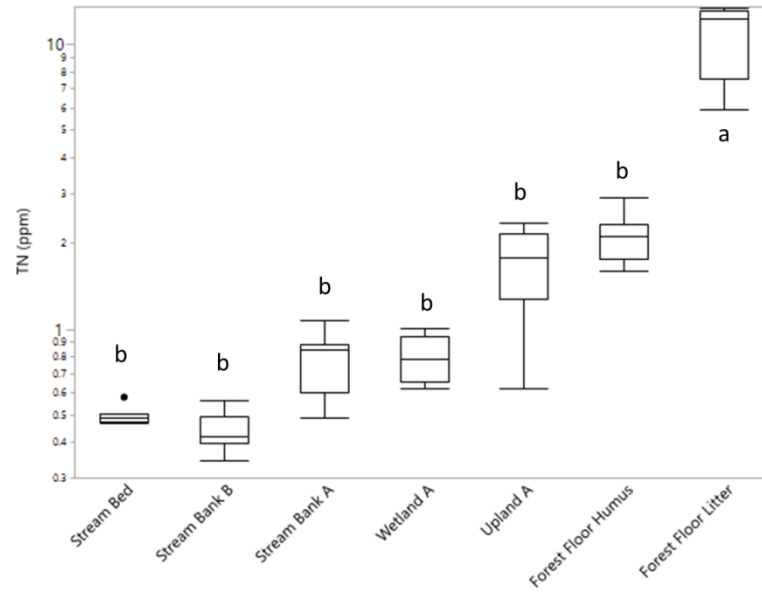


Figure 4.7: Total Nitrogen (TN) leached by all seven watershed sources. Note that the axis is on a log scale.

Fluorescence characteristics of leached POM sources

The percent protein-like fluorescence varied by source, with the highest values found in Forest Floor Litter, Forest Floor Humus and Wetland sources (Figure 4.8).

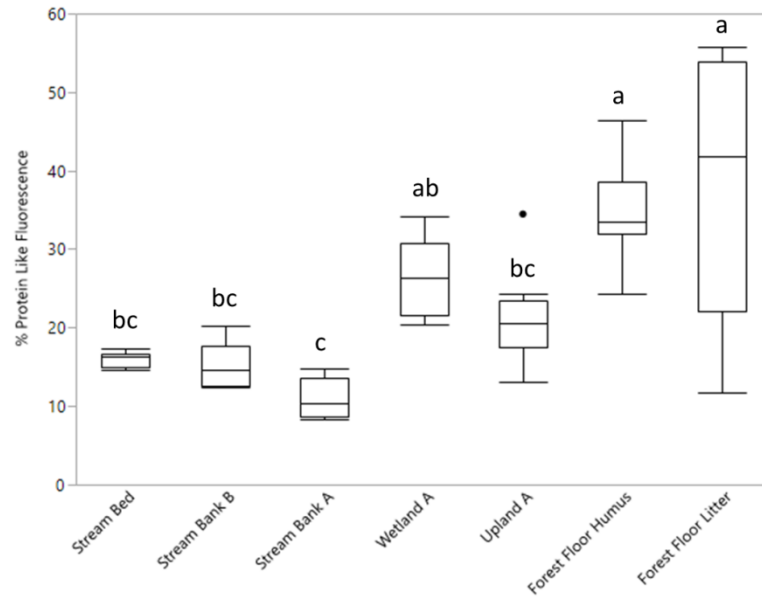


Figure 4.8: The percent protein-like fluorescence values presented for each of the seven watershed sources. Significant differences are indicated with letters.

Compared to protein-like material, there was a lack of notable trends within the humic-like fluorescence between the sources, though some significant differences existed (Figure 4.9).

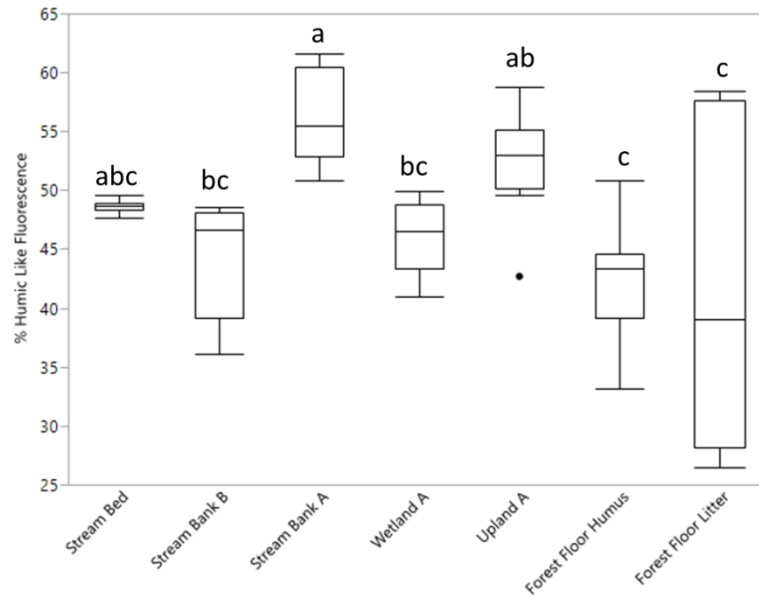


Figure 4.9: Percent humic-like fluorescence values for each of the seven watershed sources. Significant differences are noted by letters.

Percent fulvic-like fluorescence exhibited the strongest trend among the sources of the three quality components (Figure 4.10). This trend resembled the inverse pattern seen in the %C and %N data (Figure 4.1 and 4.2). Stream Bank B in particular stood out, exhibiting significantly higher values of fulvic-like fluorescence compared to all other sources, followed by Stream Bed and Stream Bank A, which were likewise significantly different from all other sources. In fact, all of the sources were significantly different from each other with the exception of Wetland A and Upland A.

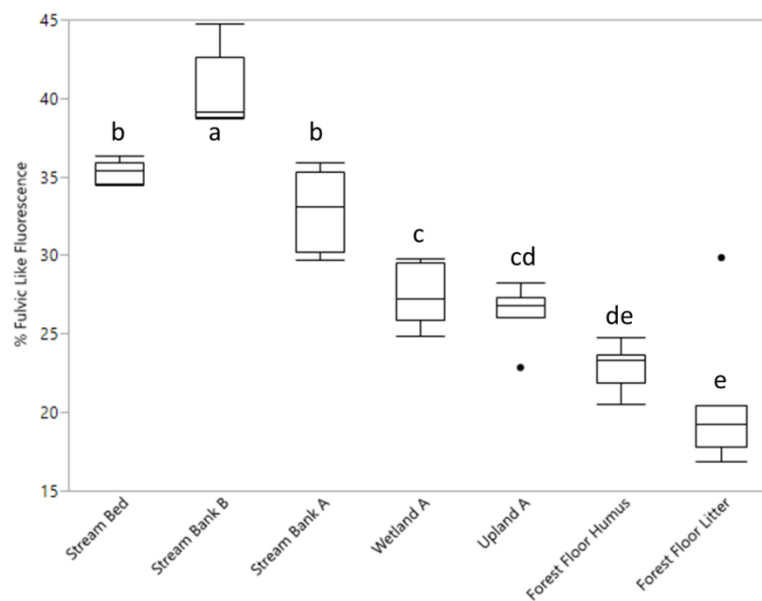


Figure 4.10: Percent fulvic-like fluorescence for all seven watershed sources. Significant differences are indicated with letters.

SUVA

The Stream Bed had the highest SUVA values and therefore was likely the most aromatic source while Forest Floor Litter exhibited the lowest SUVA values, indicating that the leachate from this source was likely the least aromatic (Figure 4.12).

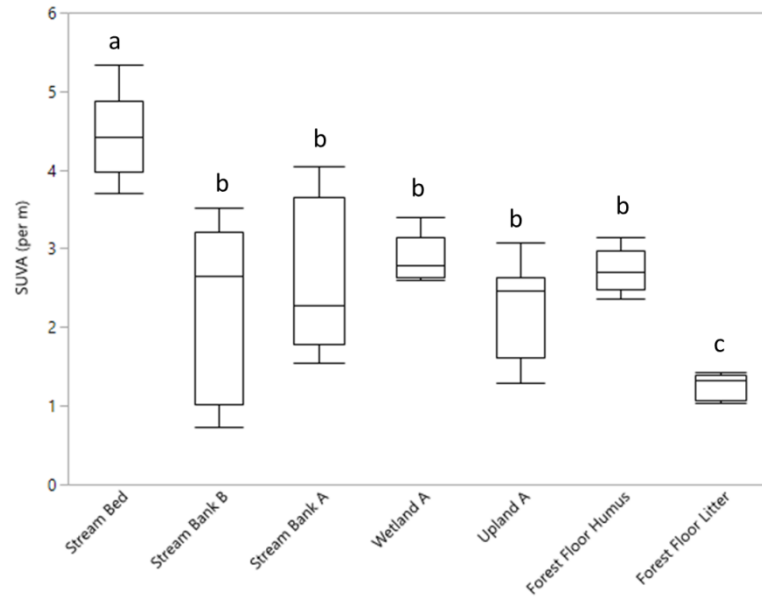


Figure 4.11: SUVA values for all seven watershed sources. Significant differences are indicated with letters.

DOC:TN (atomic)

The DOC:TN ratio was calculated to compare it to the solid phase C:N ratio (Figure 4.3). There was no distinct trend, though the Stream Bank did maintain the lowest ratio in both the solid and extracted analysis, and the Forest Floor Litter maintained the highest, though the variability increased in the extracted phase (Figure 4.12).

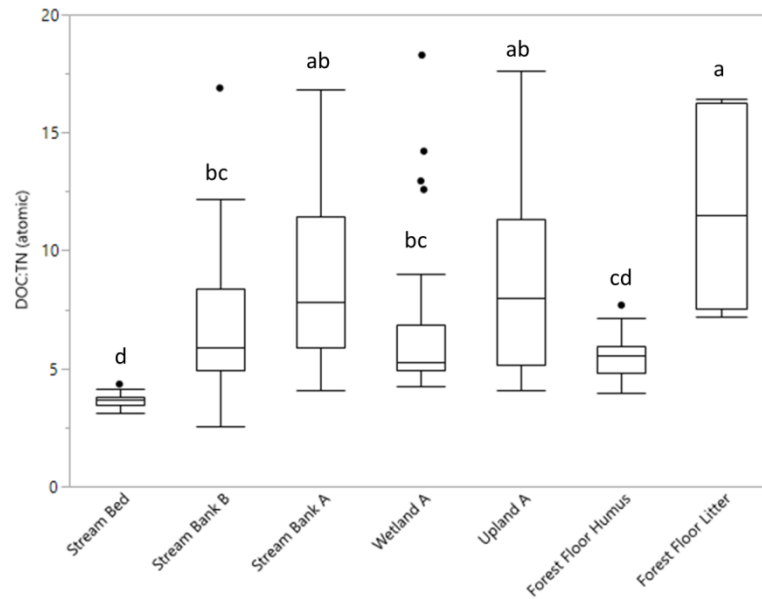


Figure 4.12: The DOC:TN ratio (atomic) is presented for all seven watershed sources. Significant differences are indicated with letters.

Storm Event Characteristics and fluvial sediment mass for the events

Five storm events were examined over the course of one year (2016) for this study. The storm events were seasonally distributed with two winter (December through February) and three summer (June through September) events, which varied in rainfall amount, duration, and intensity (Table 4.1, Figure 4.13). As indicated in Table 4.1 and Figure 4.13, the event of 2/24/16 generated the most rainfall, and was the second highest in intensity. Both winter events (2/16/16 and 2/24/16) were the longest duration while the summer event of 8/21/16 had the highest intensity. Generally, winter events seemed to be longer duration with similar rainfall amounts to the summer storms indicating that the overall intensity was lower, with the exception of the 2/24/16 event. These storm event characteristics were likely influenced by the convective nature of summer storm events and the frontal nature of winter events. The winter events in this study were atypical, and the 2/24/16 event produced the highest rainfall intensity compared to all

other winter storms recorded in the study watershed over the past 9 years. Precipitation during winter months generally comes as snowfall, however the events in this study occurred during the warmest winter on record globally to date for the contiguous U.S. (NOAA 2016). While average temperatures were higher, the temperatures were also more variable, and a “polar-vortex” influenced the mid-Atlantic region, with temperatures at the study location were below freezing for 11 days prior to the event (DEOS 2017).

Table 4.1: Storm event metrics for the five events examined in this study. API is the antecedent precipitation index, calculated as the total rainfall, in mm, for 7 or 14 days prior to the event.

Event	Season	Total	Duration	Max	API7	API14
Date		Precip.	(hr)	Intensity	(mm)	(mm)
		(mm)		(mm/hr)		
2/16/16	Winter	34.34	25	13.39	13.43	41.37
2/24/16	Winter	54.11	39	21.15	27.74	46.34
7/28/16	Summer	37.04	17	18.87	30.39	57.42
7/30/16	Summer	33.76	13	19.72	67.17	94.20
8/21/16	Summer	31.86	6	22.16	19.80	21.78

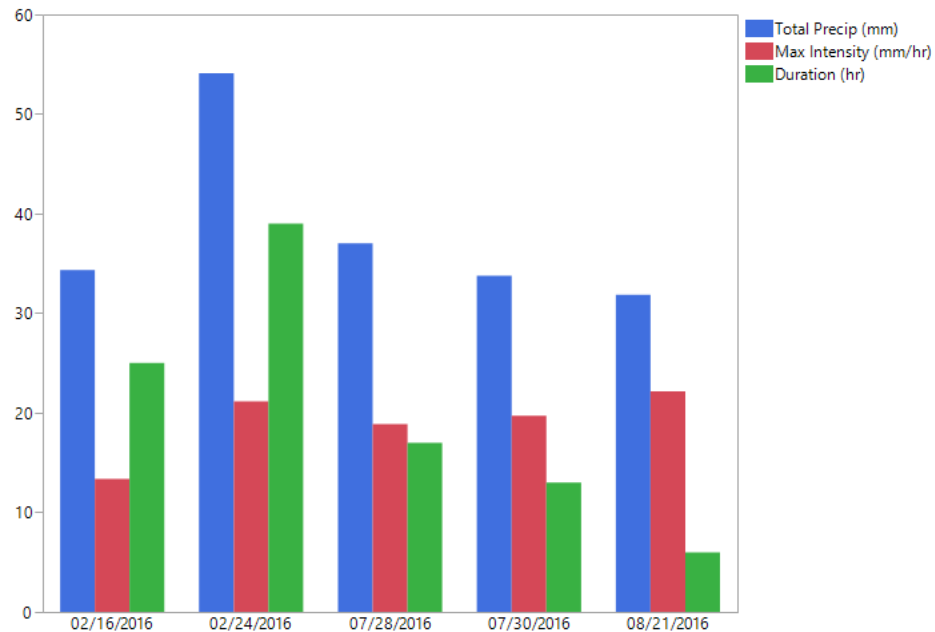


Figure 4.13: Storm event metrics showing total precipitation, maximum intensity, and duration of events

Additional differences in seasonality were observed in the amount of sediment that was collected in the stream sediment samplers. More sediment was collected in the stream samplers for the winter versus the summer events. The highest sediment mass collected was from the 2/24/16 event, and the lowest was from the 7/28/16 event (Figure 4.14). The 7/30/16 and 8/21/16 events generated similar amounts of material while the 7/28/16 event generated the least material (Figure 4.14, Table 4.2).

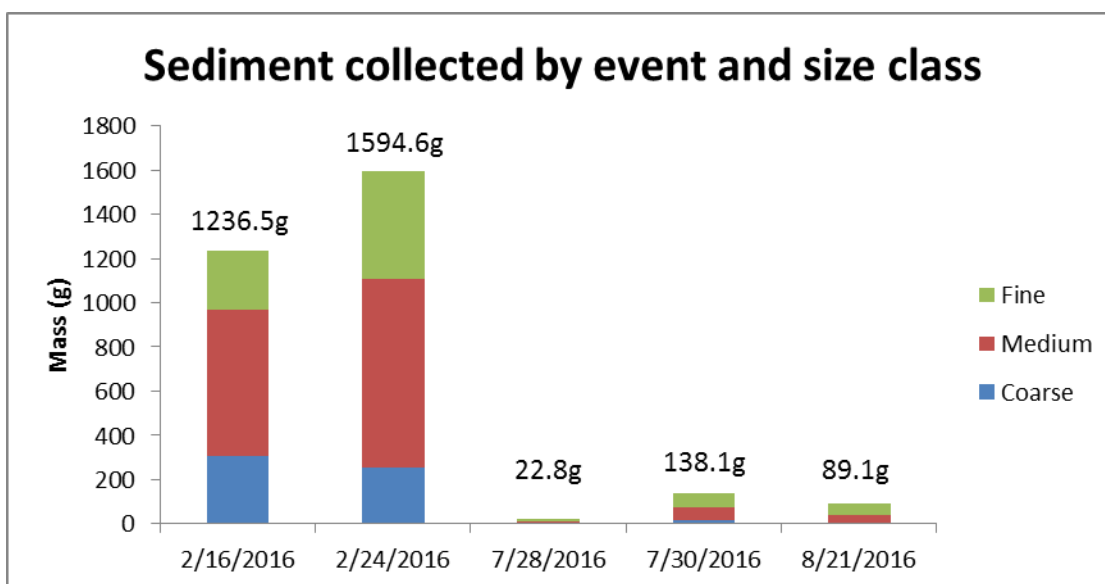


Figure 4.14: Sediment mass (g) collected from composite sediment samplers (CSS) for all events. Reported masses are a sum of all five sampling locations. The proportion of each size class collected is represented in the stacked bars.

Table 4.2: Amount of material collected (g), separated by size class for each event. All five CSS locations were summed for these calculations.

Event	Mass (g)	Mass (g)	Mass (g)	Total Mass
	Coarse	Medium	Fine	(g)
2/16/16	305.1	660.2	271.2	1236.5
2/24/16	251.9	853.2	489.5	1594.6
7/28/16	2.2	8.4	12.2	22.8
7/30/16	15.6	59.5	63.0	138.1
8/21/16	6.7	32.6	49.8	89.1

While the total sediment mass collected differed greatly between the storm events, the percent distribution of sediment mass among the particle size classes displayed

interesting trends (Table 4.3, Figure 4.15). The winter events (Figure 4.15a, 4.15b) were dominated by the Medium sediment size class with less material from both the Coarse and Fine sediment size classes. The summer events (Figure 4.15c, 4.15d, 4.15e) showed a different pattern of export. The Fine sediment size class dominated the mass in summer events, followed by the Medium size class. When comparing among the winter events (Figure 4.15a, 4.15b) in terms of the size fractions, the 2/24/16 event produced slightly smaller percentage of Coarse material and slightly higher percentage of Fine material. Both winter events generated nearly equal percentages of Medium material. The summer events (Figure 4.15c, 4.15d, 4.15e) generated similar percentages of sediment by size class. While the absolute sediment mass differed, the 7/28/16 and 8/21/16 events generated similar percentages for all size classes. The 7/30/16 event generated slightly more Coarse and Medium sediments and slightly less Fine sediment compared to the other two events, though these differences were not significant.

Table 4.3: Percent distribution of sediment within each particle size class for the storm events. All five CSS sites were summed and averaged to get a whole event composite. Percentages were calculated from this average.

Event	%Coarse	%Medium	%Fine
2/16/16	24.7	53.4	21.9
2/24/16	15.7	53.2	31.1
7/28/16	9.7	36.8	55.5
7/30/16	11.3	43.1	45.6
8/21/16	7.5	36.6	55.9

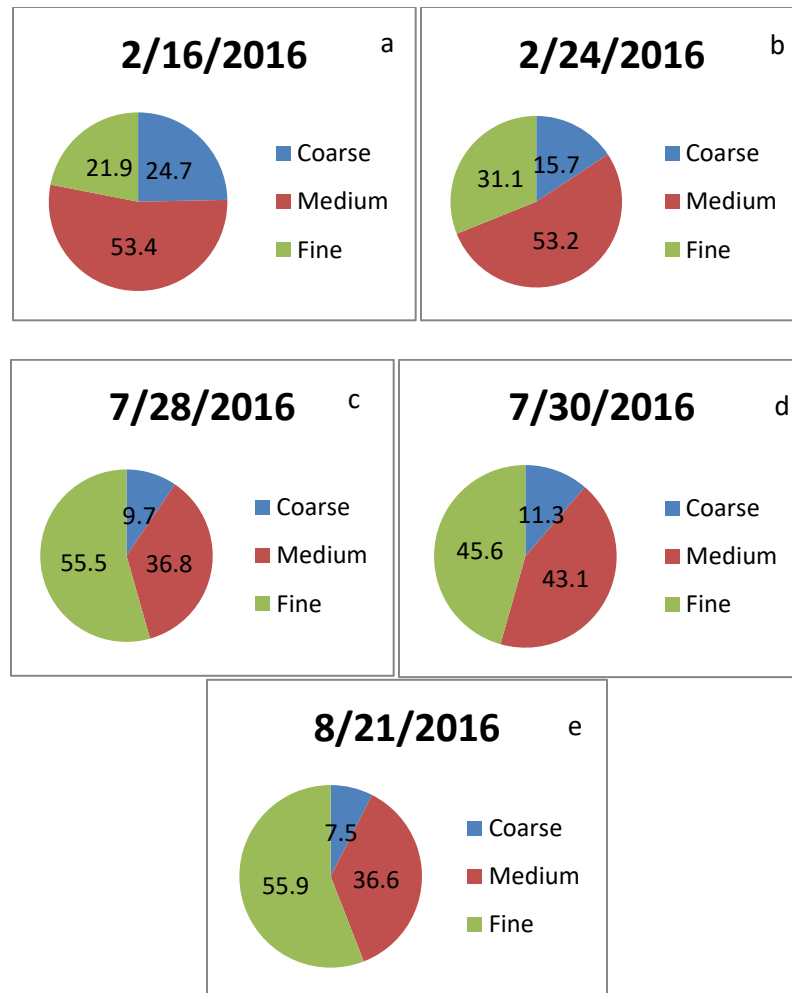


Figure 4.15a-e: Percentage of sediment in the three particle size classes for individual storm events. Samples from all CSS sites were summed to generate an event average.

Fluvial Particulate organic carbon (POC) and Particulate Nitrogen (PN)

The amount POC (Figure 4.16) and PN (Figure 4.18) for each event followed the general trend of the total sediment mass collected (Figure 4.14) with the winter events generating the highest mass, POC, and PN. Proportionally, the summer events contained more POC and PN rich material which was likely driven by the POC and PN rich Coarse material. For example, in the 8/21/16 event, the Coarse material made up 7.5% of the

total mass collected, but contributed 27.4% of the POC, indicating that it was carbon rich. This trend was seen in all of the events.

When comparing the PN generated by size class (Figure 4.19a-e) with the POC (Figure 4.17a-e) there were some contrasting patterns. The PN contribution was greatest in the Fine size class, ranging between 45 and 55% of the PN in all storm events, while the POC amounts were distributed more evenly across the size classes.

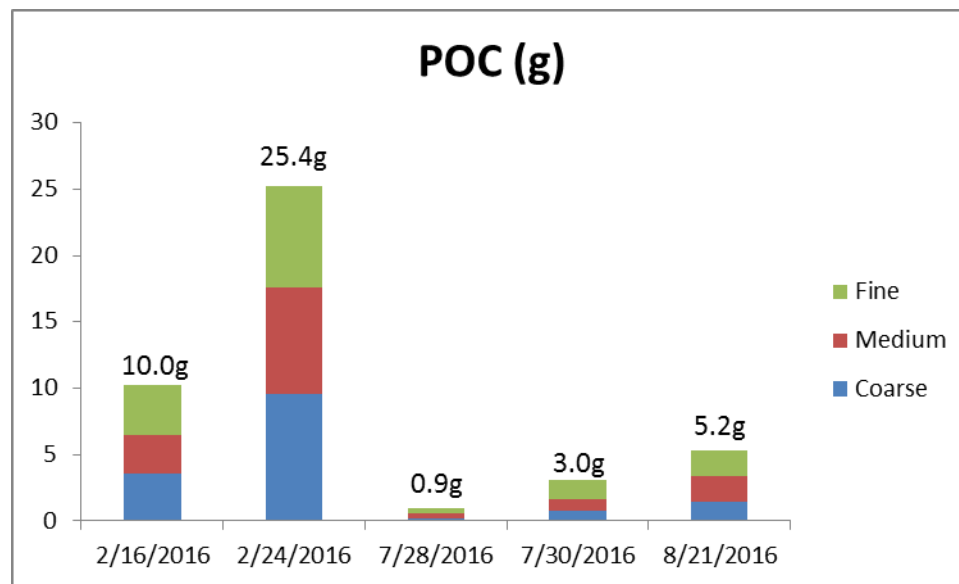


Figure 4.16: Particulate organic carbon (POC) generated by each of the events, separated by size class. This trend was driven by the amount of material generated (Figure 4.3).

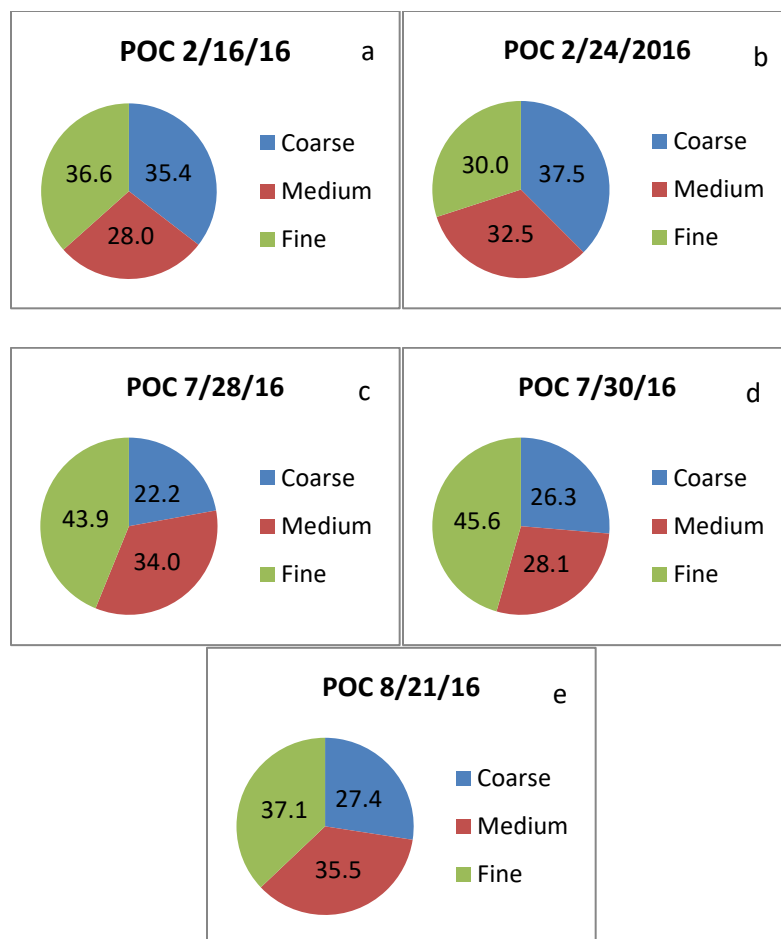


Figure 4.17a-e: Particulate organic carbon (POC) percent contributed by size class. All CSS sampling locations were summed and percent contributions of each size class were calculated from the total.

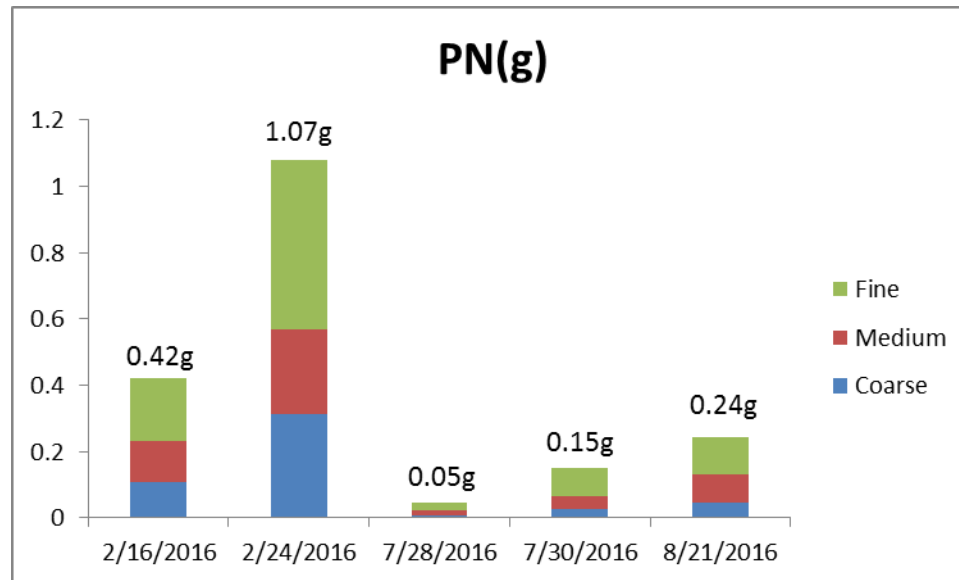


Figure 4.18: Particulate Nitrogen (PN) by size class for each event. All CSS sampling locations were summed and percent contributions of each size class were calculated from the total. This trend was partially a function of the amount of material generated (Figure 4.14).

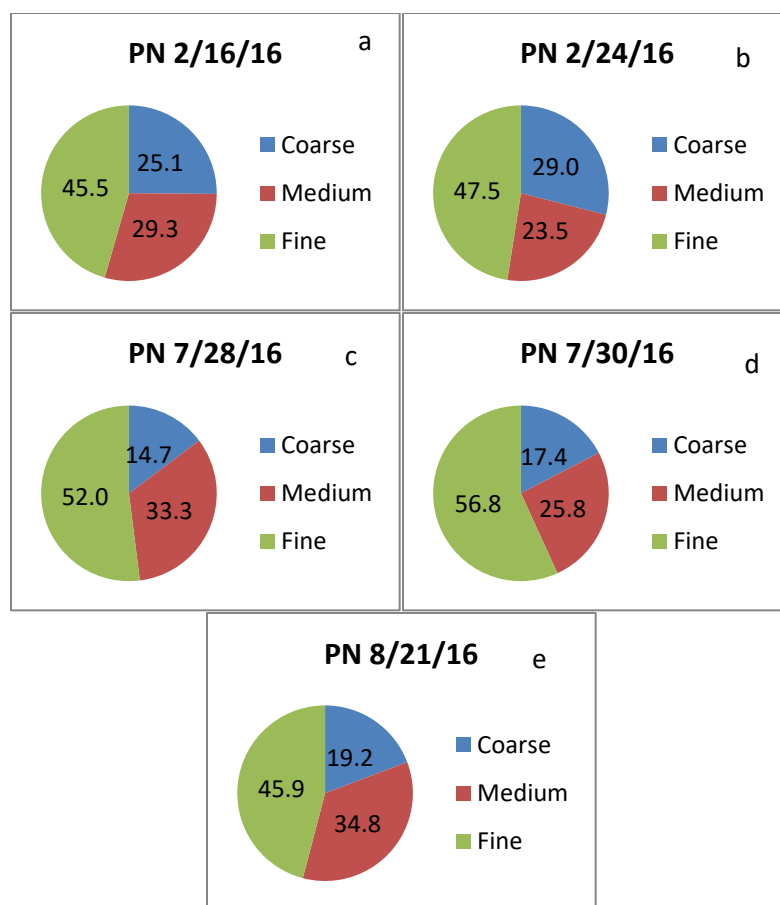


Figure 4.19: Percent PN contributed by each size class. All CSS sampling locations were summed and percent contributions of each size class were calculated from the total.

4.2 Differences in fluvial POM for storm events and particle size class

%C and %N by Event

The %C and %N of POM for the summer events was significantly higher compared to the winter events. A multiple linear regression showed that drainage location and size class were both significant predictors of % C and %N. A Tukey HSD test showed that the summer events were significantly more C and N rich compared to the winter events. This adjusted R^2 for the %C model was 0.74, and the adjusted R^2 for the %N model was 0.76. There was a wider range in the summer events due to the strong

separation between the three size classes. The outlier points in the winter events are the Coarse size class (Figure 4.20).

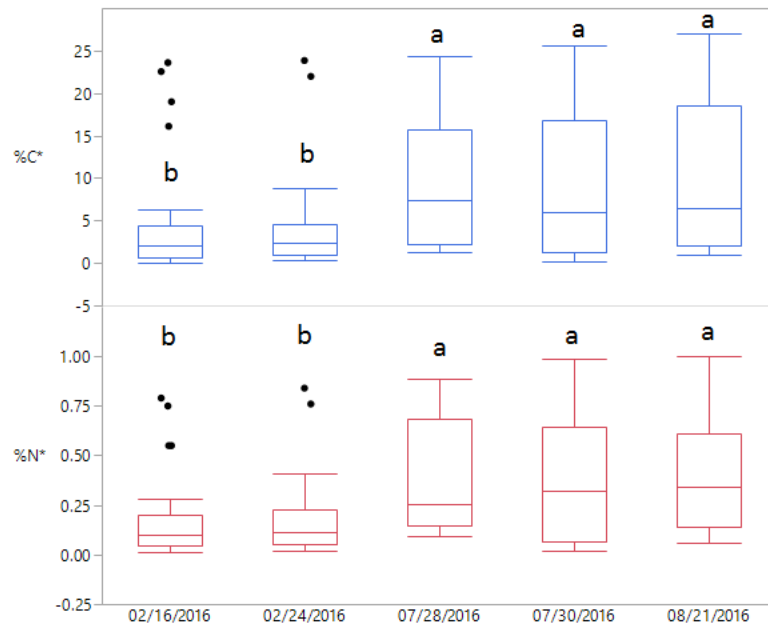


Figure 4.20: Percent C and %N values by event are presented. Significant differences are indicated by letters.

%C and %N by Particle Size Class

Evaluating %C and %N by size class, a Tukey HSD showed that the Coarse material had significantly higher C and N content compared to the other two size classes. Material from all of the events was used to calculate this, and the relationship between size classes remained consistent within individual events (Figure 4.21).

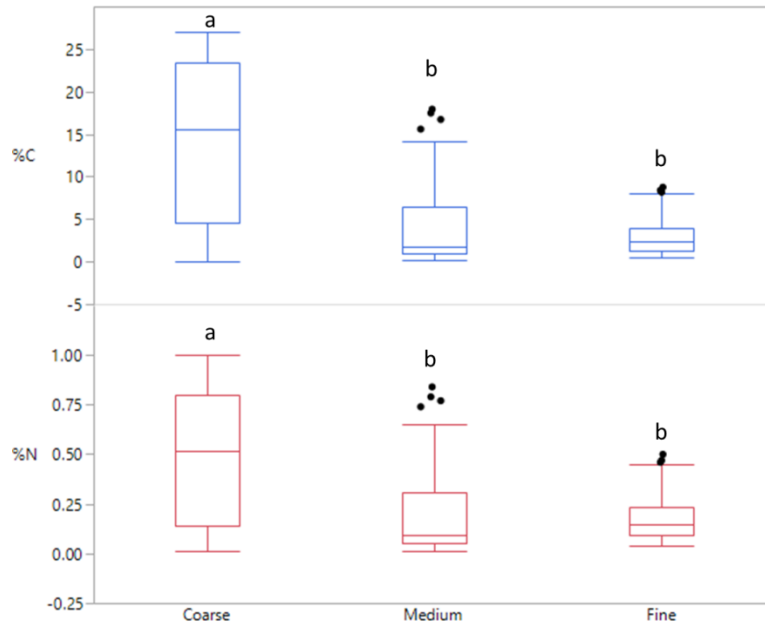


Figure 4.21: Percent C and %N presented by size class. Significant differences are indicated by letters.

Atomic C:N ratio by Event and Size Class

While carbon and nitrogen differed significantly by event, these trends were not apparent when examining the C:N ratio. The C:N ratio between all events appeared to be similar, and was driven primarily by the differences in size class. A few significant differences were found; specifically the C:N ratio for the 8/21/16 event was significantly different from the corresponding values for the 2/24/16 and 7/28/16 events. Though, the difference between the 8/21/16 and 7/28/16 event may be an artifact of the low amount of material that was collected from that event which did not generate samples at all locations (Figure 4.22). Differences in the C:N ratios were most notable between the size classes which showed significant differences between all size classes (Figure 4.23).

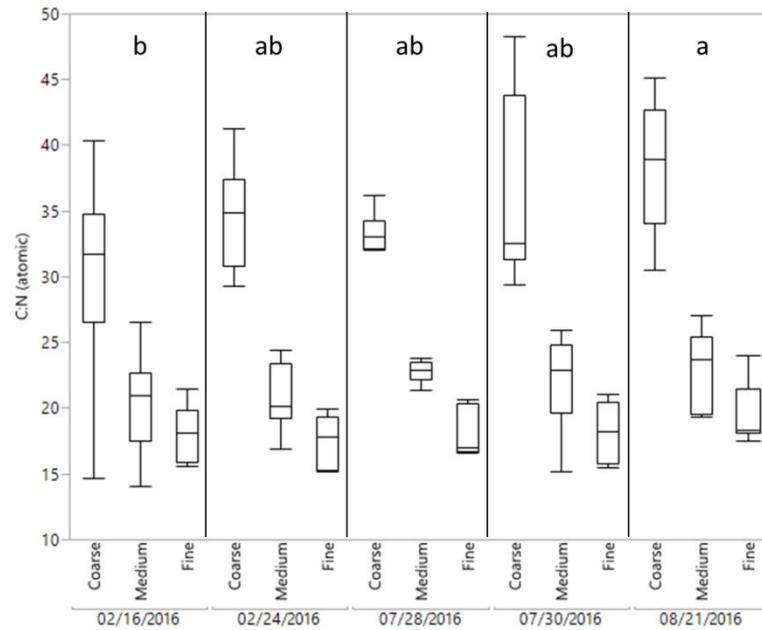


Figure 4.22: C:N ratio separated by event and size class. Significant differences are indicated by letters.

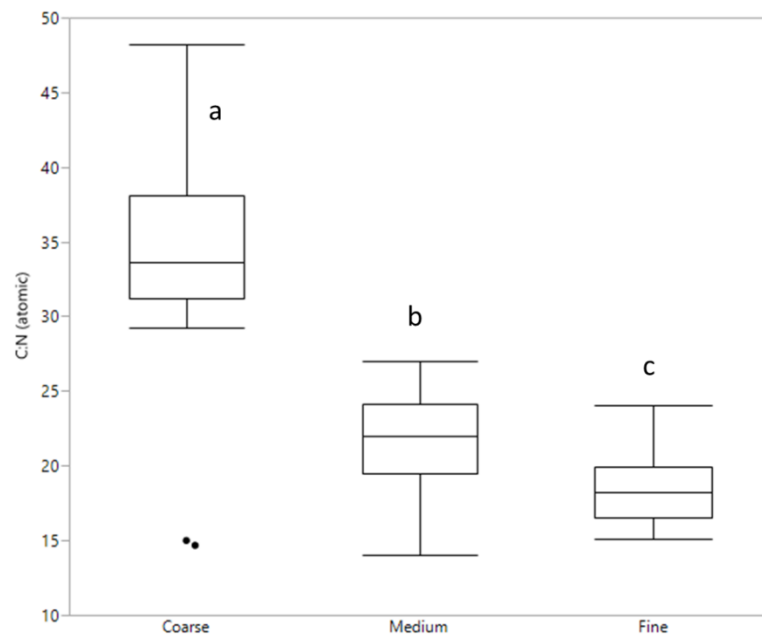


Figure 4.23: C:N ratio presented for each of the three size classes. Significant differences are indicated by letters.

Isotopes ($\delta^{15}\text{N}$ and $\delta^{13}\text{C}$)

Isotopic values for the POM samples showed the strongest separation by size class (Figure 4.24). This separation was most notable on the $\delta^{15}\text{N}$ axis. The Fine material was more enriched in the heavy isotope, giving it a more positive $\delta^{15}\text{N}$ value. A Tukey HSD showed that there were significant differences between all of the size classes, with the Fine material being the most enriched, and the Coarse material being most depleted (Figure 4.25). No significant patterns were found between events.

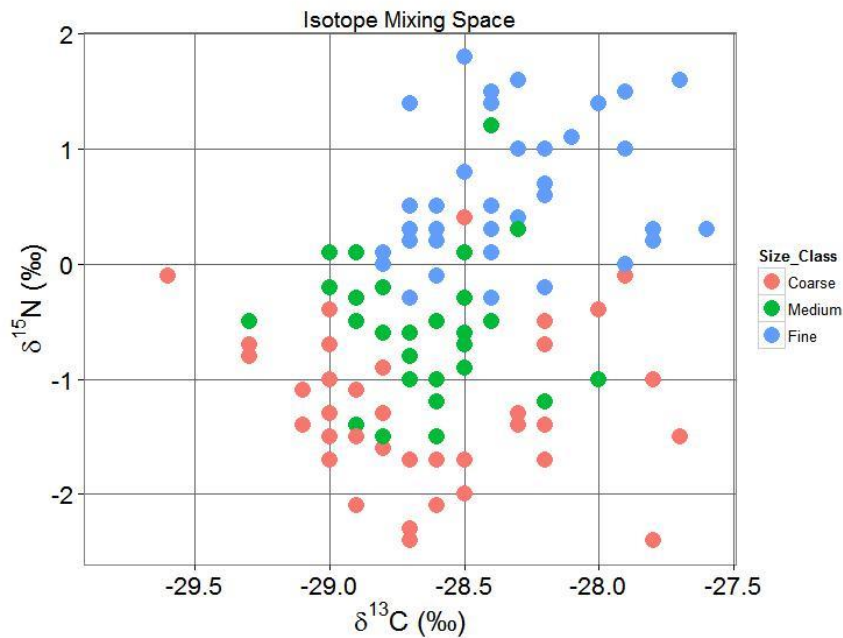


Figure 4.24: $\delta^{15}\text{N}$ and $\delta^{13}\text{C}$ mixing space shows separation between the sizes classes on the $\delta^{15}\text{N}$ axis.

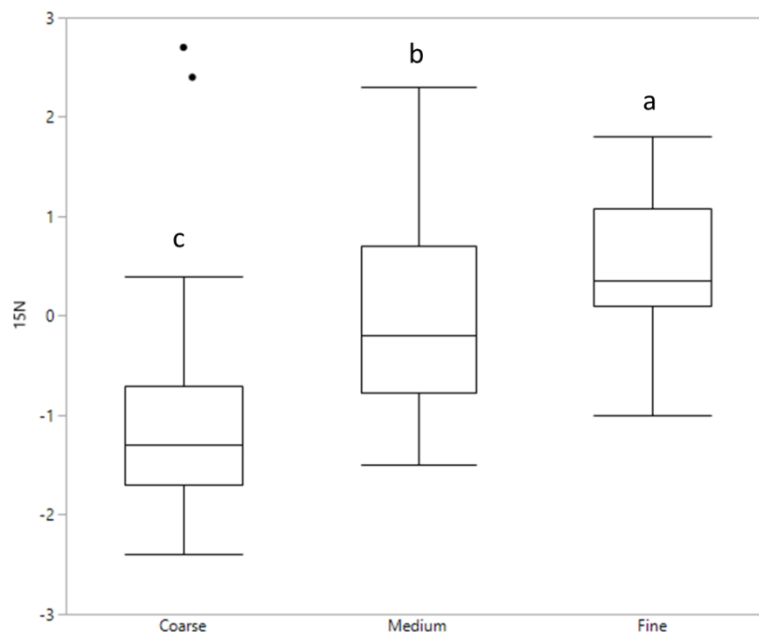


Figure 4.25: Isotopic values for $\delta^{15}\text{N}$ are presented by size class. Significant differences are indicated by letters.

Dissolved Organic Carbon (DOC)

DOC extracted from fluvial POM exhibited trends by both size class and event. A multiple linear regression was performed to analyze DOC by event, while controlling for size class and location. The results from this test indicated that generally, the winter events, on a per mass basis, yielded less DOC compared to the summer events. The only relationship that was not significant was between the 7/30/16 event and the 2/24/16 event. The adjusted R^2 for this model was 0.68. As seen in Figure 4.26 the higher DOC leached from the 8/21/16 event, compared to the other events, except the 7/28/16 event. When examining size class, the Coarse material exhibits significantly higher DOC compared to the Medium and Fine material (Figure 4.28).

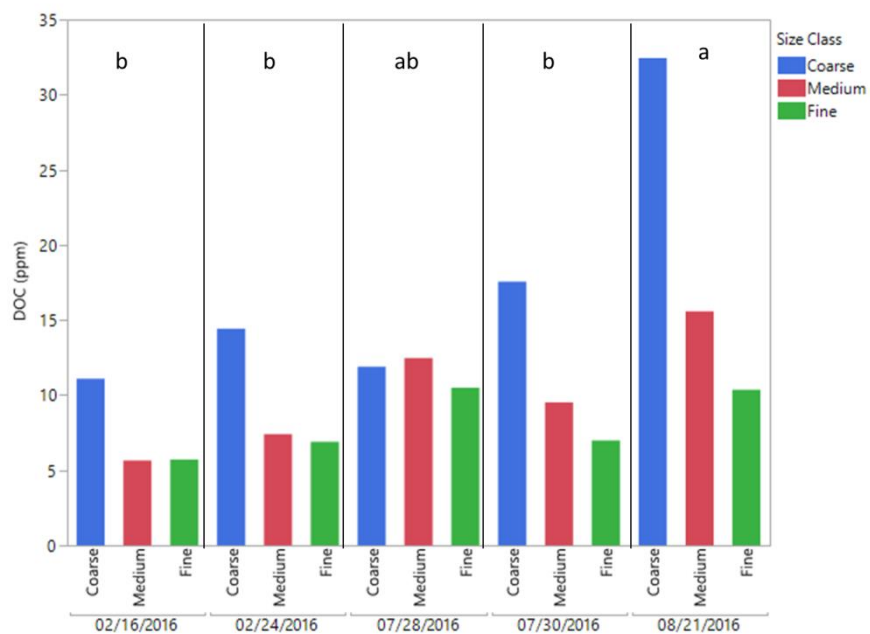


Figure 4.26: Average DOC concentration leached from each size class by event. Significant differences are indicated by letters.

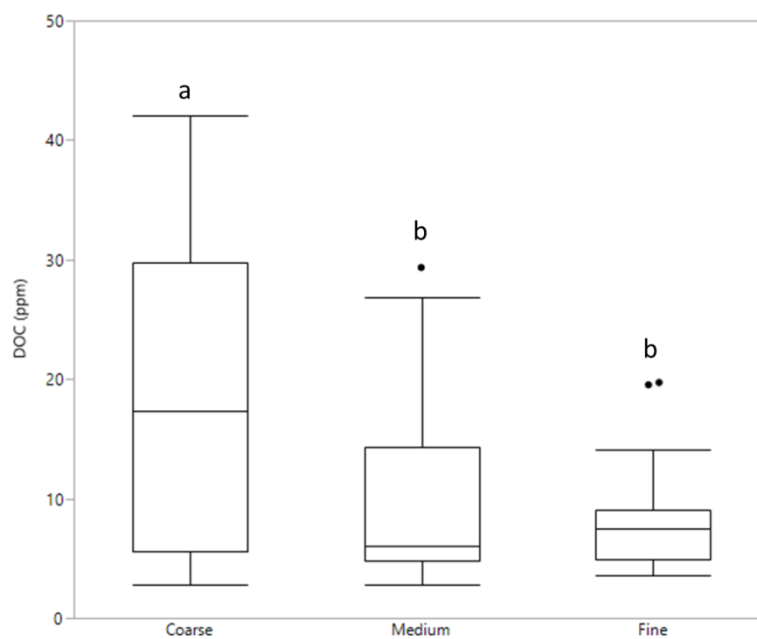


Figure 4.27: DOC amounts leached from different size classes of POM. Significant differences are noted by letters.

Taking the DOC analysis one-step further, the relative contribution of each size class based on the mass that was collected in the CSS samplers was calculated. This was done with the assumption that the samplers provided an accurate representation of the distribution of size classes moving during each event. By measuring the DOC concentration for a known mass, and multiplying that concentration by the total mass collected, allowed for a better understand which size classes may be most influential in their contribution to the total DOC (Figure 4.28).

Some interesting patterns emerged for the Coarse size class during summer events. Specifically, in the 7/30/16 and 8/21/16 events, approximately 10% of the mass (Figure 4.15d, 4.15e) contributed nearly 20% of the total DOC (Figure 4.28d, 4.28e). This indicated that the Coarse POM from the summer events was more carbon-rich than the other size classes and was also more carbon rich than the Coarse material from the winter events. The Medium size class dominated both the amount of mass, and likewise the amount of DOC produced.

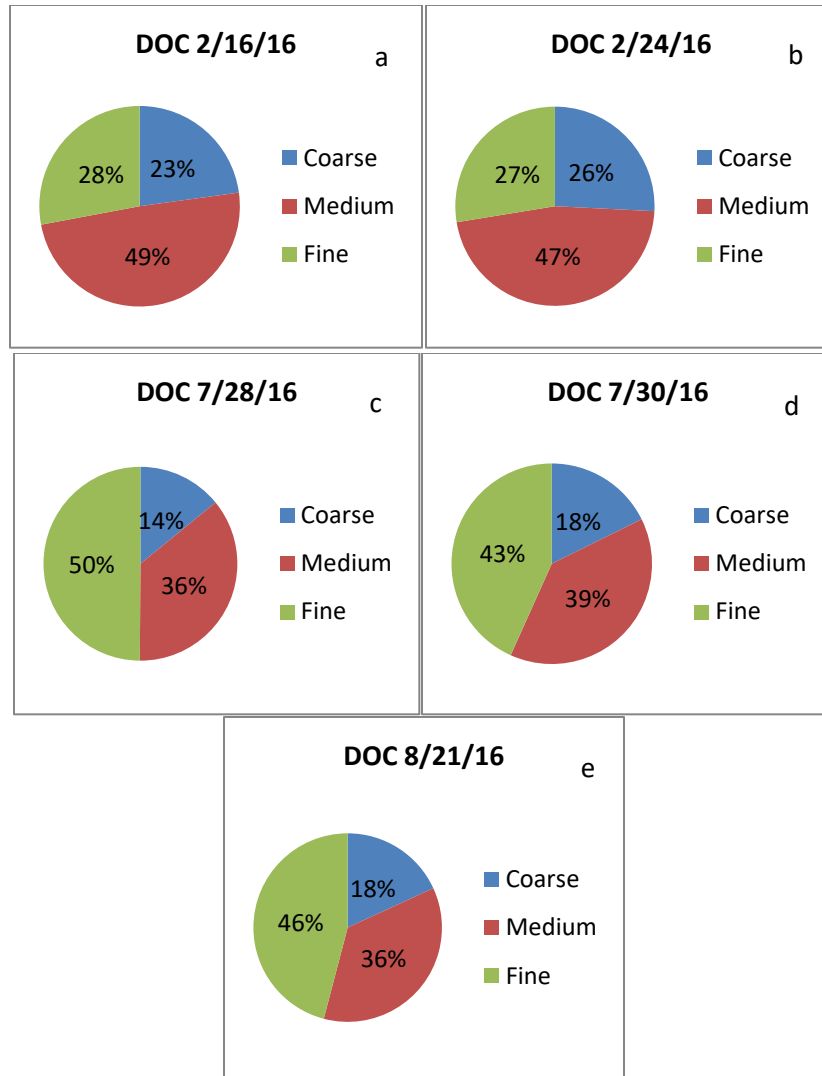


Figure 4.28a-e: DOC was leached from 0.5g of each size class. The DOC concentration obtained was multiplied by the total sample mass (Table 4.2) and the percent contribution was calculated to better understand the DOC contribution from each size class, for each event.

Total Nitrogen (TN)

Similar to the DOC results, the Coarse size class generally leached the most TN. A multiple linear regression for TN by event was run, controlling for size class and location, found that the 8/21/16 event was significantly higher in TN compared to both winter events (Figure 4.29). Contrary to the DOC results, the Fine material in some cases

leached as much or more than the Medium, though the relationship was not significant (Figure 4.30).

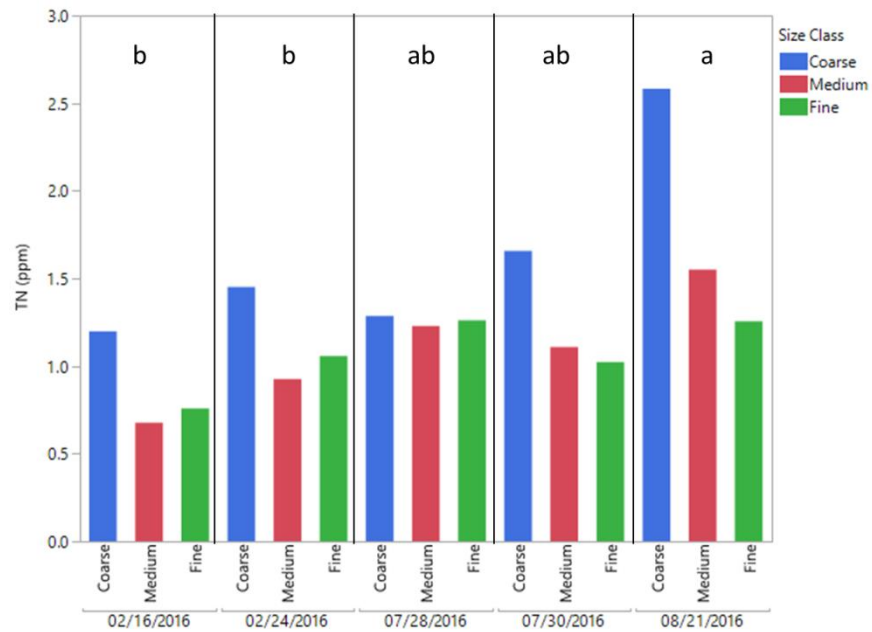


Figure 4.29: Average TN concentration leached from each size class, for each event. Significant differences are indicated by letters.

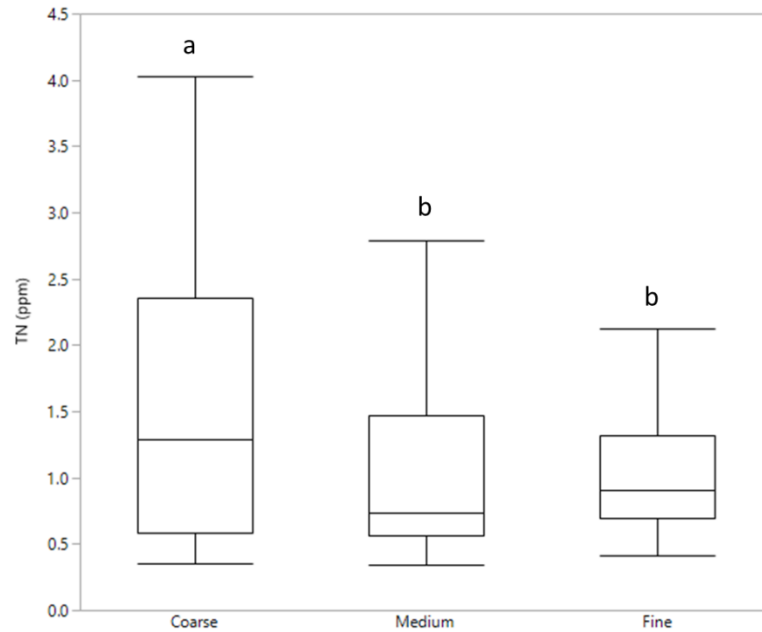


Figure 4.30: TN concentrations by size class are shown, and significant differences are indicated by letters.

Similar to DOC, the TN analysis was taken one-step further, by calculating the relative contribution of each size class based on the mass collected in the CSS sampler, with the assumption that this represented the distribution of size classes transported during an event (Figure 4.31). Interestingly, in the 8/21/16 event there was a large discrepancy between the percent of DOC (36%) (Figure 4.28e) and TN (51%) (Figure 4.31e) attributed to the Medium size class. The other events were more consistent between these two metrics across size classes and events.

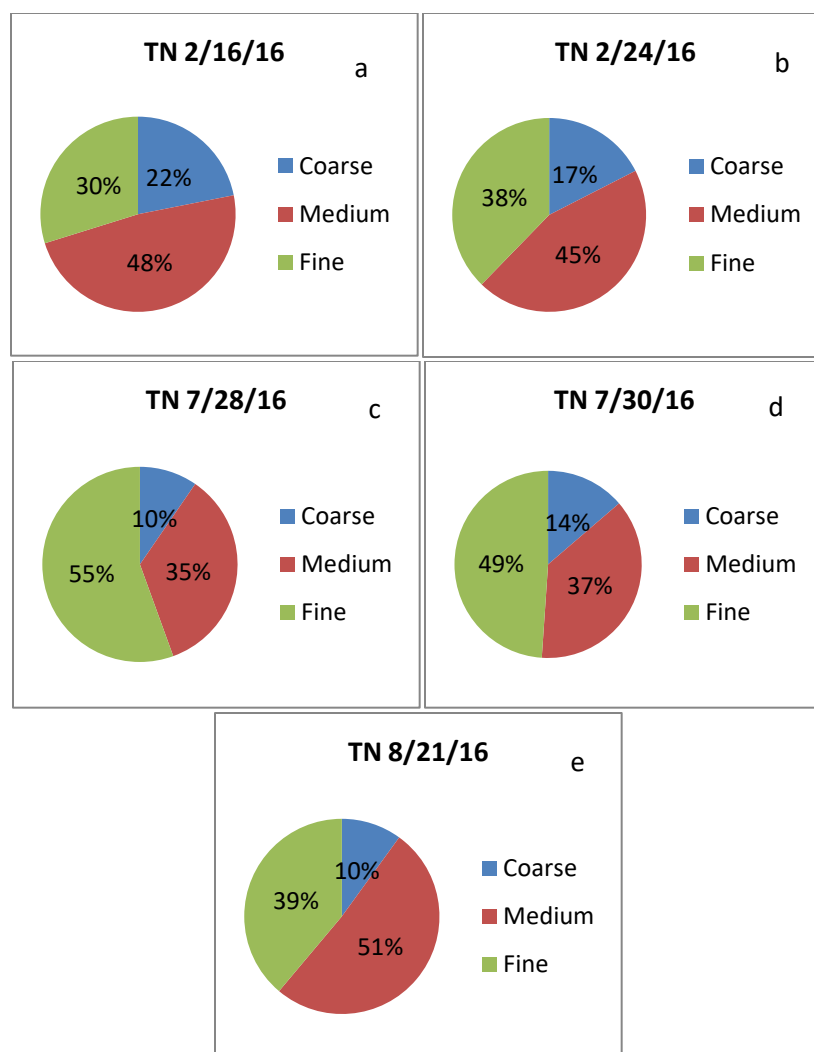


Figure 4.31a-e: TN was leached from 0.5g of each size class. The TN concentration obtained was multiplied by the total sample mass (Table 4.2) and the percent contribution was calculated to better understand the TN contribution from each size class, for each event

Fluorescence parameters

Examining the %protein-like fluorescence showed differences in the composition of material by event. A multiple linear regression was performed for %protein-like fluorescence, while controlling for size class and location. A Tukey HSD showed that the 2/24/16 event had significantly lower %protein-like fluorescence compared to all other events (including the 2/16/16 event). The 2/16/16 event was also significantly

lower than the 7/28/16 and 8/21/16 events but not the 7/30/16 event (Figure 4.32). The size classes were all significantly different from each other, with Coarse showing the highest %protein-like fluorescence, and Fine showing the lowest (Figure 4.33).

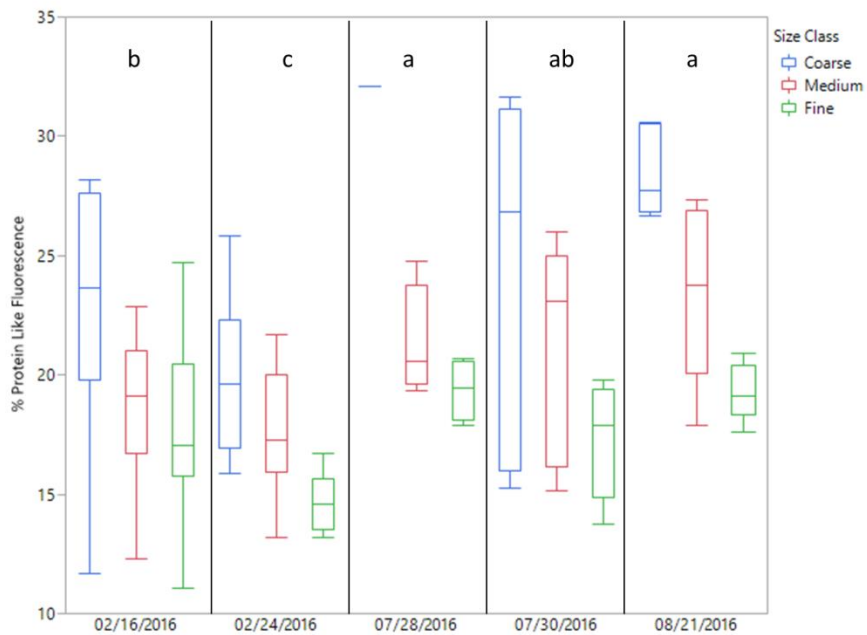


Figure 4.32: Protein-like fluorescence values are presented by event and size class. Significant differences are indicated by letters.

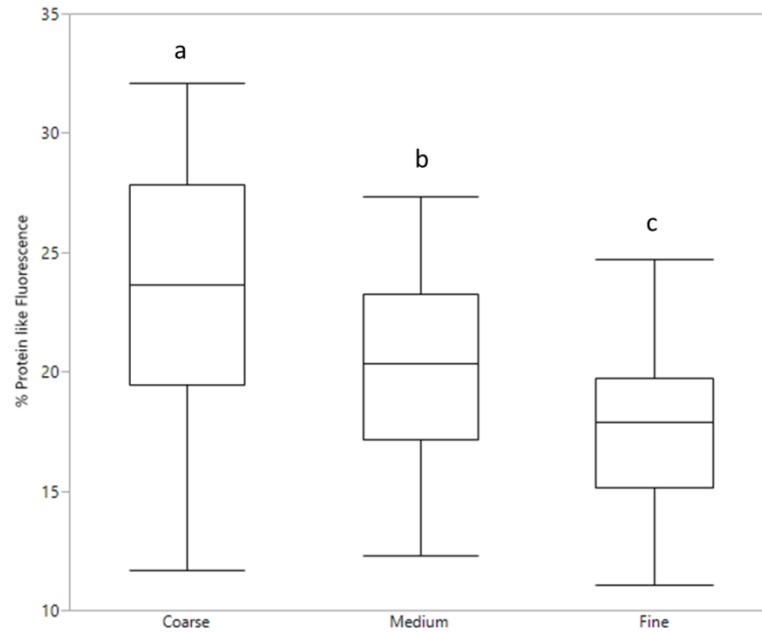


Figure 4.33: Percent protein-like fluorescence is presented by size class. Significant differences are indicated by letters.

Percent humic-like fluorescence by event was evaluated through a multiple linear regression, controlling for size class. The winter events (2/16/16 and 2/24/16) had significantly higher %humic-like fluorescence compared to the 7/30/16 and 8/21/16 events. The 7/28/16 event was not significantly different from the 2/16/16 event. Location did not significantly contribute to explaining the model (Figure 4.34). Each size class was significantly different with the Fine material exhibiting the highest humic-like fluorescence and Coarse generating the lowest (Figure 4.35).

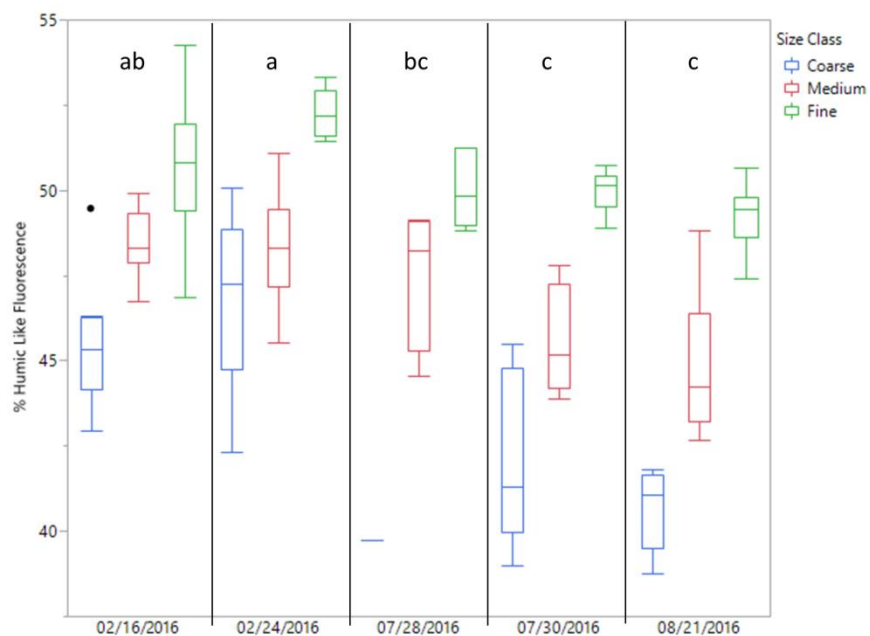


Figure 4.34: Percent humic-like fluorescence is presented by event and size class. Significant differences are indicated by letters.

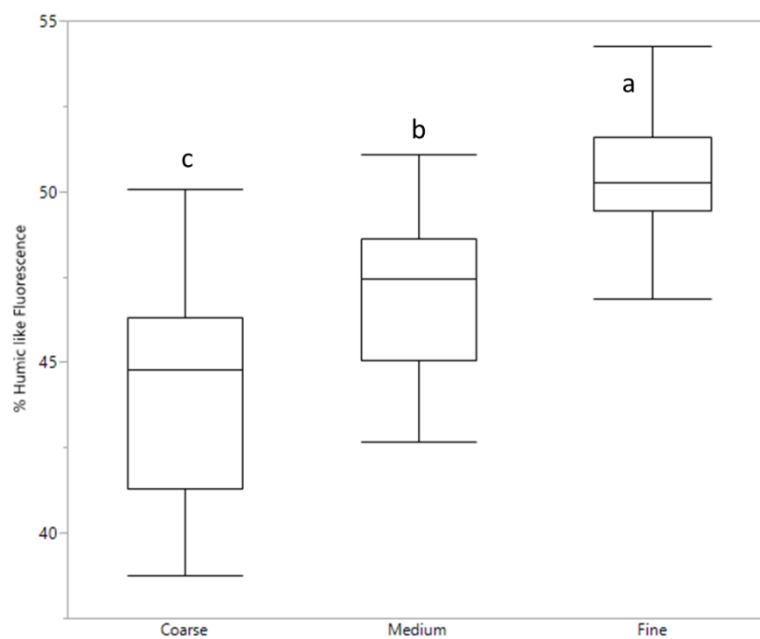


Figure 4.35: Percent humic-like fluorescence is shown by size class. Significant differences are indicated by letters.

A multiple linear regression was run for %fulvic-like fluorescence by event, controlling for location. A Tukey HSD showed that the 2/24/16 event was significantly higher in fulvic-like fluorescence compared to all other events except the 7/30/16 event (Figure 4.36). Size class did not significantly help to explain the model, and was not significant when examined alone (Figure 4.37).

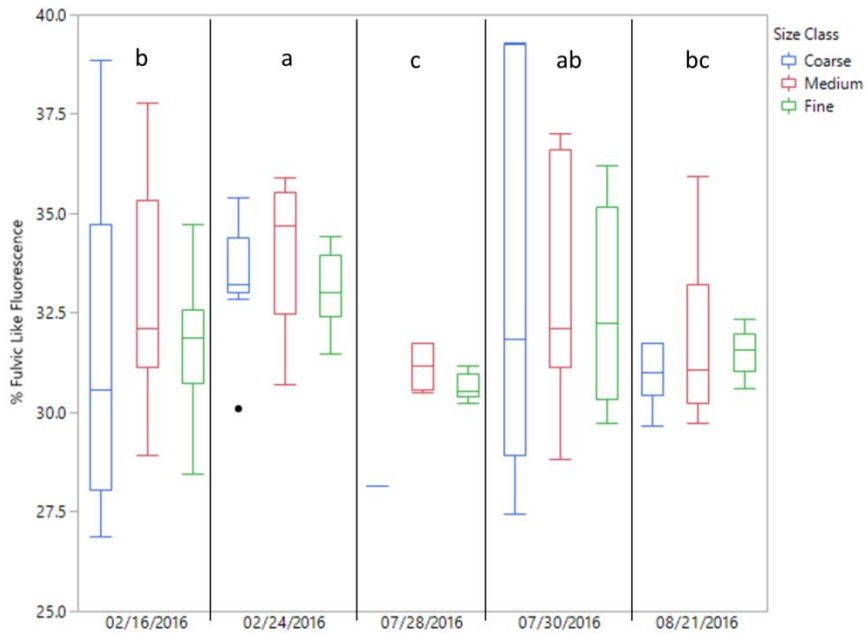


Figure 4.36: Percent fulvic-like fluorescence presented by event and size class. Significant differences are indicated by letters.

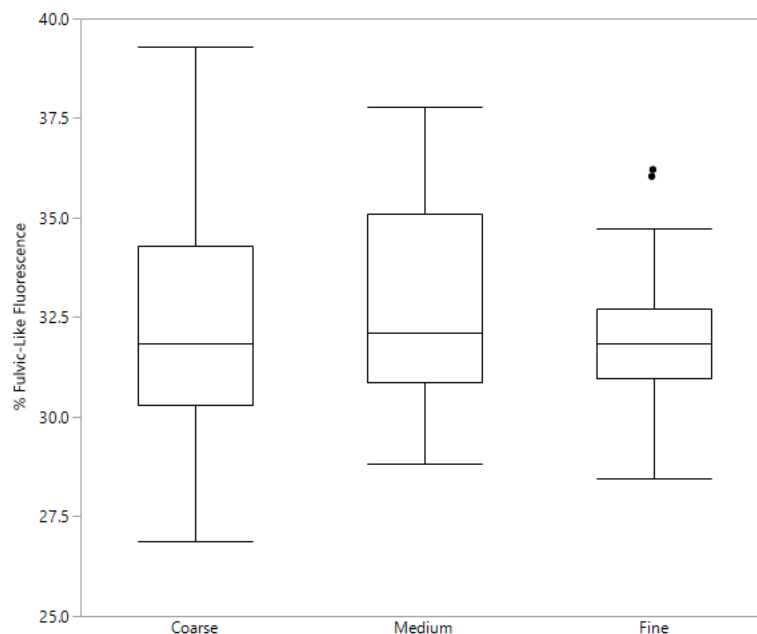


Figure 4.37: Percent fulvic-like fluorescence presented by size class. No significant differences were found.

A multiple linear regression was run to assess the differences in SUVA by event. While there were no significant differences between event alone, when a model was run controlling for size class and location, the 2/16/16 and 2/24/16 events had higher SUVA compared to the 7/28/16 and 8/21/16 events. The difference was not significant for the 7/30/16 event (Figure 4.38). When examining SUVA by size class the Coarse size class was significantly lower compared to the other two size classes, indicating that it was less aromatic compared to the Medium and Fine material (Figure 4.39).

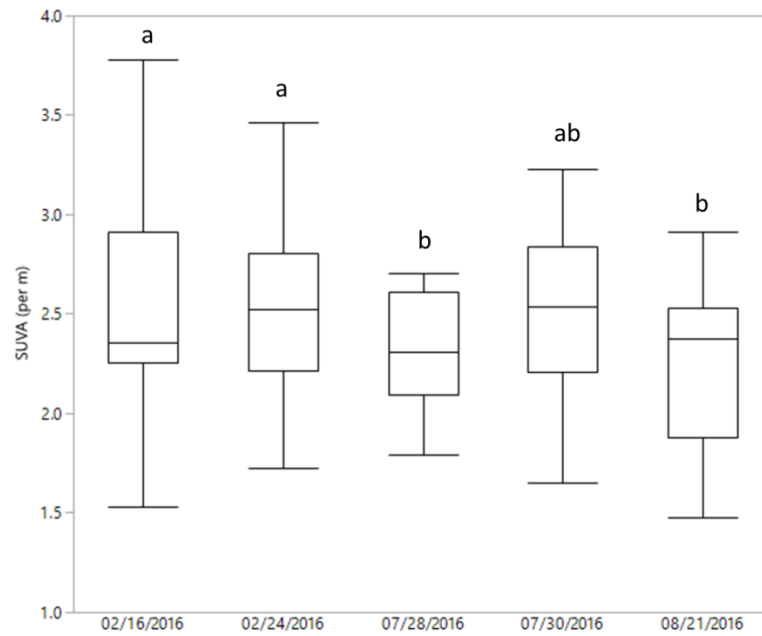


Figure 4.38: SUVA values presented by event. Significant differences indicated by letters.

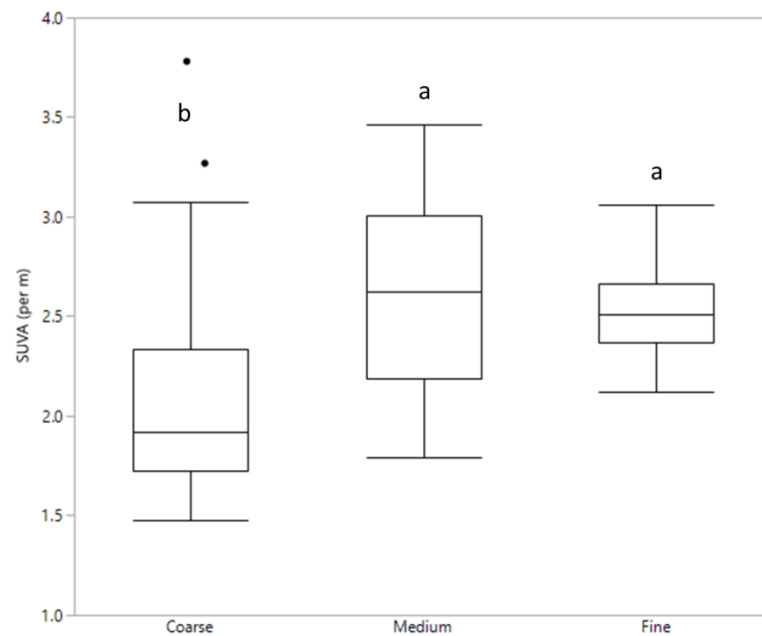


Figure 4.39: SUVA presented by size class. Significant differences indicated by letters.

The DOC:TN ratio (atomic) (Figure 4.40) was calculated to compare to the solid C:N ratio (Figure 4.23). The DOC:TN ratio, evaluated by size class was similar to the C:N ratio trends by size class. Significant differences were found between all size classes with Coarse having the highest DOC:TN ratio and Fine having the lowest (Figure 4.40). When the DOC:TN ratio was examined by event, significant differences were found between the 8/21/16 event, which showed the highest ratio and the 2/16/16, 2/24/16, and 7/30/16 events which showed a significantly lower DOC:TN ratio (Figure 4.41).

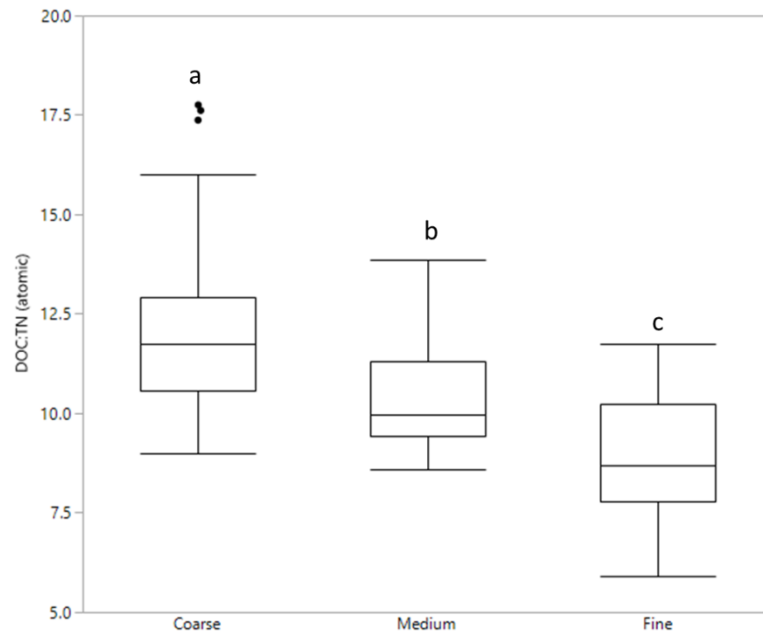


Figure 4.40: DOC:TN ratio presented by size class. Significant differences are indicated by letters. Similar results are presented in Figure 4.23.

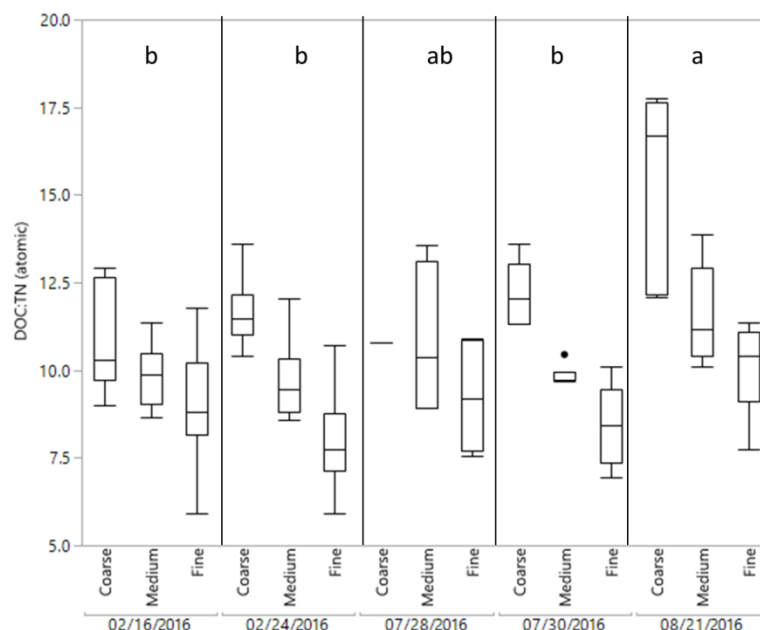


Figure 4.41: DOC:TN ratio presented by event. Significant differences are indicated by letters.

Correlations between solid phase and leached POM metrics

A correlation matrix was created with POM samples from all events. The events were examined separately but show consistent patterns and relationships with each other and therefore the full correlation with all events is reported in Appendix A (Table A3) along with the p-values for the correlation (Table A4). The table is summarized here. There was a correlation strong negative between the isotopic values and the carbon and nitrogen. Carbon was negatively correlated with $\delta^{15}\text{N}$ ($r=-0.59$) and $\delta^{13}\text{C}$ ($r=-0.41$). Nitrogen showed a strong negative correlation to $\delta^{15}\text{N}$ ($r=-0.53$) and $\delta^{13}\text{C}$ ($r=-0.47$). There was a negative correlation between %protein-like fluorescence and $\delta^{15}\text{N}$ ($r=-0.59$). The relationship between %protein-like fluorescence and C:N ratio was strong and positive ($r=0.56$). All quality metrics (%humic, %fulvic, and %protein) were highly correlated with %C and %N. %C and %humic ($r=-0.62$), %fulvic ($r=-0.55$), and %protein ($r=0.75$) showed strong correlation as did %N and %humic ($r=-0.52$), %fulvic

($r=-0.61$), and %protein ($r=0.71$). The quality metrics did correlated relatively strongly with DOC and TN. DOC and %humic ($r=-0.61$), %fulvic ($r=-0.51$), and %protein ($r=0.71$) showed strong correlation as did TN and %humic ($r=-0.47$), %fulvic ($r=-0.59$), and %protein ($r=0.65$).

4.3 Comparison of watershed sources against fluvial POM in chemical and isotopic mixing space

The following section presents results comparing the solid and extracted parameters of fluvial POM and source POM in order to better understand the sources of POM contributed to the stream during large storm events.

Comparisons in isotope mixing space

The isotopic composition of the sources varied widely, as seen in Figure 4.4. Figure 4.42 presents the source values, plotted along with three fluvial POM values per event, which represent the average value for each of the three size classes. These average values included samples from all five CSS locations and showed clear separation between the size classes and events. The different POM size classes separated most strongly on the $\delta^{15}\text{N}$ axis with Coarse material falling closest to the Forest Floor Litter and Forest Floor Humus sources. The Fine material was more enriched in $\delta^{15}\text{N}$, indicating its similarity to the Stream Bed, Upland, or the Stream Bank sources. Moving from Coarse to Fine material there was enrichment along the $\delta^{15}\text{N}$ axis. There was also enrichment along the $\delta^{13}\text{C}$ axis moving down in size class in all events except 8/21/16. The events tended to cluster in groups along the $\delta^{13}\text{C}$ axis, with the winter events (2/16/16 and 2/24/16) being generally more enriched along the $\delta^{13}\text{C}$ axis while two of the summer events (7/28/16 and 7/30/16) were more depleted. The 8/21/16 event fell in the middle of these two groups, though notably, there was little separation by size class along the $\delta^{13}\text{C}$ axis for the 8/21/16 event (Figure 4.42).

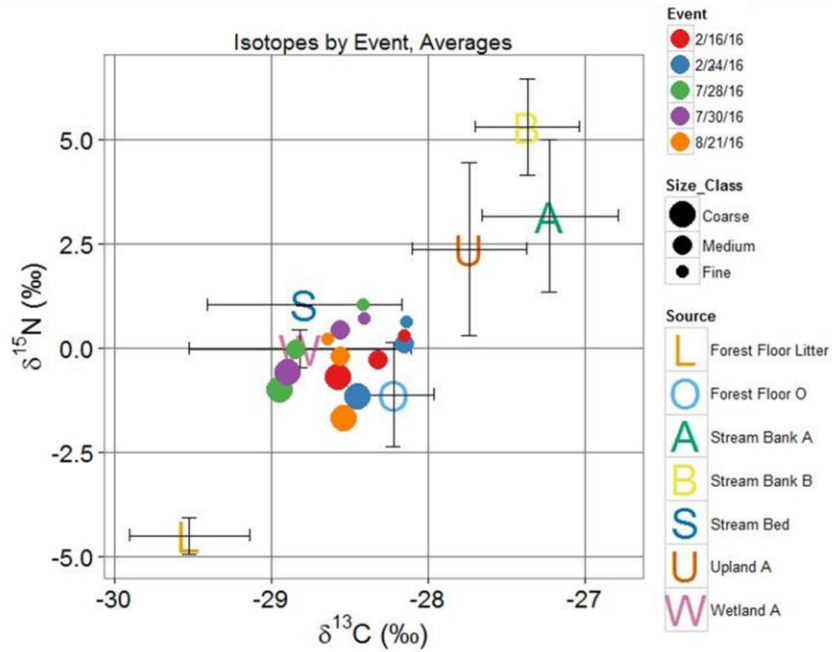


Figure 4.42: Isotope mixing space of $\delta^{15}\text{N}$ and $\delta^{13}\text{C}$ with sources plotted as letters and event POM plotted as dots. Dots are sized by size class and colored by event.

Each of the size classes was examined individually to assess the similarity to the watershed POM sources, and how the POM varied with event. All of the Coarse material appeared to be more similar to the Forest Floor Litter, Humus, and Wetland sources, though the 7/28/16 and 7/30/16 events seemed to be more similar to the Wetland source. The 8/21/16 event was the most depleted in $\delta^{15}\text{N}$, potentially indicating increased contributions from the Forest Floor Litter source. The Coarse material from the 2/16/16 and 2/24/16 events was likely more similar to the Forest Floor Humus (Figure 4.43).

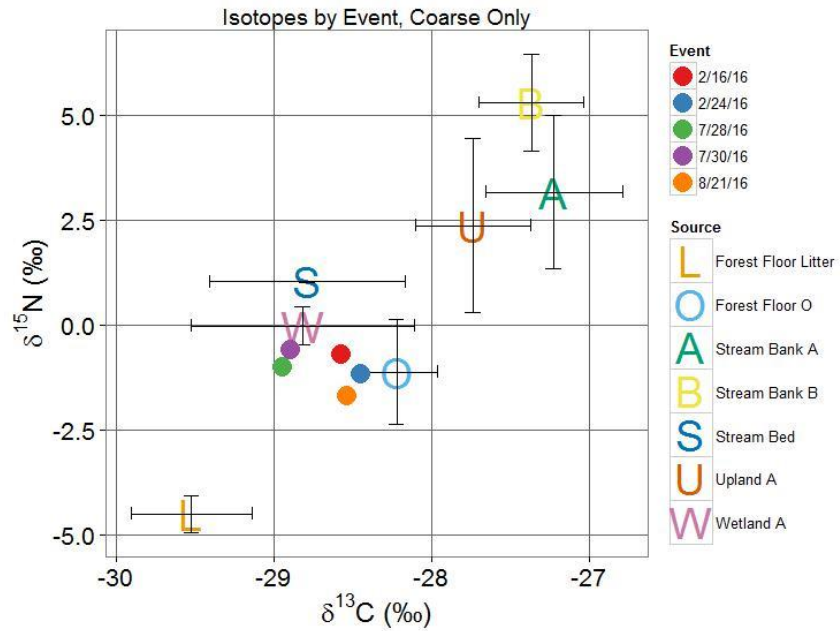


Figure 4.43: Coarse material only is presented for all five events, along with the sources.

The Medium size class hardly separated on the $\delta^{15}\text{N}$ axis, but did separate on the $\delta^{13}\text{C}$ axis. The winter events (2/16/16, 2/24/16) were more enriched while the summer events were more depleted (Figure 4.44).

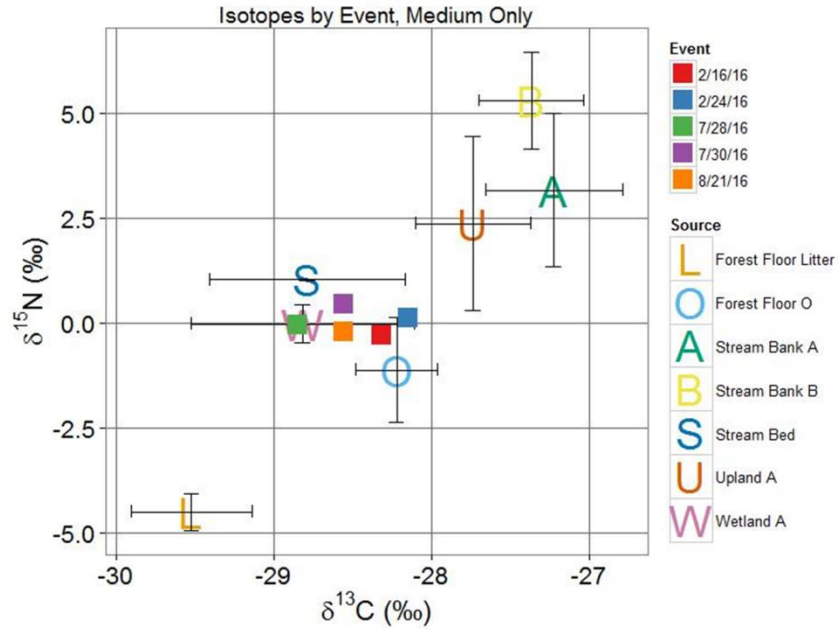


Figure 4.44: Medium material only is presented for each of the five events, along with the sources.

The Fine size class showed slight separation along the $\delta^{15}\text{N}$ axis but more pronounced separation on the $\delta^{13}\text{C}$ axis. The winter events were more enriched in $\delta^{13}\text{C}$ while the summer events were more depleted. The 8/21/16 event was shifted slightly closer to the Wetland source compared to the other events (Figure 4.45).

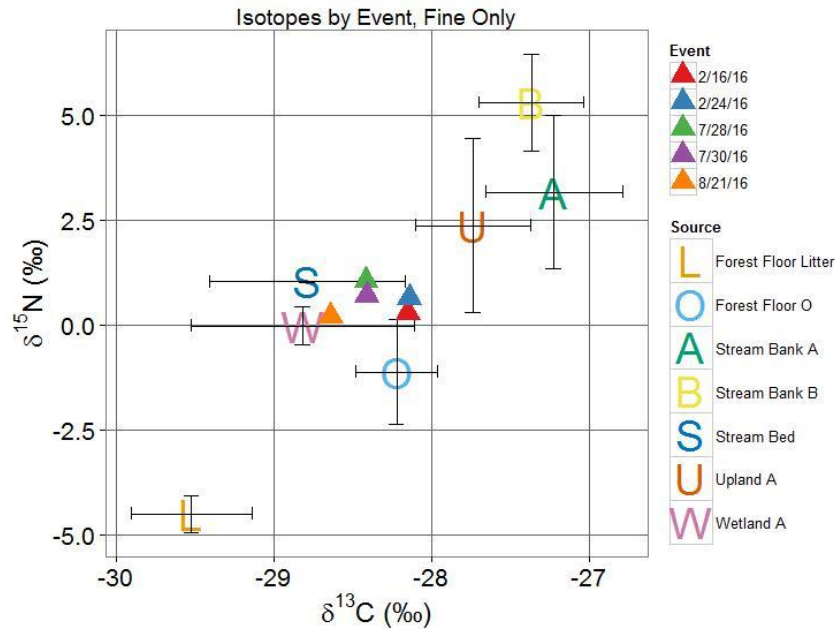


Figure 4.45: The Fine material only is presented by event, along with the sources.

Principal Component Analysis (PCA)

After a first run of the PCA SUVA was removed due to its lack of explanatory power. The final PCA was run with all source POM and fluvial POM samples and included the variables %C, C:N, %N, $\delta^{13}\text{C}$, $\delta^{15}\text{N}$, DOC, TN, %Protein, %Humic, and %Fulvic-like fluorescence.

Principal Component 1 (PC1) explained 61.6% of the variability in the samples and was most strongly associated with the carbon and nitrogen components of %C, %N, TN, DOC loading positively, and $\delta^{15}\text{N}$ and $\delta^{13}\text{C}$ loading negatively. Principal Component 2 (PC2) explained 13.7% of the variability and was more strongly driven by the quality metrics of %Humic and %Protein-like fluorescence (Figure 4.46).

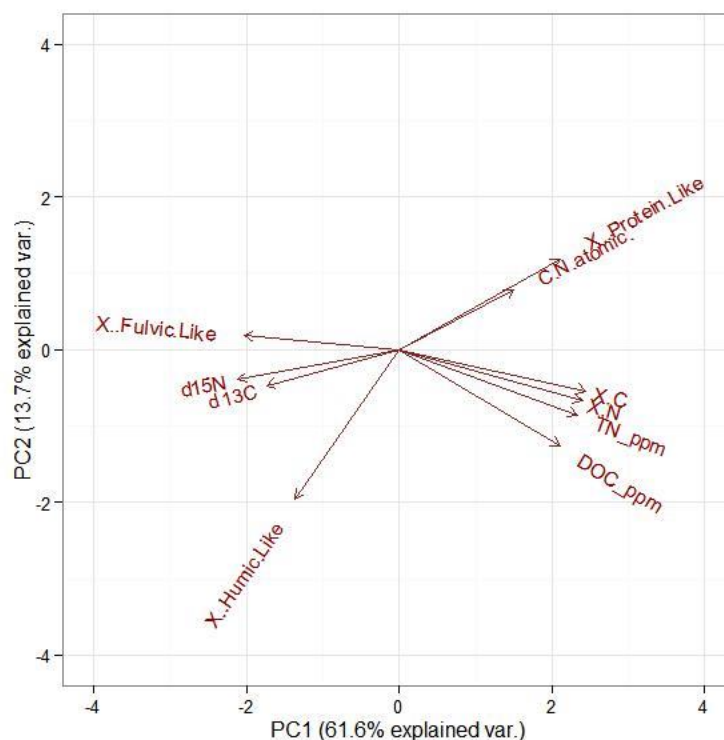


Figure 4.46: Loading plot of PCA components shows that PC1 was best explained by the carbon and nitrogen components, while PC2 was best explained by the “quality” components.

By examining all of the metrics in concert, general composition and quality differences among the sources were evaluated. The Forest Floor Litter source was included in the PCA analysis, but excluded from the remaining graphics for scale. The coordinates for Forest Floor Litter were (8.74,-1.91).

Forest Floor Litter (not pictured) loaded positively on PC1, indicating that the carbon and nitrogen content was high, and slightly negatively on PC2 which likely was driven by the slight negative position of the carbon and nitrogen components, as this source was found to be more protein-like than humic-like in the individual quality analysis. Forest Floor Humus loaded positively on PC1, again representing the strong influence of the carbon and nitrogen components. Forest Floor Humus also loaded

positively on PC2, indicating that it was represented more by the %protein-like composition compared to the %humic-like. Wetland loaded positively on PC1 and PC2 showing higher carbon and nitrogen values as well as higher protein-like values, respectively. The Upland source loaded slightly negative on PC1 and PC2 indicating that it likely contained more depleted isotopic values and humic-like material. Stream Bed loaded negatively on PC1 and almost neutral on PC2. This position in the mixing space showed an association with more depleted isotopic values as well as increase in fulvic-like fluorescence. Stream Bank B loaded negatively on PC1 and neutral on PC2. This material was strongly associated with the fulvic-like fluorescence as well as depleted isotopic values. Stream Bank A loaded negatively on both PC1 and PC2 indicating that it contained material with depleted isotopic values as well as humic-like fluorescent qualities (Figure 4.46, 4.47). When an ANOVA, and a post hoc Tukey HSD were run on the principal components there were significant differences between the sources on both the PC1 and PC2 axes. Levels of significance are denoted by letter/letters in parentheses. For PC1 ($F=225.07$, $p<0.001$) Forest Floor Litter (a) Forest Floor Humus (b) Wetland and Upland (c) Stream Bed (d) Stream Bank A (de) Stream Bank B (e). For PC2 ($F=5.609$, $p=0.0002$) Forest Floor Humus and Wetland (a), Stream Bed, Stream Bank B and Upland (ab), Forest Floor Litter and Stream Bank A (b).

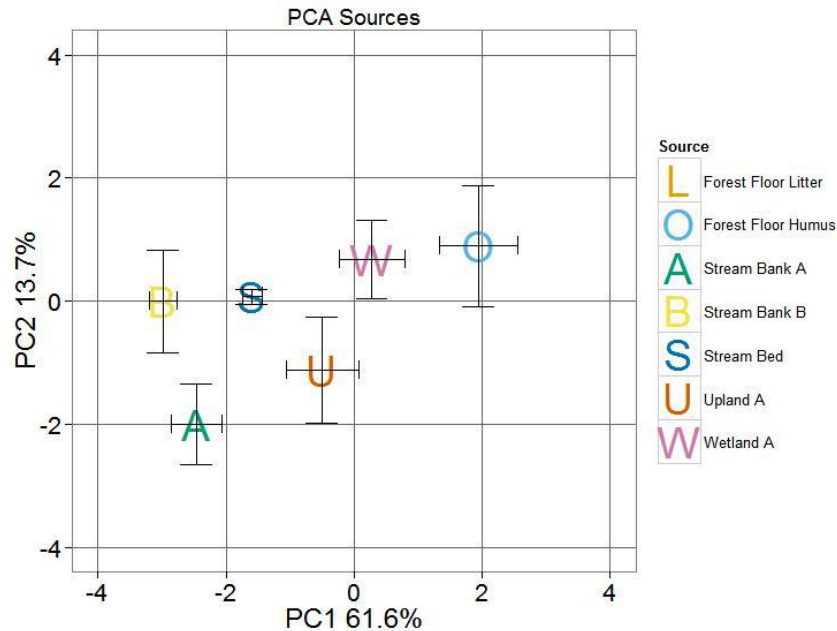


Figure 4.47: Comparing the sources in component space with the PC component loadings (Figure 4.46) provides information about the quality of the sources.

Examining the fluvial POM in component space along with the sources showed distinct separations by event and size class. Each point represents an average value for each size class which includes samples from all five CSS locations. Coarse material was best explained by the C:N ratio and the %Protein-like fluorescence variables, and was most strongly associated with the Forest Floor Humus source. On the contrary the Fine material was associated more strongly by the %humic-like fluorescence and the isotope components, particularly with a depleted $\delta^{15}\text{N}$. These POM characteristics were most closely aligned with the Stream Banks and Upland sources (Figure 4.48).

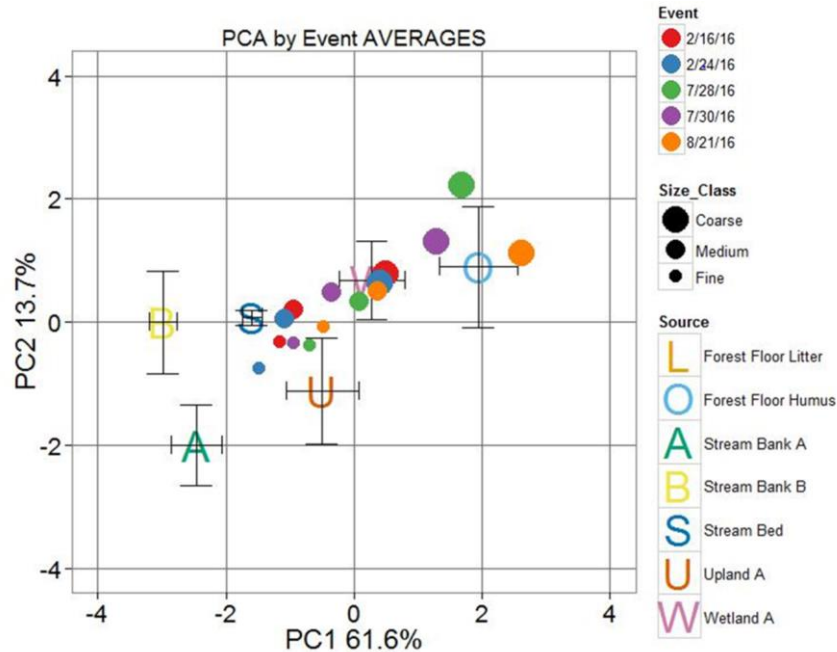


Figure 4.48: Average values for POM, by size class, for each event. Plotted with sources in PCA mixing space.

Size classes were examined individually to assess between-event trends. While all of the Coarse material loads positively on PC1 and PC2 indicating the higher carbon and nitrogen content and protein-like composition of the material, there are some smaller shifts that allow for distinctions between events. For the Coarse material there was a strong coupling of the winter events close to the Wetland source. The 7/28/16 and 7/30/16 events appear to more closely resemble the Forest Floor Humus source, while the 8/21/16 event could be influenced by the Forest Floor Litter source (8.74,-1.91) (Figure 4.49). When an ANOVA, and a post hoc Tukey HSD were run on the principal components the 8/21/16 event was significantly higher on PC1 compared to the 2/24/16 event ($F=2.65$, $p=0.05$). No significant differences were found on the PC2 axis.

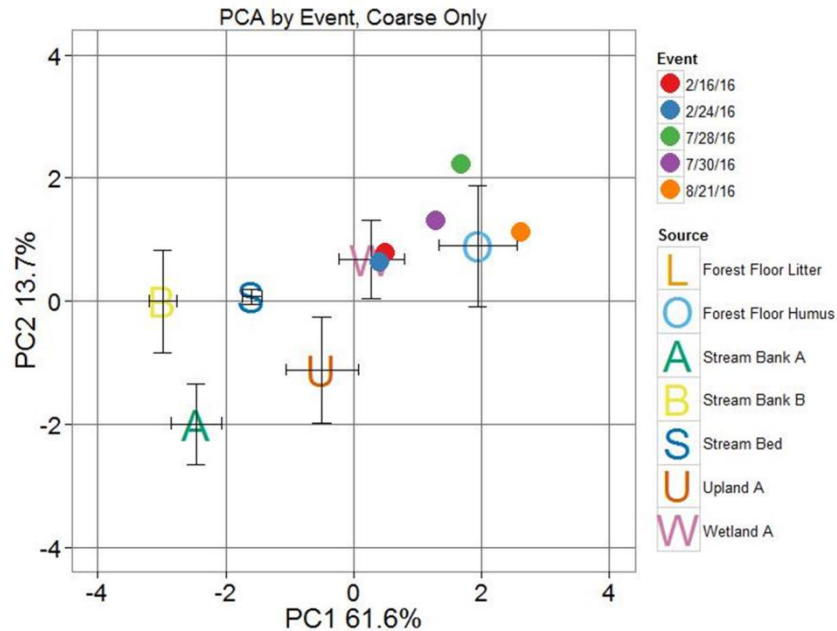


Figure 4.49: The average value of Coarse material for each event is presented. Sources are also plotted in this PCA mixing space.

The Medium size class separated almost exclusively on the PC1 axis, indicating differences in carbon and nitrogen content, isotopic signatures, and potentially %fulvic-like composition. The winter events were more similar to the Stream Bed and Stream Bank B sources, indicating that this material was also likely more depleted in $\delta^{15}\text{N}$ and $\delta^{13}\text{C}$, and potentially had a stronger fulvic-like character. The summer events clustered closer to the Wetland source, indicating higher carbon and nitrogen content compared to the winter events (Figure 4.50). An ANOVA found no significant difference between the samples for either the PC1 or PC2 components, however when drainage location was controlled for, a significant difference was found between two groups, 8/21/16 and 7/28/16 were higher on PC1 compared to 2/16/16 and 2/24/16 ($F=13.75$, $p < 0.001$). No significant differences were found for PC2.

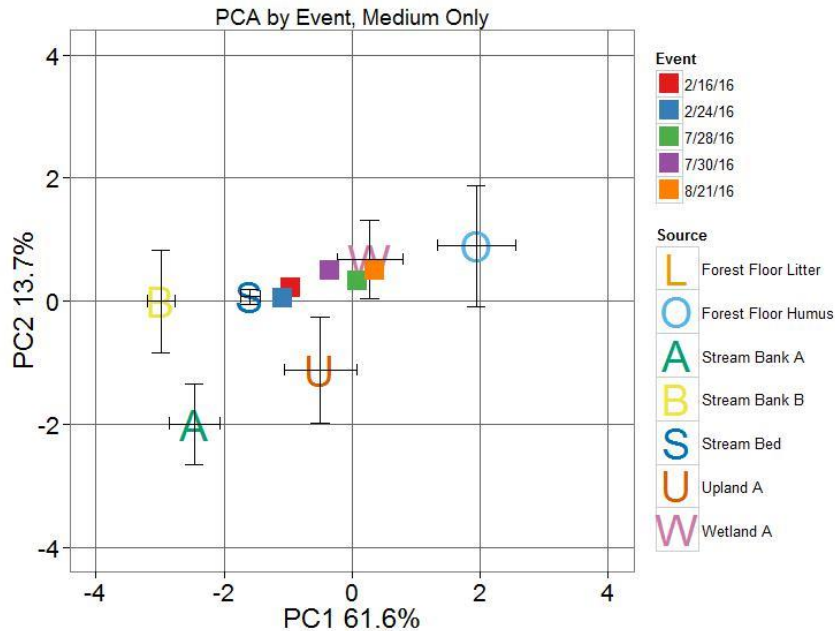


Figure 4.50: The average value of Medium material for each event is presented. Sources are also plotted in this PCA mixing space.

The Fine size class showed less separation compared to the other size classes, but did show slight shifts on both the PC1 and PC2 axis. On the PC1 axis the summer events loaded more strongly in the direction of the carbon and nitrogen components, while the winter events loaded more strongly with the isotope parameters. On the PC2 axis there was a small shift between the 2/24/16 and the 8/21/16 events which showed that the 8/21/16 event was likely slightly more protein-like compared to the other events, and the 2/24/16 event was likely slightly more humic-like. The close clustering made it difficult to assess the similarity of the fine material to specific sources by event (Figure 4.51). When an ANOVA, and a post hoc Tukey HSD were run on the principal components there was a significant difference between the events ($F=3.27$, $p=0.02$) with the 8/21/16 event being significantly higher compared to the 2/24/16 event. This difference became even greater when location was controlled for ($F=14.35$, $p<0.001$) 8/21/16 (a), 7/28/16

(ab), 7/30/16 (bc), 2/16/16 (cd), 2/24/16 (d). There were also significant differences found on the PC2 axis ($F=6.045$, $p=0.0007$) where the 8/21/16 and 2/16/16 events were significantly different from the 2/24/16 event. No additional differences were found when controlling for location.

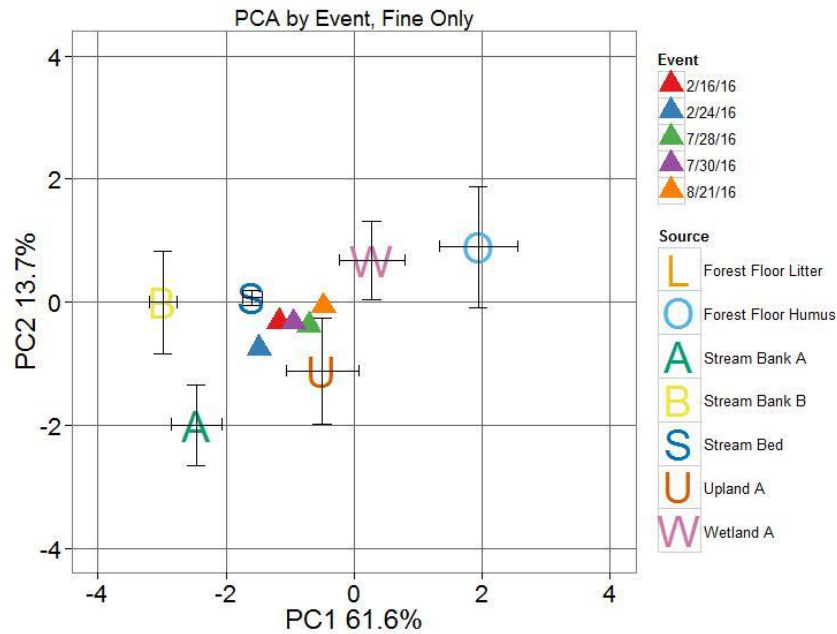


Figure 4.51: The average value of Fine material for each event is presented. Sources are also plotted in this PCA mixing space..

The POM composition was evaluated by drainage location to assess spatial trends in fluvial POM composition. Distinct separation was found between size classes and location. The size class trends were similar to those found in Figure 4.48. Coarse, Medium, and Fine material from CSS3 loaded the most positively on PC1 compared to all of the other locations indicating that this location produced material that was rich in carbon and nitrogen. The CSS10 and CSS11 locations were intermediate, and the CSS12 site showed negative loading on PC1 indicating similarity to the depleted isotopic values

and fulvic-like fluorescence. For all locations, separation on the PC2 axis was driven primarily by the differences in size class, and did not vary greatly between locations (Figure 4.52).

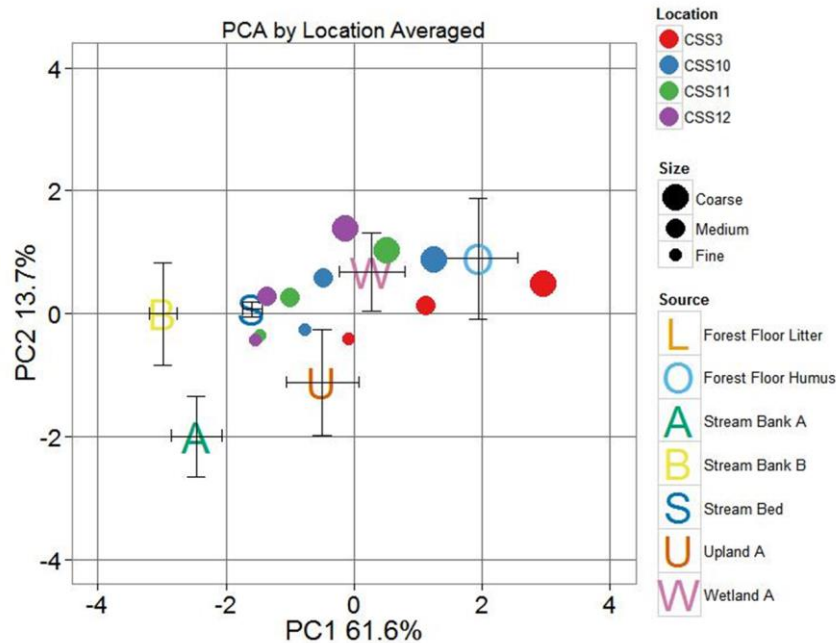


Figure 4.52: POM averaged by location for all events shows is presented, along with the sources in PCA mixing space.

The Coarse material separates most strongly on PC1, indicating that moving downstream resulted in a decrease in carbon and nitrogen content and an increase in the depletion of the carbon and nitrogen isotopes. Coarse material in upstream locations was more similar to Forest Floor Humus, while downstream locations were more similar to the Wetland source (Figure 4.53). When an ANOVA, and a post hoc Tukey HSD were run on the principal components there was a significant difference between the drainage locations ($F=9.85$, $p=0.0002$) with site CSS3 being significantly higher than all other locations. This difference became even greater when event was controlled for ($F=15.15$,

$p < 0.001$) CSS3 (a), CSS10 (b), CSS11 (bc), CSS12 (c). There were also significant differences found on the PC2 axis ($F=3.16$, $p=0.043$) where the CSS3 site was significantly lower compared to the CSS12 site. No additional differences were found when controlling for event.

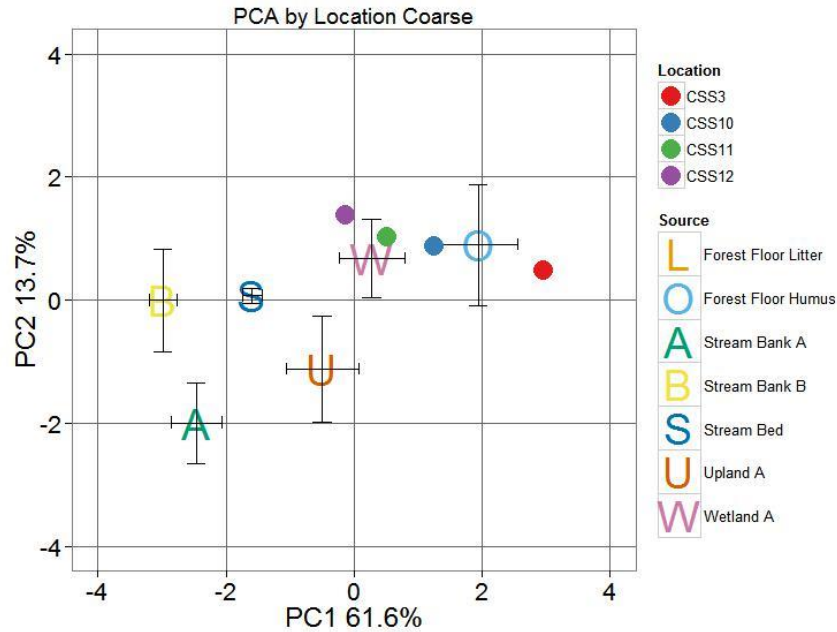


Figure 4.53: The average value of Coarse material for each location is presented. Sources are also plotted in this PCA mixing space.

The Medium material from all locations separated most on the PC1 axis, indicating differences in carbon and nitrogen content. CSS3 showed similarity to the Forest Floor Humus source, while all three downstream locations clustered between the Stream Bed and Wetland sources (Figure 4.54). When an ANOVA, and a post hoc Tukey HSD were run on PC1 there was a significant difference between the drainage locations ($F=13.8$, $p < 0.0001$) with site CSS3 being significantly higher than all other locations. This difference became even greater when event was controlled for ($F=13.36$,

$p < 0.001$) CSS3 (a), CSS10 (b), CSS11 (bc), CSS12 (c). There were no significant differences found on PC2.

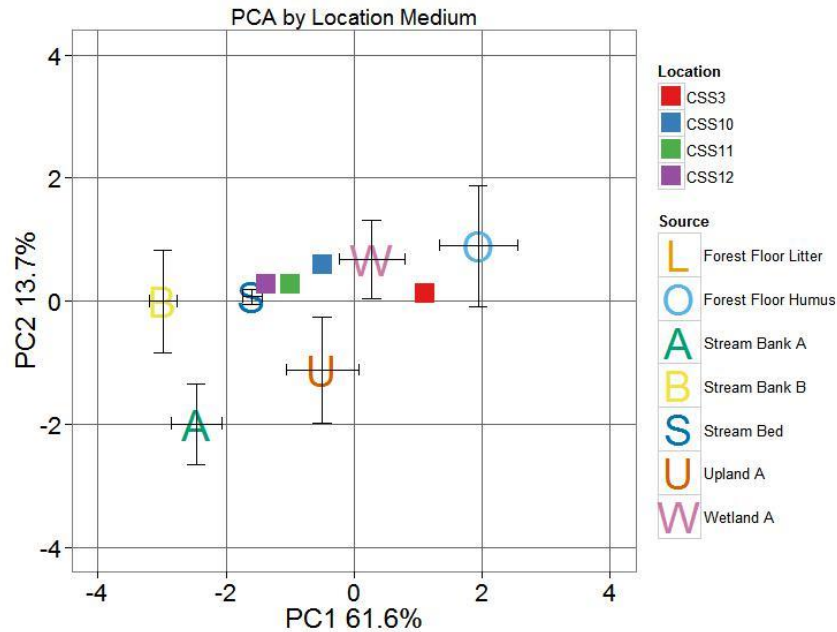


Figure 4.54: The average value of Medium material for each location is presented. Sources are also plotted in this PCA mixing space.

Again, Fine material separated most distinctly on PC1, indicating that the largest difference by location was the carbon and nitrogen content, as the quality did not differ greatly within individual size classes. The CSS3 location loaded most positively on PC1, while material from the CSS11 and CSS12 locations had a similar composition, and was most similar to the Stream Bed source (Figure 4.55). When an ANOVA, and a post hoc Tukey HSD were run on the principal components there was a significant difference between the drainage locations ($F=22.67$, $p < 0.001$) CSS3 (a), CSS10 (b), CSS11 (c), CSS12 (c). No additional differences were found when event was controlled for. There were no significant differences for PC2.

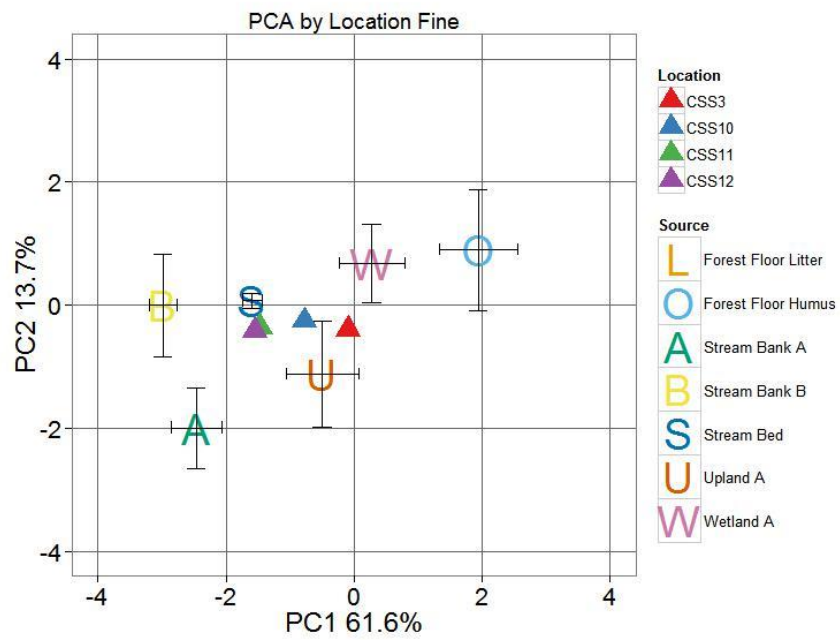


Figure 4.55: The average value of Fine material for each location is presented. Sources are also plotted in this PCA mixing space.

Chapter 5

DISCUSSION

Results from this study show that POM composition could vary substantially with watershed source, storm events, and particle size class and has the potential to significantly impact downstream water quality. The discussion below elaborates on the key factors that influence POM composition and evaluates them against observations from previous studies. Finally, broader environmental implications are identified to develop a comprehensive understanding of the potential POM impacts to fluvial systems both now and with a changing climate.

5.1 POM composition for Watershed Sources

The composition and quality of POM sources within a watershed provides critical information about the inputs and impacts of POM on downstream ecosystem processes (Webster et al. 1999; Tank et al. 2010). Composition and quality are both critical metrics to analyze, as composition provides information regarding the richness of elemental carbon and nitrogen, while the quality dictates the lability and potential bioavailability of the material (Webster et al. 1999; Fellman et al. 2009).

In forested systems, such as this study location, autochthonous sources of POM are negligible and therefore differences in carbon and nitrogen content as well as C:N ratio are strongly driven by decomposition (Brady and Weil, 2008). Fresher surficial sources, such as Forest Floor Litter contained the most carbon and nitrogen and had the highest C:N ratio indicating that this material was likely the least degraded. Contrary to this, the Stream Bed and Stream Bank A and B sources generally had the lowest carbon and nitrogen content and C:N ratio, indicating higher degradation and processing of the material from these sources. The amount of degradation also influences the isotopic composition of the source material and therefore results in an inverse relationship

between the carbon and nitrogen content and isotopic composition. Sources with high carbon and nitrogen content also tend to have more depleted (negative) isotopic values, and break down to produce sources with lower carbon and nitrogen content and more enriched (positive) isotopic values due to the fractionation that occurs in early diagenesis (Engle and Macko 1993). The most depleted $\delta^{13}\text{C}$ and $\delta^{15}\text{N}$ values were found in the Forest Floor Litter, Forest Floor Humus, and Wetland sources which was likely a function of the lower decomposition as well as a dominance of $\delta^{13}\text{C}$ depleted lignin compounds found in leaf material (Benner et al. 1987). Stream Bank A, B, and Upland demonstrated more enriched values for $\delta^{13}\text{C}$ and $\delta^{15}\text{N}$ indicating that these sources were more degraded, and contained less lignin compounds. Stream Bed showed relatively depleted $\delta^{13}\text{C}$ values which could be driven by benthic algal production or microbial biomass, both of which have been found to produce depleted $\delta^{13}\text{C}$ values (Rosenfeld and Roff 1992). This pattern of enrichment is consistent with natural decomposition processes which cause $\delta^{13}\text{C}$ and $\delta^{15}\text{N}$ values to increase, with greater changes per mil in $\delta^{15}\text{N}$ compared to $\delta^{13}\text{C}$ (Benner et al. 1987; Kendall et al. 2001). Additionally, the division between surficial and subsurface sources was consistent with the findings of Jung et al. (2012) who found increasing $\delta^{13}\text{C}$ and $\delta^{15}\text{N}$ values with soil depth in a mountainous watershed in South Korea, indicating that surficial forest soils were more depleted in $\delta^{13}\text{C}$ and $\delta^{15}\text{N}$ while subsurface soils were more enriched.

The carbon and nitrogen content of the sources also provides valuable information about their leaching potential of dissolved carbon and nitrogen. C:N ratios have been shown to predict DOC export from ecosystems (Aitkenhead and McDowell 2000). As predicted, the lowest amount of DOC and TN was leached from the most carbon and nitrogen poor sources with the lowest C:N ratios (Stream Bed, Stream Bank B, and Stream Bank A) and the most DOC and TN was leached from sources that were more carbon and nitrogen rich with higher C:N ratios (Wetland, Upland A, Forest Floor Humus, and Forest Floor Litter). In a study of two small forested mountainous rivers

Goñi et al. (2013) found that factors such as vegetation cover, productivity, and soil carbon in the sources directly influenced the composition of the POM. This indicates the sources mobilized during storm events have a direct influence on the amount of DOM influencing the fluvial system (Yoshimura et al. 2010).

While the leachable DOC provides important information on quantity, what it fails to address is the quality of the material, a critical metric for understanding the biogeochemical implications for water quality. To address this lack of knowledge fluorescence spectroscopy was used to develop a better understating of the quality of dissolved material leached from the POM. Fluorescence spectroscopy has previously been used to successfully distinguish between terrestrial and estuarine derived DOM and POM after the passage of a hurricane in the Neuse River Estuary, NC (Osburn et al. 2012). These findings indicate that different POM sources are distinguishable solely based on their fluorescent properties and can therefore provide key parallels to water quality parameters (Osburn et al. 2012). In this study the leachates that exhibited higher protein-like fluorescence, an indicator of DOM bioavailability (Fellman et al. 2009), were produced by the sources with higher carbon, nitrogen, and C:N ratios such as Forest Floor Litter, Forest Floor Humus, and Wetland. Other studies have found similar results, demonstrating that protein-like components were preferentially metabolized, and therefore considered more labile, compared to humic and fulvic-like components (Hur et al. 2009). Another study found that the majority (80%) of leaf litter leachate was bioavailable, and considered either readily, or intermediately labile (Wiegner et al. 2005). On the contrary, humic-like and fulvic-like fluorescence metrics are collectively thought to be more degraded and refractory (Fellman et al. 2010). This type of material, primarily derived from secondary plant compounds, has also been shown to inhibit microbial activity and degradation (Bianchi and Bauer 2011). Humic-like compounds dominated the Stream Bank A and Upland A sources which could be a function of humic substances becoming immobilized in shallow subsurface horizons, while fulvic-like

compounds are able to percolate farther down into the soil profile therefore explaining the dominance of fulvic-like fluorescence in the in the Stream Bank B source (Ussiri and Johnson 2003). Sources dominated by humic and fulvic-like fluorescence, were likewise lower in carbon, nitrogen, and C:N ratio indicating that mobilization of these sources would contribute less carbon and nitrogen of more degraded quality compared to the carbon and nitrogen rich protein-like sources. Performing an in depth characterization of sources, especially within a single land use can provide important information about the POM character seen during storm events.

Similar to the approach taken in this study, Larsen et al. (2015) used fluorescence, and a subsequent PCA analysis to develop end member mixing analysis (EMMA) for baseflow and stormflow samples taken from a restored and an unrestored stream in an urban watershed in Maryland. They were able to distinguish between multiple sources, though the majority of samples fell closest to a poorly characterized “general allochthonous” source which exhibited low specific fluorescence (Larsen et al. 2015). Even within a single land use, such as in the current study, important distinctions can be made between the sources by evaluating multiple composition and quality metrics. For example, one distinctive signature within the sources was the fulvic-like fluorescence in the Stream Bank B source. The Stream Bank B exhibited higher fulvic-like fluorescence compared to all other sources and therefore, strong fulvic-like signatures from storm event POM samples could be a key indicator of contributions from stream banks. This is especially relevant as stream banks have been shown to contribute a large proportion of the total sediment during storm events in some mid-Atlantic systems (Gellis et al. 2016). Since the Stream Bank B samples were taken from legacy sediments, this fulvic-like signature could serve as a unique indicator for this widespread and pervasive source of sediment in mid-Atlantic watersheds (Walter and Merritts 2008). Further research should be done to determine if legacy sediments consistently exhibit a fulvic-like signature as well as what the functional groups associated with this fulvic-like material are. This

fulvic-like signature could serve as an accurate indicator of legacy sediment mobilization during storm events, and could provide important information about the quality of organic matter coming from legacy sediments.

5.2 Fluvial POM composition with particle size class and storm events

POM composition with Storm Event magnitude/intensity and seasonal timing

The three major factors influencing the POM composition during storm events are (1) the different source contributions, (2) the hydrology and flow paths activated, and (3) the biological influences on the POM. These factors vary with event magnitude and intensity as well as seasonal timing which subsequently produces variability in POM quality for different events.

The sources available in a watershed directly regulate the quality of POM contributed to streams during storm events. A principal component analysis (PCA) (Figure 4.46, 4.47) showed that the sources in this watershed/study can be collectively grouped into two overarching categories based on their loading along the PC1 axis. Sources with higher C, N, C:N ratio, DOC, and TN along with depleted isotopic values and higher protein-like composition loading positively on the PC1 axis can broadly be termed *rich-labile* sources. These include the Forest Floor Litter, Forest Floor Humus and Wetland sources. Sources with lower C, N, C:N ratio, DOC, and TN coupled with enriched isotope values and higher humic and fulvic-like composition loading negatively on the PC1 axis can broadly be termed *poor-refractory* sources. These include Upland, Stream Bank A, Stream Bank B, and Stream Bed. These differences in composition and quality of the sources are directly related to the fluvial POM signature seen during storm events. In a study of fine sediment and organic matter in Australia, Garzon-Garcia et al. (2016) found that the litter contributed the main source of carbon to the stream, and that the subsoil was the main nitrogen source. However, in a wet year Garzon-Garcia et al.

(2016) found that surficial soils became the dominant N source. This indicates that with variable climatic conditions the different sources may play a larger/smaller role due to differences in mobilization and quality (i.e. rich-labile or poor-refractory), even within a single watershed.

The POM quality is also dependent on the hydrology and flow paths that are activated during a storm event. Storm event characteristics such as magnitude, intensity, antecedent moisture conditions and seasonal timing exert a strong control on the hydrology and flow paths and the subsequent sources that are intercepted/mobilized (Jung et al. 2012; Goñi et al. 2013; Dhillon and Inamdar 2014; Ziegler et al. 2016). In this study, summer storms were convective systems with high intensity and short duration, while winter events were generally frontal storm systems with longer duration, though they also produced periods of high intensity. The composition of POM in summer and winter events differed significantly on multiple quality metrics, indicating the activation of different sources and different amounts of material from those sources. Summer events tended to be more intense, leading to the potential for greater saturation overland flow and thus higher erosion and delivery of surficial POM sources such as Forest Floor Litter and Humus. On the contrary, winter events in this study operated under vastly different antecedent conditions, which were atypical even for a winter event. An unseasonably high rainfall amount and intensity occurred on patchy snow cover after a sharp freeze-thaw episode in February 2016 resulting in the highest recorded suspended sediment concentrations (SSC) in the mid-Atlantic study watershed over the past 10 years. The sources mobilized during these events were likely very different from those activated during summer storms. Patchy snow cover may have resulted in lower transport of surficial sources as some studies have observed only small pulses of DOC and POC during rain-on-snow events (Jeong et al. 2012). However high suspended sediment loads in these winter events point to increased contributions from the stream banks, as antecedent freeze-thaw of stream banks has previously been found to result in

increased contribution during winter events (Gellis and Noe 2013). This stream bank source is also particularly relevant in mid-Atlantic Piedmont watersheds where there is a large supply of legacy sediments in valley bottoms (Merritts et al. 2011). Given these unique winter event characteristics and antecedent conditions, along with the lower %C and %N values, it is likely that more poor-refractory sources such as Stream Banks and Stream Bed were the primary sources mobilized in these events.

The differences between summer and winter events was confirmed in the PCA analysis (Figure 4.48), as summer events were more similar to the rich-labile sources, while winter events appeared to be more similar to the poor-refractory sources. Similar results presented by Dhillon and Inamdar (2014) showed higher %POC in summer events compared to winter events and a correlation between high intensity events and high POC concentrations in a forested mid-Atlantic watershed. They also found that high intensity events generated a greater diversity of sources, including more distal and upland sources which tend to be carbon and nitrogen rich, while lower intensity events primarily mobilized near stream sources which tend to be more carbon poor (Dhillon and Inamdar 2014). On the contrary, in a mountainous watershed in South Korea Jung et al. (2012) found that lower flows (or non-peak flows) transported younger and fresher POC while high flows and intense rainfall increased contributions from deeper mineral soils which were older and more degraded. This indicates that the sources of POM within watersheds, and the flow paths that are activated may be very different, even under similar climatic conditions such as intense rainfall events.

In this study, both the solid and extracted analyses indicate the summer events contributed more carbon and nitrogen of higher quality to the system, however, it should be recognized that the winter events generated a greater amount of sediment and POM (Figure 4.14). This suggests that the actual mass input to the fluvial system was higher during the winter events, despite the lower C and N content and more degraded quality of the material. As this material is transported into new aquatic environments either directly

as a result of the storm event, or is remobilized in subsequent storm events it could be subject to additional degradation and processing. These processes could have significant implications for downstream water quality.

Another key factor influencing POM quality is the levels of biological processes affecting the POM. Drying and wetting cycles, and increased microbial activity due to higher temperatures, such as those generally present in summer month, can facilitate breakdown of C and N and enhance mineralization compared to more consistent moisture levels (Borken and Matzner 2009). This would generate a large pool of available nutrients that could be flushed out in subsequent storm events. On the contrary, colder temperatures with more consistent moisture may result in slower microbial decomposition and less C and N mineralization. In a study of seasonal and longitudinal changes in POM quality in a mountainous region in Argentina, Díaz Villanueva et al. (2016) found that seasonal stoichiometric differences existed within the POM and DOM and showed higher POM C:N and C:P ratios in the autumn, indicating that seasonal changes in the composition of the sources may subsequently influence the dissolved phases. While this study shows that different sources are mobilized during different seasons as a function of the storm magnitude/intensity and antecedent conditions, differences within seasons may best be explained by the differences in biological processing of the material.

5.3 POM compositional changes with Particle Size Class

The most notable and significant differences in POM were observed for different POM particle size classes. It is widely accepted the degradation and processing of Coarse POM (CPOM) results in the generation of Fine POM (FPOM) and that CPOM breakdown is a direct control on the chemical properties of FPOM (Yoshimura et al. 2008; Tank et al. 2010; Sakamaki and Richardson 2011; Tant et al. 2013). It therefore follows that significantly higher %C and %N was observed for the Coarse POM

compared to the Medium and Fine size classes. The breakdown process also influences the C:N ratio (Brady and Weil, 2008), which decreased significantly moving down in size class. Degradation resulted in enrichment of the $\delta^{15}\text{N}$ and $\delta^{13}\text{C}$ isotopic values moving down in size class, due to the preferential use of the lighter ^{12}C and the subsequent fractionation (Engle and Macko 1993). Similar trends for %C, %N, C:N ratio, and $\delta^{15}\text{N}$ and $\delta^{13}\text{C}$ isotopes were found by size class for past source tracking studies in this watershed (Rowland et al. 2017).

The CPOM was more C and N rich and resulted in higher extracted DOC and TN compared to the other two size classes, and therefore likely was derived from sources which had similar composition. The fluorescence components show a strong trend with size class with %protein-like fluorescence significantly decreasing, and %humic-like fluorescence increasing moving down in size class. This trend has been attributed to the preferential use of more protein-like and labile components, leaving behind more humic-like and refractory components during the microbial processing and breakdown of organic matter (Yoshimura et al. 2008; Hur et al. 2009). Yoshimura et al. (2010) also analyzed the leaching rate of Coarse and Fine POM and found that CPOM had a higher initial leaching rate but that the leaching rates became similar after approximately two weeks. In this study, approximately 50 percent of the POM from summer events in this study was in the Fine fraction, indicating that while CPOM is an important initial source of DOC, the larger contribution of FPOM can be a sustained source of DOC long after a storm event is over.

Examining the size classes in PCA mixing space along with the sources provides information about the overall quality of the material as well as the sources from which the POM may have been derived. The material from the Coarse size class from all events shares similar characteristics to the rich-labile sources (Figure 4.49). However, the Coarse size class also showed differences between events. The winter events showed more similarity to the Wetland source while the summer events showed increased

influence from the Forest Floor Humus, and likely the Forest Floor Litter, especially for the 8/21/16 event (Figure 4.49). The Medium size class was not distinguishable between the rich-labile or poor-refractory sources, but spanned an area in the mixing space between the Coarse and Fine material (Figure 4.50). However, the Medium material did show seasonal differences, with the winter POM falling closer to more poor-refractory sources such as the Stream Bed and the summer POM demonstrating a stronger association to the rich-labile material in the Wetland. Material from the Fine size class showed a much stronger association for the poor-refractory sources (Figure 4.51), and was significantly different from the Coarse material on nearly all of the metrics, indicating lower C, N, and C:N ratio, more enriched isotopes, lower DOC and TN, and higher %humic-like fluorescence. The Fine size class was likely the most similar between the events, indicating that it may be more homogeneous material or that similar sources of fine material are activated in all seasons.

5.4 Broader environmental implications of POM composition

Impacts on water quality and aquatic nutrient cycling

Large storm events can contribute huge quantities of POM to fluvial systems (Jeong et al. 2012; Jung et al. 2012; Dhillon and Inamdar 2013; Lloret et al. 2013; Inamdar et al. 2015; Lee et al. 2016). However, far fewer studies have investigated the quality of POM mobilized during large events and its potential impact on water quality and aquatic nutrient cycling (Osburn et al. 2012; Goñi et al. 2013; Jung et al. 2014a; Stelzer et al. 2014; Larsen et al. 2015). Understanding POM quality is critical for understanding the biogeochemical and ecological implications of large POM pulses in fluvial systems, which are likely to rise with increases in extreme storm events due to climate change.

After POM is delivered to aquatic systems, a variety of conditions such as excess nutrients, microbial exudates, light exposure, and salinity gradients can affect the availability of POM (Bianchi 2011). Other studies have shown similar changes in organic matter lability, or a “priming” effect, with exposure to increased nutrients and other sources of labile organic matter (Stelzer et al. 2003; Tant et al. 2013; Guenet et al. 2014). In a small forested watershed Stelzer et al. (2003) found that increasing nutrients caused a stimulation of microbial respiration on POM, and that the POM quality was a controlling factor in the level of respiration. Since storm events provide both a source of POM as well as increased nutrients, higher respiration and increased nutrient inputs and cycling are likely to occur. Size class may also be a regulating factor as Tant et al. (2013) found that the microbial respiration was simulated more on Coarse compared to Fine POM. Though, similar to the findings of Stelzer et al. (2003), Tant et al. (2013) recognized that substrate quality is likely an influential factor on the respiration level. This “priming” effect, where microbial respiration is stimulated by the addition of nutrients may be especially relevant for winter storm events. This study showed that these events mobilized large amounts of material from more poor-refractory sources, and while they may not initially leach large amounts of nutrients to the system, a priming effect may stimulate these previously refractory sources causing them to become a large source of nutrients to downstream systems.

Additions of POM may also have a direct influence on the nitrogen processing in the fluvial systems. In a carbon burial experiment Stelzer et al. (2014) found that the POC quality was an influential factor in determining the nitrogen processing in the sediments. Specifically, they found that the burial of leaves, a high quality POM source, resulted in higher nitrate retention, higher total dissolved nitrogen retention, as well as higher denitrification rates compared to lower quality POM. In fact, denitrification accounted for approximately 60% of the nitrate removal in the leaf treatments. This was attributed to the creation of favorable redox conditions along with a sufficient supply of

organic carbon (Stelzer et al. 2014). They also found an increase in %N as microbes colonized the leaves and immobilized N from the water column. These findings indicate that contributions of surficial, labile sources such as Forest Floor Litter and Humus may influence aquatic nutrient cycling, and result in more nitrate retention or denitrification than previously thought. Given favorable conditions, labile POM inputs may result in an N sink through denitrification, thereby affecting the net N budget in the system. While favorable conditions may create an N sink, Stelzer et al. (2014) found that if anoxic conditions are not present, such as in the field experiment portion of their study, then nitrate removal through the process of denitrification is less influential. This could therefore make the sediments an N source. Nitrate contributions from POM could have important implications for downstream water quality, and could exacerbate challenges such as eutrophication (Horowitz 2013).

Future increases in the frequency and intensity of large storm events, coupled with elevated antecedent moisture conditions (e.g., Yellen et al. 2016) could exacerbate water quality concerns as a result of POM contributions. The large inputs during winter events in this study points to changing and variable climatic conditions as a mechanism for eliciting large scale POM responses. Variability in winter temperatures, resulting in freeze-thaw conditions can facilitate stream bank erosion, which can be a dominant source in winter events (Gellis and Noe 2013). Intensity of the largest storms (especially tropical storms) may also be increasing (Melillo et al. 2014). The increased intensity may facilitate the mobilization of more Coarse material, especially from surficial sources which tend to be organic rich. Large contributions of labile surficial sources could impact water quality and nutrient cycling locally, as Coarse particles may not be transported very far and possibly buried in the sediments. It may also affect downstream reaches, as nutrients are leached and the CPOM is broken down into smaller size fractions. These changes are an important consideration when planning for future water quality challenges.

Microbial communities, aquatic food web and stream metabolism

Since allochthonous inputs are well known to be the primary fuel for the base of food webs, changes in the allochthonous material or its dynamics could have a large influence on ecosystem metabolism (Tank et al. 2010). In a study of nutrient enrichment, Tant et al. (2013) found that nutrient enrichment resulted in higher respiration of POM. This increase was greatest for CPOM (~300%) but also increased for the FPOM (~50%) indicating that shifts in nutrient enrichment could result in the activation of large carbon loss pathways and affect the resource quality of the base of the food web (Tant et al. 2013). This change in resource quality also affects the amount and rate at which energy is supplied to higher trophic levels (Wiegner et al. 2005). In a stream metabolism study, Wiegner et al. (2005) concluded that readily labile DOC would be consumed over a shorter distance compared to intermediately labile DOC. This has direct implications for stream metabolism, as large pulses of readily labile DOC may immediately impact metabolism at the reach scale, while intermediately labile DOC has implications on a longer spatial and temporal scale (Wiegner et al. 2005). These findings indicate that changing inputs of DOM and POM into fluvial systems have implications over wide spatial and temporal scales.

Fluvial flux and GHG budgets

POM inputs into fluvial systems also have the ability to increase CO₂ fluxes from inland waters, further increasing greenhouse gas (GHG) emissions to the atmosphere. Conventionally thought to be passive pipe systems, inland waters have been shown to release significant amounts of CO₂ to the atmosphere (Battin et al. 2009a; Aufdenkampe et al. 2011). It has been estimated that approximately two times as much carbon enters inland waters than what is exported to the ocean, indicating that outgassing along with inland storage can be significant (Cole et al. 2007). A study in the UK found that soils, a

traditional carbon sink, became a net source of CO₂ due to significant erosion and subsequent mineralization of DOC and POC in fluvial systems (Worrall et al. 2014). In fact, Worrall et al. (2014) showed that 70% of the POC load in UK rivers was lost to the atmosphere on its way to the ocean. On a smaller time scale, Goulsbra et al. (2016) measured CO₂ outgassing caused by POC additions from peatland soils. They found significant carbon loss to the atmosphere, particularly within the first 24 hours, indicating that POC additions, such as those seen in large storm events could cause “hot moments” of carbon processing (Goulsbra et al. 2016). Increasing inputs of POM to fluvial systems could increase CO₂ fluxes to the atmosphere, becoming an even more significant source of GHG’s. Further downstream impacts are being investigated in estuarine systems where POM quality is analyzed using fluorescence to evaluate the potential influence of POM inputs on CO₂ fluxes from marsh systems, which are globally important areas of blue carbon storage (Osburn et al. 2015). The quality of POM may be a large regulating factor in CO₂ fluxes in marsh systems, due to differences in lability. In an assessment of DOC biodegradability in the Schelde estuary, Muylaert et al. (2005) found that labile DOC produced in summer months was respired more than refractory DOC produced in winter months. This ranged from a mean of 3% in February to a mean of 24% in July (Muylaert et al. 2005). This indicates that the impact of POM and leached DOM from summer events may result in higher CO₂ fluxes from downstream systems due to the bioavailable nature of the material.

Chapter 6

CONCLUSION

This study provided novel insight into the composition and quality of POM mobilized by large storm events and delivered to the fluvial network. The combination of traditional solid-state compositional analysis of POM along with fluorescence spectroscopy on leached POM provided detailed information about the sources of POM and the biogeochemical significance of POM inputs to fluvial systems.

Key conclusions from this study are:

Source influence: Carbon and nitrogen rich, and isotopically depleted surficial sources produced higher dissolved carbon and nitrogen, as well as higher protein-like fluorescence. This indicated that these sources had the potential to contribute large amounts of labile material to downstream systems during storm events. Carbon and nitrogen poor and isotopically enriched near stream sources produced lower dissolved carbon and nitrogen and higher humic-like fluorescence, indicating that mobilization of these sources could result in inputs of more recalcitrant material.

- (1) Storm event impact on POM: POM transported during storm events varied in amount and quality by storm magnitude, intensity, antecedent moisture conditions, and seasonal occurrence. High-intensity summer storms tended to mobilize more carbon and nitrogen rich labile POM, indicating contributions from upland surficial sources, while winter events tended to mobilize more carbon and nitrogen poor and refractory POM from near stream sources such as stream banks. Thus, the nature of POM delivered to aquatic ecosystems is expected to vary seasonally.

(2) Particle size effects: Different size classes of POM consistently exhibited distinct differences in composition and quality across all events and stream drainage locations. Coarse material contained significantly more carbon and nitrogen, and leached significantly higher protein-like fluorescence compared to the other size classes. On the contrary, Fine material was more carbon and nitrogen poor, more isotopically enriched, as well as more humic-like, indicating that this material was more degraded and processed. The compositional differences between the size classes indicated that while CPOM may be quickly processed and degraded, FPOM may store large amounts of humic and refractory carbon for longer periods of time.

(3) Drainage locations: POM composition and quality differed by drainage location with the upper reaches of the watershed containing more carbon and nitrogen, and protein-like material compared to lower reaches. These differences were attributed to the availability and activation of different sources at each location. The upper reaches of the watershed were heavily influenced by upland surficial sources, while the lower reaches receive increased influence from incised stream banks and other more near-stream degraded sources.

These results clearly show that inputs of POM amount and quality can be affected by a wide variety of factors such as – storm magnitude and intensity, seasonal timing, watershed sources, and particle size. POM inputs can have significant implications for watershed water quality. Water quality models that are used for watershed management and regulatory compliance (e.g., total maximum daily load TMDL; Chesapeake Bay Program, 2017) typically do not account for POM inputs rigorously. Even less consideration is given to POM composition and its long-term impact on water quality through leaching and dissolution of POM. Thus, insights from this study will help in the development of mechanistic and numerical models of POM. Large POM inputs to aquatic ecosystems can also substantially alter in-stream microbial communities and benthic

habitat and observations from this study could aid in that assessment. There has also been an increased emphasis on developing better budgets for greenhouse gas fluxes and POM inputs to fluvial systems could play an important role (Worrall et al. 2016). Given that future climate variability may increase the intensity of storm events, and thus increase the input of POM to aquatic ecosystems, greater attention needs to be paid to understanding the sources, composition and fate of POM.

REFERENCES

- Aitkenhead JA, McDowell WH (2000) Soil C : N ratio as a predictor of annual riverine DOC flux at local and global scales tropical estimated the total export of carbon from land to the oceans $\times 10^6 \text{ Tg yr}^{-1}$. *Global Biogeochem Cycles* 14:127–138. doi: 10.1029/1999GB900083
- Akamatsu F, Kobayashi S, Amano K, et al (2011) Longitudinal and seasonal changes in the origin and quality of transported particulate organic matter along a gravel-bed river. *Hydrobiologia* 669:183–197. doi: 10.1007/s10750-011-0682-8
- Alvarez-Cobelas M, Angeler DG, Sánchez-Carrillo S, Almendros G (2012) A worldwide view of organic carbon export from catchments. *Biogeochemistry* 107:275–293. doi: 10.1007/s10533-010-9553-z
- Anderson D, Glibert P, Burkholder J (2002) Harmful algal blooms and eutrophication: nutrient sources, compositions, and consequences. *Estuaries* 25:704–726. doi: 10.1016/j.hal.2008.08.017
- Atkinson CL, Golladay SW, Opsahl SP, Covich AP (2009) Stream discharge and floodplain connections affect seston quality and stable isotopic signatures in a coastal plain stream. *J North Am Benthol Soc* 28:360–370. doi: 10.1899/08-102.1
- Aufdenkampe AK, Mayorga E, Raymond PA, et al (2011) Riverine coupling of biogeochemical cycles between land, oceans, and atmosphere. *Front Ecol Environ* 9:53–60. doi: 10.1890/100014
- Barker T (2007) Climate Change 2007 : An Assessment of the Intergovernmental Panel on Climate Change. *Change* 446:12–17. doi: 10.1256/004316502320517344
- Bass AM, Munksgaard NC, Leblanc M, et al (2014) Contrasting carbon export dynamics of human impacted and pristine tropical catchments in response to a short-lived discharge event. *Hydrol Process* 28:1835–1843. doi: 10.1002/hyp.9716
- Battin TJ, Kaplan L a., Findlay S, et al (2009a) Biophysical controls on organic carbon fluxes in fluvial networks. *Nat Geosci* 2:595–595. doi: 10.1038/ngeo602
- Battin TJ, Luyssaert S, Kaplan L a., et al (2009b) The boundless carbon cycle. *Nat Geosci* 2:598–600. doi: 10.1038/ngeo618
- Benner R, Fogel ML, Sprague EK, Hodson RE (1987) Depletion of ^{13}C in lignin and its implication for stable carbon isotope studies. *Nature* 329:708–710. doi: 10.1038/329708a0
- Bianchi TS (2011) The role of terrestrially derived organic carbon in the coastal ocean: A changing paradigm and the priming effect. *Proc Natl Acad Sci* 108:19473–19481. doi: 10.1073/pnas.
- Bianchi TS, Bauer JE (2011) *Particulate Organic Carbon Cycling and Transformation*. Elsevier Inc.

- Blackmer GC (2005) PRELIMINARY BEDROCK GEOLOGIC MAP OF A PORTION OF THE WILMINGTON 30- BY 60-MINUTE QUADRANGLE, SOUTHEASTERN PENNSYLVANIA.
- Borken W, Matzner E (2009) Reappraisal of drying and wetting effects on C and N mineralization and fluxes in soils. *Glob Chang Biol* 15:808–824. doi: 10.1111/j.1365-2486.2008.01681.x
- Chesapeake Bay Program (2017), Phase 5.3 Watershed Model. Web page <http://www.chesapeakebay.net/about/programs/modeling/53/> (last accessed May 31, 2017).
- Cole JJ, Prairie YT, Caraco NF, et al (2007) Plumbing the global carbon cycle: Integrating inland waters into the terrestrial carbon budget. *Ecosystems* 10:171–184. doi: 10.1007/s10021-006-9013-8
- Cory RM, McKnight DM (2005) Fluorescence Spectroscopy Reveals Ubiquitous Presence of Oxidized and Reduced Quinones in Dissolved Organic Matter
Fluorescence Spectroscopy Reveals Ubiquitous Presence of Oxidized and Reduced Quinones in Dissolved Organic Matter. *Environ Sci Technol* 39:8142–8149. doi: 10.1021/es0506962
- DEOS (Delaware Environmental Observing System) (2017), Data Access Portal <http://deos.udel.edu/data/> (last accessed May 26, 2017).
- Dhillon GS, Inamdar S (2013) Extreme storms and changes in particulate and dissolved organic carbon in runoff: Entering uncharted waters? *Geophys Res Lett* 40:1322–1327. doi: 10.1002/grl.50306
- Dhillon GS, Inamdar S (2014) Storm event patterns of particulate organic carbon (POC) for large storms and differences with dissolved organic carbon (DOC). *Biogeochemistry* 118:61–81. doi: 10.1007/s10533-013-9905-6
- Díaz Villanueva V, Bastidas Navarro M, Albariño R (2016) Seasonal patterns of organic matter stoichiometry along a mountain catchment. *Hydrobiologia* 771:227–238. doi: 10.1007/s10750-015-2636-z
- Engle MH, Mako SA. *Organic Geochemistry Principles and Applications*. NY, NY: Plenum Press; p. 211-219
- Fellman JB, Hood E, D'Amore D V., et al (2009) Seasonal changes in the chemical quality and biodegradability of dissolved organic matter exported from soils to streams in coastal temperate rainforest watersheds. *Biogeochemistry* 95:277–293. doi: 10.1007/s10533-009-9336-6
- Fellman JB, Hood E, Spencer RGM (2010) Fluorescence spectroscopy opens new windows into dissolved organic matter dynamics in freshwater ecosystems: A review. *Limnol Oceanogr* 55:2452–2462. doi: 10.4319/lo.2010.55.6.2452
- Finlay JC, Kendall C (2007) Stable Isotopes tracing of temporal and spatial variability in organic matter sources to freshwater ecosystems. *Stable Isot Ecol Environ Sci* 283–333.

- Gabor RS, Burns M a., Lee RH, et al (2015) Influence of Leaching Solution and Catchment Location on the Fluorescence of Water-Soluble Organic Matter. *Environ Sci Technol* 150309144001005. doi: 10.1021/es504881t
- Gabor RS, Eilers K, McKnight DM, et al (2014) From the litter layer to the saprolite: Chemical changes in water-soluble soil organic matter and their correlation to microbial community composition. *Soil Biol Biochem* 68:166–176. doi: 10.1016/j.soilbio.2013.09.029
- Garzon-Garcia A, Laceby JP, Olley JM, Bunn SE (2016) Differentiating the sources of fine sediment , organic matter and nitrogen in a subtropical Australian catchment. *Sci Total Environ*. doi: 10.1016/j.scitotenv.2016.09.219
- Gellis AC, Myers MK, Noe GB, et al (2016) Storms, channel changes, and a sediment budget for an urban-suburban stream, Difficult Run, Virginia, USA. *Geomorphology* 278:128–148. doi: 10.1016/j.geomorph.2016.10.031
- Gellis AC, Noe GB (2013) Sediment source analysis in the Linganore Creek watershed, Maryland, USA, using the sediment fingerprinting approach: 2008 to 2010. *J Soils Sediments* 13:1735–1753. doi: 10.1007/s11368-013-0771-6
- Goñi MA, Hatten JA, Wheatcroft RA, Borgeld JC (2013) Particulate organic matter export by two contrasting small mountainous rivers from the Pacific Northwest, U.S.A. *J Geophys Res Biogeosciences* 118:112–134. doi: 10.1002/jgrg.20024
- Goulsbra CS, Evans MG, Allott TEH (2016) Rates of CO₂ efflux and changes in DOC concentration resulting from the addition of POC to the fluvial system in peatlands. *Aquat Sci*. doi: 10.1007/s00027-016-0471-6
- Guenet B, Danger M, Harrault L, et al (2014) Fast mineralization of land-born C in inland waters: First experimental evidences of aquatic priming effect. *Hydrobiologia* 721:35–44. doi: 10.1007/s10750-013-1635-1
- Hirsch RM (2012) Flux of Nitrogen, Phosphorus, and Suspended Sediment from the Susquehanna River Basin to the Chesapeake Bay during Tropical Storm Lee, September 2011, as an indicator of the effects of reservoir sedimentation on water quality. *US Geol Surv Sci Investig Rep* 2012–5185 17.
- Hoover DJ, MacKenzie FT (2009) Fluvial fluxes of water, suspended particulate matter, and nutrients and potential impacts on tropical coastal water Biogeochemistry: Oahu, Hawai'i. *Aquat Geochemistry* 15:547–570. doi: 10.1007/s10498-009-9067-2
- Horowitz AJ (2013) A review of selected inorganic surface water quality-monitoring practices: Are we really measuring what we think, and if so, are we doing it right? *Environ Sci Technol* 47:2471–2486. doi: 10.1021/es304058q
- Hrudey SE (2009) Chlorination disinfection by-products, public health risk tradeoffs and me. *Water Res* 43:2057–2092. doi: 10.1016/j.watres.2009.02.011
- Hur J, Park MH, Schlautman MA (2009) Microbial Transformation of Dissolved Leaf Litter Organic Matter and Its Effects on Selected Organic Matter Operational Descriptors. *Environ Sci Technol* 43:2315–2321. doi: 10.1021/es802773b
- Inamdar S, Dhillon G, Singh S, et al (2015) Particulate nitrogen exports in stream runoff exceed dissolved nitrogen forms during large tropical storms in a temperate,

- headwater, forested watershed. 1–19. doi: 10.1002/2015JG002909. Received
- Inamdar S, Finger N, Singh S, et al (2012) Dissolved organic matter (DOM) concentration and quality in a forested mid-Atlantic watershed, USA. *Biogeochemistry* 108:55–76. doi: 10.1007/s10533-011-9572-4
- Inamdar S, Singh S, Dutta S, et al (2011) Fluorescence characteristics and sources of dissolved organic matter for streamwater during storm events in a forested mid-Atlantic watershed. *J Geophys Res Biogeosciences*. doi: 10.1029/2011JG001735
- Jeong JJ, Bartsch S, Fleckenstein JH, et al (2012) Differential storm responses of dissolved and particulate organic carbon in a mountainous headwater stream, investigated by high-frequency, in situ optical measurements. *J Geophys Res Biogeosciences* 117:1–13. doi: 10.1029/2012JG001999
- Jung B-J, Jeanneau L, Alewell C, et al (2014a) Downstream alteration of the composition and biodegradability of particulate organic carbon in a mountainous, mixed land-use watershed. *Biogeochemistry* 122:79–99. doi: 10.1007/s10533-014-0032-9
- Jung B-J, Lee J-K, Kim H, Park J-H (2014b) Export, biodegradation, and disinfection byproduct formation of dissolved and particulate organic carbon in a forested headwater stream during extreme rainfall events. *Biogeosciences Discuss* 11:6877–6908. doi: 10.5194/bgd-11-6877-2014
- Jung BJ, Lee HJ, Jeong JJ, et al (2012) Storm pulses and varying sources of hydrologic carbon export from a mountainous watershed. *J Hydrol* 440–441:90–101. doi: 10.1016/j.jhydrol.2012.03.030
- Karanfil T, Krasner SW, Westerhoff P, Xie Y (2008) Recent Advances in Disinfection By-Product Formation , Occurrence , Control , Health Effects , and Regulations. 2–19.
- Kaushal SS, Mayer PM, Vidon PG, et al (2014) Land use and climate variability amplify carbon, nutrient, and contaminant pulses: A review with management implications. *J Am Water Resour Assoc* 50:585–614. doi: 10.1111/jawr.12204
- Kendall C, Silva SR, Kelly VJ (2001) Carbon and nitrogen isotopic compositions of particulate organic matter in four large river systems across the United States. *Hydrol Process* 15:1301–1346. doi: 10.1002/hyp.216
- Kraus TEC, Bergamaschi BA, Hernes PJ, et al (2008) Assessing the contribution of wetlands and subsided islands to dissolved organic matter and disinfection byproduct precursors in the Sacramento-San Joaquin River Delta: A geochemical approach. *Org Geochem* 39:1302–1318. doi: 10.1016/j.orggeochem.2008.05.012
- Larsen L, Harvey J, Skalak K, Goodman M (2015) Fluorescence-based source tracking of organic sediment in restored and unrestored urban streams. *Limnol Oceanogr* n/a–n/a. doi: 10.1002/lno.10108
- Lee M-H, Payeur-Poirier J-L, Park J-H, Matzner E (2016) Variability in runoff fluxes of dissolved and particulate carbon and nitrogen from two watersheds of different tree species during intense storm events. *Biogeosciences* 13:5421–5432. doi: 10.5194/bg-13-5421-2016
- Levia DF, Van Stan JT, Mage SM, Kelley-Hauske PW (2010) Temporal variability of

- stemflow volume in a beech-yellow poplar forest in relation to tree species and size. *J Hydrol* 380:112–120. doi: 10.1016/j.jhydrol.2009.10.028
- Lloret E, Dessert C, Pastor L, et al (2013) Dynamic of particulate and dissolved organic carbon in small volcanic mountainous tropical watersheds. *Chem Geol* 351:229–244. doi: 10.1016/j.chemgeo.2013.05.023
- Lu YH, Canuel EA, Bauer JE, Chambers RM (2014) Effects of watershed land use on sources and nutritional value of particulate organic matter in temperate headwater streams. *Aquat Sci* 76:419–436. doi: 10.1007/s00027-014-0344-9
- McClain ME, Boyer EW, Dent CL, et al (2003) Biogeochemical Hot Spots and Hot Moments at the Interface of Terrestrial and Aquatic Ecosystems. *Ecosystems* 6:301–312. doi: 10.1007/s10021-003-0161-9
- Melillo JM, Richmond T (T. C., Yohe GW (2014) Climate Change Impacts in the United States.
- Merriitts D, Walter R, Rahnis M, et al (2011) Anthropocene streams and base-level controls from historic dams in the unglaciated mid-Atlantic region, USA. *Philos Trans R Soc A Math Phys Eng Sci* 369:976–1009. doi: 10.1098/rsta.2010.0335
- Muylaeert K, Dasseville R, De Brabandere L, et al (2005) Dissolved organic carbon in the freshwater tidal reaches of the Schelde estuary. *Estuar Coast Shelf Sci* 64:591–600. doi: 10.1016/j.ecss.2005.04.010
- NOAA (2016), Winter was record warm for the contiguous U.S.
<http://www.noaa.gov/news/winter-was-record-warm-for-contiguous-us> (last accessed 390 March 21, 2017).
- Osburn CL, Handsel LT, Mikan MP, et al (2012) Fluorescence tracking of dissolved and particulate organic matter quality in a river-dominated estuary. *Environ Sci Technol* 46:8628–8636. doi: 10.1021/es3007723
- Osburn CL, Mikan MP, Etheridge JR, et al (2015) Seasonal variation in the quality of dissolved and particulate organic matter exchanged between a salt marsh and its adjacent estuary. 1–20. doi: 10.1002/2014JG002897.Received
- Park J-H, Duan L, Kim B, et al (2010) Potential effects of climate change and variability on watershed biogeochemical processes and water quality in Northeast Asia. *Environ Int* 36:212–225. doi: 10.1016/j.envint.2009.10.008
- Perdrial N, Perdrial N (2016) Impacts of Sampling Dissolved Organic Matter with Passive Capillary Wicks Versus Aqueous Soil Extraction. doi: 10.2136/sssaj2012.0061
- Raymond PA, Saiers JE, Sobczak W V. (2016) Hydrological and biogeochemical controls on watershed dissolved organic matter transport: pulse-shunt concept. *Ecology* 97:5–16. doi: 10.1890/07-1861.1
- Rosenfeld JS, Roff JC (1992) Examination of the Carbon Base in Southern Ontario Streams Using Stable Isotopes. *J North Am Benthol Soc* 11:1–10. doi: 10.2307/1467877
- Rowland R, Inamdar S, Parr T (2017) Evolution of particulate organic matter (POM)

- along a headwater drainage: role of sources, particle size class, and storm magnitude. *Biogeochemistry*. doi: 10.1007/s10533-017-0325-x
- Sadro S, Melack JM (2012) The Effect of an Extreme Rain Event on the Biogeochemistry and Ecosystem Metabolism of an Oligotrophic High-Elevation Lake. *Arctic, Antarct Alp Res* 44:222–231. doi: 10.1657/1938-4246-44.2.222
- Sakamaki T, Richardson JS (2011) Biogeochemical properties of fine particulate organic matter as an indicator of local and catchment impacts on forested streams. *J Appl Ecol* 48:1462–1471. doi: 10.1111/j.1365-2664.2011.02038.x
- Seitzinger SP, Sanders RW, Styles R (2002) Bioavailability of DON from natural and anthropogenic sources to estuarine plankton. *Limnol Oceanogr* 47:353–366. doi: 10.4319/lo.2002.47.2.0353
- Singh S, Inamdar S, Scott D (2013) Comparison of Two PARAFAC Models of Dissolved Organic Matter Fluorescence for a Mid-Atlantic Forested Watershed in the USA. *J Ecosyst* 2013:1–16. doi: 10.1155/2013/532424
- Stanley EH, Powers SM, Lottig NR, et al (2012) Contemporary changes in dissolved organic carbon (DOC) in human-dominated rivers: Is there a role for DOC management? *Freshw Biol* 57:26–42. doi: 10.1111/j.1365-2427.2011.02613.x
- Stedmon CC a, Markager S, Bro R (2003) Tracing dissolved organic matter in aquatic environments using a new approach to fluorescence spectroscopy. *Mar Chem* 82:239–254. doi: 10.1016/S0304-4203(03)00072-0
- Stelzer RS, Heffernan J, Likens GE (2003) The influence of dissolved nutrients and particulate organic matter quality on microbial respiration and biomass in a forest stream. *Freshw Biol* 48:1925–1937. doi: 10.1046/j.1365-2427.2003.01141.x
- Stelzer RS, Thad Scott J, Bartsch LA, Parr TB (2014) Particulate organic matter quality influences nitrate retention and denitrification in stream sediments: Evidence from a carbon burial experiment. *Biogeochemistry* 119:387–402. doi: 10.1007/s10533-014-9975-0
- Tank J, Rosi-Marshall E, Griffiths N a., et al (2010) A review of allochthonous organic matter dynamics and metabolism in streams. *J North Am Benthol Soc* 29:118–146. doi: 10.1899/08-170.1
- Tant CJ, Rosemond AD, First MR (2013) Stream nutrient enrichment has a greater effect on coarse than on fine benthic organic matter. *Freshw Sci* 32:1111–1121. doi: 10.1899/12-049.1
- Trimmer M, Grey J, Heppell CM, et al (2012) River bed carbon and nitrogen cycling: State of play and some new directions. *Sci Total Environ* 434:143–158. doi: 10.1016/j.scitotenv.2011.10.074
- Ussiri DAN, Johnson CE (2003) Characterization of organic matter in a northern hardwood forest soil by C-13 NMR spectroscopy and chemical methods. *Geoderma* 111:123–149. doi: Pii S0016-7061(02)00257-4rDoi 10.1016/S0016-7061(02)00257-4
- Vannote RL, Minshall GW, Cummins KW, Sedell JR, Cushing CE. The River Continuum Concept. *Canadian Journal of Fisheries and Aquatic Sciences*.

1980;37:130–7.

- Walter RC, Merritts DJ (2008) Natural streams and the legacy of water-powered mills. *Science* 319:299–304. doi: 10.1126/science.1151716
- Webster JR, Benfield EF, Ehrman TP, et al (1999) What happens to allochthonous material that falls into streams? A synthesis of new and published information from Coweeta. *Freshw Biol* 41:687–705. doi: 10.1046/j.1365-2427.1999.00409.x
- Wiegner TN, Kaplan L a, Newbold JD, et al (2005) Contribution of dissolved organic C to stream metabolism : a mesocosm study using ^{13}C -enriched tree-tissue leachate. *J North Am Benthol Soc* 24:48–67. doi: 10.1899/0887-3593(2005)024<0048:CODOCT>2.0.CO;2
- Worrall F, Burt TP, Howden NJK (2016) The fluvial flux of particulate organic matter from the UK: The emission factor of soil erosion. *Earth Surf Process Landforms* 41:61–71. doi: 10.1002/esp.3795
- Worrall F, Burt TP, Howden NJK (2014) The fluvial flux of particulate organic matter from the UK: Quantifying in-stream losses and carbon sinks. *J Hydrol* 519:611–625. doi: 10.1016/j.jhydrol.2014.07.051
- Yellen B, Woodruff JD, Cook TL, Newton RM (2016) Historically unprecedented erosion from Tropical Storm Irene due to high antecedent precipitation. *Earth Surf Process Landforms* 41:677–684. doi: 10.1002/esp.3896
- Yoshimura C, Fujii M, Omura T, Tockner K (2010) Instream release of dissolved organic matter from coarse and fine particulate organic matter of different origins. *Biogeochemistry* 100:151–165. doi: 10.1007/s10533-010-9412-y
- Yoshimura C, Gessner MO, Tockner K, Furumai H (2008) Chemical properties, microbial respiration, and decomposition of coarse and fine particulate organic matter. *J North Am Benthol Soc* 27:664–673. doi: 10.1899/07-106.1
- Ziegler AD, Benner SG, Kunkel ML, et al (2016) Particulate carbon and nitrogen dynamics in a headwater catchment in Northern Thailand: hysteresis, high yields, and hot spots. *Hydrol Process* 30:3339–3360. doi: 10.1002/hyp.10840

Appendix A

SUPPLEMENTAL DATA

A.1 Inorganic Nitrogen species

Overall, very weak or non-existent trends existed in the nutrient data. This was likely an artifact of the sample storage and preservation techniques, and does not represent the potential nutrient contributions and processing dynamics that may occur. NO₃-N did not vary between events (Figure A1) or between size classes (Figure A2). Notably, it also did not deviate strongly from the average value of the streamwater blank (horizontal line), indicating that negligible amounts of nitrate were produced. NH₄-N only varied significantly between two events (2/16/17, 8/21/16) (Figure A3) and did not vary by size class (Figure A4) though the values were significantly higher than the streamwater blank, which read below the detection limit of the instrument. Dissolved organic nitrogen (DON), measured as $(\text{TN}) - (\text{NO}_3\text{-N}) - (\text{NH}_4\text{-N})$ showed trends by size class, similar to TN, indicating that this trend was likely an artifact of the TN values and was not influenced by the NO₃-N or NH₄-N values (Figure A5).

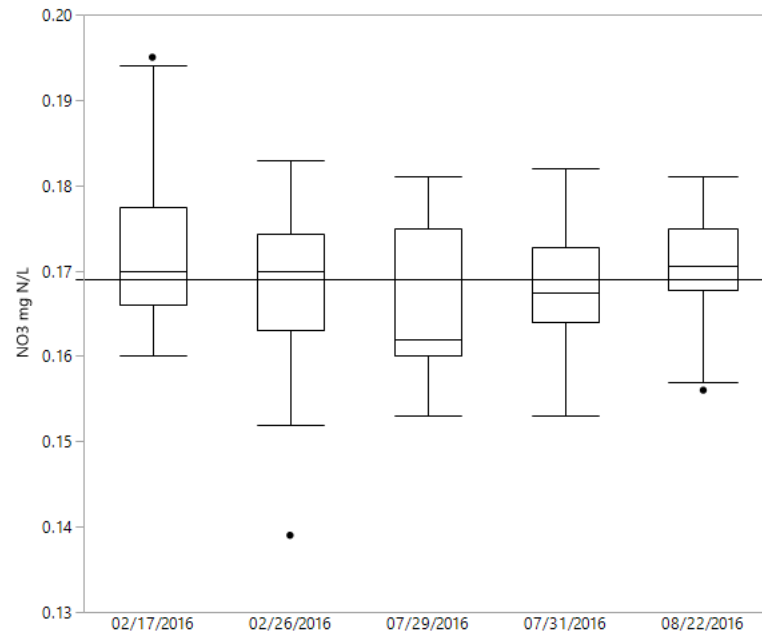


Figure A1: Nitrate, measured as NO₃-N, showed no significant differences by event. The horizontal line represents the average streamwater concentration, from which the event values did not significantly deviate.

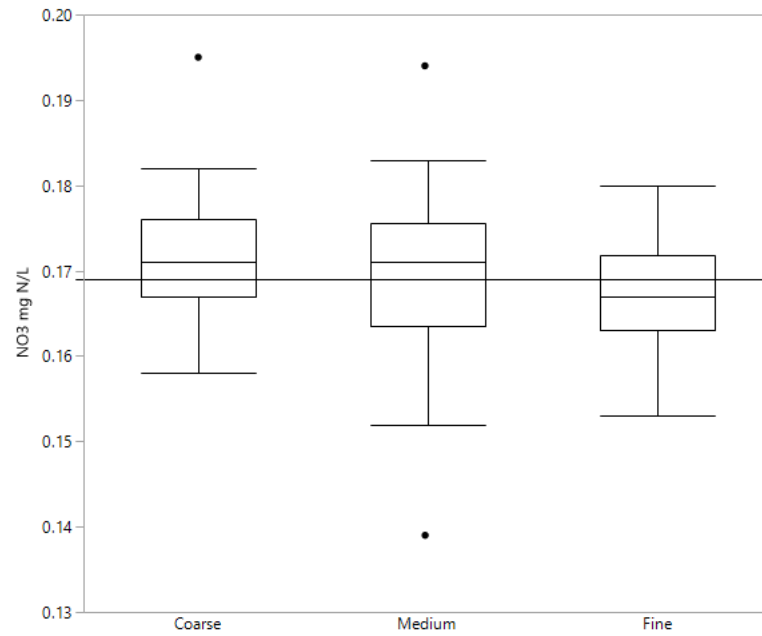


Figure A2: Nitrate, measured as NO₃-N, showed no significant differences by size class. The horizontal line represents the average streamwater blank sample from which the size classes did not deviate significantly.

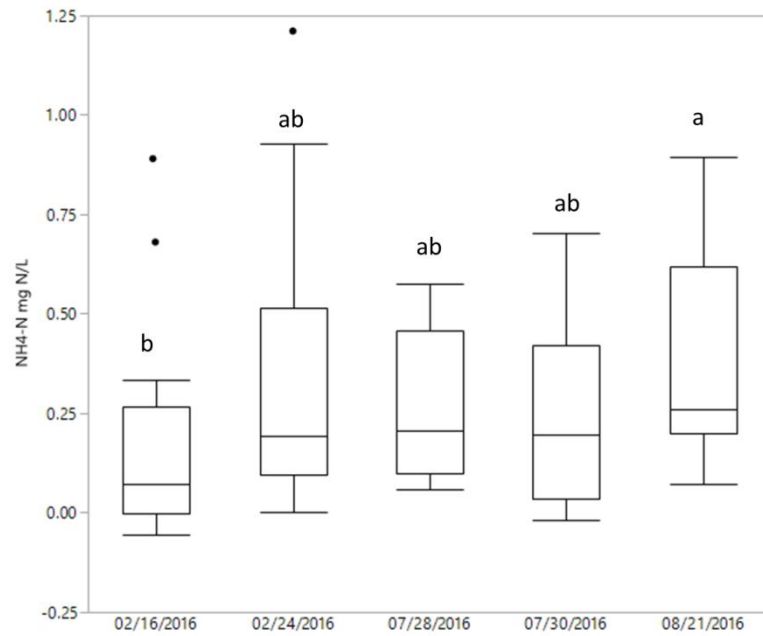


Figure A3: Ammonium, measured as NH₄-N, only showed a significant difference between the 2/16/16 and 8/21/16 events, and was significantly higher than streamwater blank which read below the detection limit of the instrument.

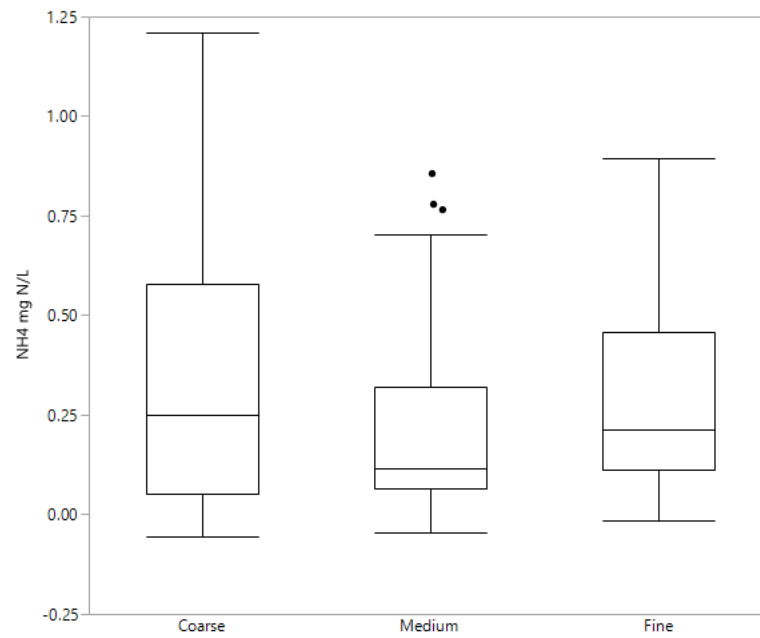


Figure A4: Ammonium, measured as NH₄-N, showed no significant difference between size classes.

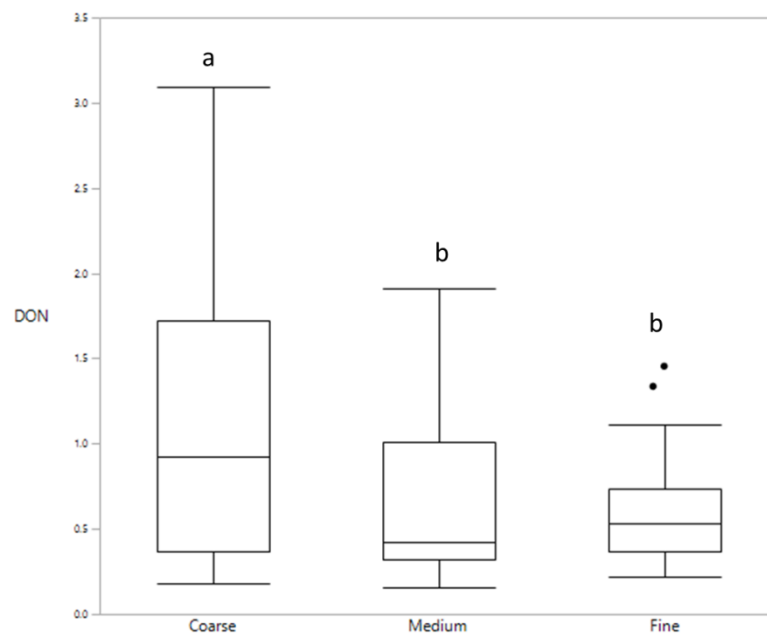


Figure A5: DON (ppm), calculated as $TN - NO_3-N - NH_4-N$. The Coarse size class was significantly different from Medium and Fine. No significant differences were found between events. This trend mirrors the TN trend by size class indicating that this relationship was an artifact of the TN values and was not influenced by the NO_3-N or NH_4-N values.

A.2 Average values for extracted and solid POM metrics

Table A1: Average values and standard deviations of solid POM metrics

Event	Size Class	%N	dev %N	%C	dev %C	C:N (atm)	$\delta^{15}\text{N}$	dev $\delta^{15}\text{N}$	$\delta^{13}\text{C}$	dev $\delta^{13}\text{C}$
2/16/2016	Coarse	0.50	0.28	11.48	9.78	34.78	-1.95	0.26	-28.63	0.24
	Medium	0.14	0.08	2.29	2.02	22.76	-1.13	0.39	-28.66	0.34
	Fine	0.15	0.05	2.08	1.26	18.71	0.02	0.71	-28.34	0.45
2/24/2016	Coarse	0.27	0.29	7.93	8.26	34.69	-1.16	0.67	-28.46	0.43
	Medium	0.18	0.17	2.40	3.20	22.09	-0.67	0.67	-28.51	0.33
	Fine	0.13	0.07	2.09	1.19	17.47	0.66	0.76	-28.15	0.29
7/28/2016	Coarse	0.27	NA	8.28	NA	36.18	-0.38	NA	-29.05	NA
	Medium	0.26	0.27	5.30	5.49	22.74	-0.03	0.37	-28.89	0.31
	Fine	0.25	0.19	4.04	3.46	18.04	1.05	0.53	-28.40	0.17
7/30/2016	Coarse	0.46	0.41	12.21	10.38	37.37	-0.63	0.62	-28.77	0.41
	Medium	0.33	0.31	4.89	6.34	23.34	-0.05	0.73	-28.95	0.49
	Fine	0.23	0.18	3.98	3.34	18.19	0.71	0.46	-28.42	0.30
8/21/2016	Coarse	0.65	0.27	20.57	5.46	38.57	-1.76	0.48	-28.56	0.65
	Medium	0.44	0.27	7.67	6.64	23.99	-0.47	0.42	-28.61	0.23
	Fine	0.21	0.10	3.76	2.18	19.76	0.23	0.23	-28.65	-28.65

Table A2: Average and standard deviations of extracted event POM metric.

Event	Size Class	DOC (mg/L)	dev	TN (mg/L)	dev	% Humic	% Fulvic	% Protein	NH4-N mg N/L	dev	NO3-N mg N/L	dev
2/16/2016	Coarse	11.09	8.13	1.20	0.89	45.55	31.65	22.80	0.25	0.33	0.17	0.01
	Medium	5.65	2.51	0.68	0.34	48.40	33.00	18.60	0.08	0.13	0.17	0.01
	Fine	5.73	1.54	0.76	0.23	50.67	31.59	17.74	0.16	0.13	0.17	0.01
2/24/2016	Coarse	14.42	10.57	1.45	1.10	46.66	33.42	19.92	0.37	0.42	0.17	0.01
	Medium	7.41	4.62	0.93	0.66	48.31	34.08	17.61	0.25	0.26	0.17	0.01
	Fine	6.90	1.78	1.06	0.42	52.27	33.09	14.64	0.35	0.26	0.17	0.01
7/29/2016	Coarse	11.90	NA	1.29	NA	39.74	28.17	32.09	0.20	NA	0.16	NA
	Medium	12.47	11.35	1.23	0.86	47.53	31.15	21.31	0.20	0.17	0.17	0.01
	Fine	10.49	7.15	1.26	0.69	49.99	30.64	19.37	0.30	0.21	0.16	0.01
7/31/2016	Coarse	17.55	12.57	1.66	1.17	42.15	33.64	24.20	0.26	0.26	0.17	0.01
	Medium	9.53	7.58	1.11	0.88	45.62	32.86	21.52	0.22	0.25	0.17	0.01
	Fine	6.99	3.42	1.02	0.60	49.99	32.61	17.40	0.29	0.26	0.16	0.01
8/22/2016	Coarse	32.45	8.86	2.58	1.13	40.68	30.97	28.35	0.49	0.27	0.17	0.00
	Medium	15.58	9.04	1.55	0.90	44.91	31.84	23.25	0.36	0.30	0.17	0.01
	Fine	10.36	2.35	1.26	0.47	49.18	31.50	19.32	0.38	0.26	0.17	0.00

A.3 Correlation Matrix

Table A3: Correlation matrix for all POM samples

	%N	%C	$\delta^{15}\text{N}$	$\delta^{13}\text{C}$	C:N	TN	DOC	Humic	Fulvic	Protein	IC	TC
%N	1.000	0.969	-0.526	-0.472	0.503	0.963	0.934	-0.523	-0.613	0.706	-0.332	0.932
%C	0.969	1.000	-0.594	-0.411	0.632	0.919	0.950	-0.625	-0.554	0.750	-0.292	0.950
$\delta^{15}\text{N}$	-0.526	-0.594	1.000	0.387	-0.761	-0.486	-0.540	0.488	0.445	-0.592	0.267	-0.536
$\delta^{13}\text{C}$	-0.472	-0.411	0.387	1.000	-0.274	-0.468	-0.395	0.418	0.424	-0.530	-0.012	-0.400
C:N (atm)	0.503	0.632	-0.761	-0.274	1.000	0.399	0.532	-0.647	-0.167	0.565	-0.073	0.535
TN (ppm)	0.963	0.919	-0.486	-0.468	0.399	1.000	0.942	-0.467	-0.586	0.650	-0.435	0.936
DOC (ppm)	0.934	0.950	-0.540	-0.395	0.532	0.942	1.000	-0.610	-0.507	0.715	-0.313	0.999
% Humic	-0.523	-0.625	0.488	0.418	-0.647	-0.467	-0.610	1.000	0.237	-0.862	-0.157	-0.622
% Fulvic	-0.613	-0.554	0.445	0.424	-0.167	-0.586	-0.507	0.237	1.000	-0.696	0.173	-0.506
% Protein	0.706	0.750	-0.592	-0.530	0.565	0.650	0.715	-0.862	-0.696	1.000	0.026	0.723
IC (ppm)	-0.332	-0.292	0.267	-0.012	-0.073	-0.435	-0.313	-0.157	0.173	0.026	1.000	-0.281
TC (ppm)	0.932	0.950	-0.536	-0.400	0.535	0.936	0.999	-0.622	-0.506	0.723	-0.281	1.000

Table A4: p-values of correlation matrix presented in Table A3

	%N	%C	$\delta^{15}\text{N}$	$\delta^{13}\text{C}$	C:N	TN	DOC	Humic	Fulvic	Protein	IC	TC
%N	0.0001	0.0001	0.0001	0.0001	0.0001	0.0001	0.0001	0.0001	0.0001	0.0001	0.0003	0.0001
%C	0.0001	0.0001	0.0001	0.0001	0.0001	0.0001	0.0001	0.0001	0.0001	0.0001	0.0014	0.0001
$\delta^{15}\text{N}$	0.0001	0.0001	0.0001	0.0001	0.0001	0.0001	0.0001	0.0001	0.0001	0.0001	0.0036	0.0001
$\delta^{13}\text{C}$	0.0001	0.0001	0.0001	0.0001	0.0028	0.0001	0.0001	0.0001	0.0001	0.0001	0.8985	0.0001
C:N(atomic)	0.0001	0.0001	0.0001	0.0028	0.0001	0.0001	0.0001	0.0001	0.0717	0.0001	0.434	0.0001
TN (ppm)	0.0001	0.0001	0.0001	0.0001	0.0001	0.0001	0.0001	0.0001	0.0001	0.0001	0.0001	0.0001
DOC (ppm)	0.0001	0.0001	0.0001	0.0001	0.0001	0.0001	0.0001	0.0001	0.0001	0.0001	0.0006	0.0001
% Humic	0.0001	0.0001	0.0001	0.0001	0.0001	0.0001	0.0001	0.0001	0.01	0.0001	0.0915	0.0001
% Fulvic	0.0001	0.0001	0.0001	0.0001	0.0717	0.0001	0.0001	0.01	0.0001	0.0001	0.0623	0.0001
% Protein	0.0001	0.0001	0.0001	0.0001	0.0001	0.0001	0.0001	0.0001	0.0001	0.0001	0.782	0.0001
IC (ppm)	0.0003	0.0014	0.0036	0.8985	0.434	0.0001	0.0006	0.0915	0.0623	0.782	0.0001	0.0021
TC (ppm)	0.0001	0.0001	0.0001	0.0001	0.0001	0.0001	0.0001	0.0001	0.0001	0.0001	0.0021	0.0001

